



3 4456 0021433 7

ORNL-2748  
Part A  
2nd Issue

RADIATION ACCIDENTS: DOSIMETRIC  
ASPECTS OF NEUTRON AND  
GAMMA-RAY EXPOSURE

G. S. Hurst  
R. H. Ritchie  
Editors

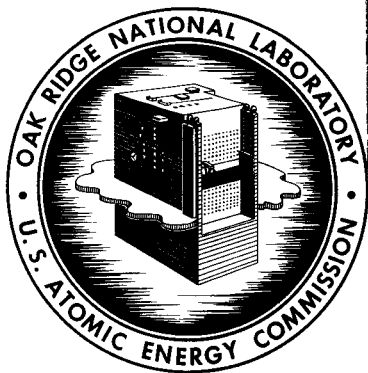
OAK RIDGE NATIONAL LABORATORY  
CENTRAL RESEARCH LIBRARY  
CIRCULATION SECTION  
4500N ROOM 175

**LIBRARY LOAN COPY**

DO NOT TRANSFER TO ANOTHER PERSON

If you wish someone else to see this  
report, send in name with report and  
the library will arrange a loan.

UCN-7969 (3-9-77)



**OAK RIDGE NATIONAL LABORATORY**

operated by

**UNION CARBIDE CORPORATION**

for the

**U.S. ATOMIC ENERGY COMMISSION**

Printed in USA. Price \$2.75. Available from the  
Office of Technical Services  
Department of Commerce  
Washington 25, D.C.

LEGAL NOTICE

This report was prepared as an account of Government sponsored work. Neither the United States, nor the Commission, nor any person acting on behalf of the Commission:

- A. Makes any warranty or representation, expressed or implied, with respect to the accuracy, completeness, or usefulness of the information contained in this report, or that the use of any information, apparatus, method, or process disclosed in this report may not infringe privately owned rights; or
- B. Assumes any liabilities with respect to the use of, or for damages resulting from the use of any information, apparatus, method, or process disclosed in this report.

As used in the above, "person acting on behalf of the Commission" includes any employee or contractor of the Commission, or employee of such contractor, to the extent that such employee or contractor of the Commission, or employee of such contractor prepares, disseminates, or provides access to, any information pursuant to his employment or contract with the Commission, or his employment with such contractor.

UNCLASSIFIED

ORNL-2748

Part A

ERRATA

RADIATION ACCIDENTS: DOSIMETRIC ASPECTS  
OF NEUTRON AND GAMMA-RAY EXPOSURES

Page Nos.	Errata
iii	F. J. Davis should be added to list of contributors.
45	U <sup>235</sup> in 6th line from bottom should be corrected to U <sup>238</sup> .
47	0.75 g of Pu <sup>239</sup> in 6th line from bottom should read 0.075 g of Pu <sup>239</sup> .
	0.03380 g of U <sup>235</sup> in 7th line from bottom should read 0.03360 g of U <sup>235</sup> .
55	Fig. 19 - 2nd value in 9th column should be 4549. 3rd and 4th values in last column should be 23.4 and 23.6, respectively.
63	Table VI - last column of numbers should be corrected, from top to bottom, to 2,325; 1,265; 215; and 54.
95	Ref. 17 in 6th line from top should be Ref. 2.

OAK RIDGE NATIONAL LABORATORY LIBRARY



3 4456 0021433 7

UNCLASSIFIED

ORNL-2748

Part A

Second Issue

RADIATION ACCIDENTS: DOSIMETRIC ASPECTS OF  
NEUTRON AND GAMMA-RAY EXPOSURES

G. S. Hurst and R. H. Ritchie  
Editors

HEALTH PHYSICS DIVISION

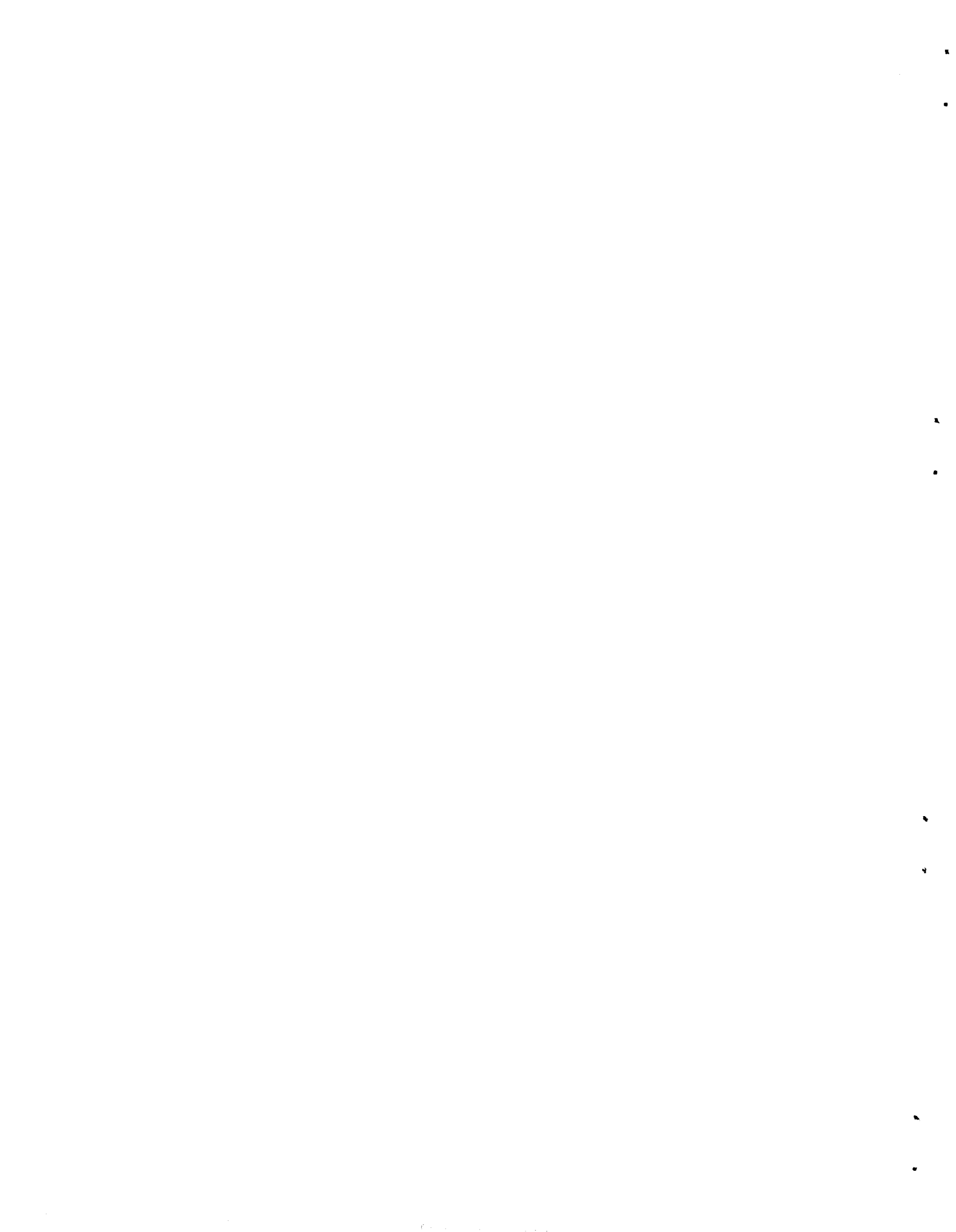
Date Issued

MAY 9 1961

---

Contract No. W-7405-eng-26  
Oak Ridge National Laboratory  
Oak Ridge, Tennessee  
Operated by  
Union Carbide Corporation  
for the  
U. S. Atomic Energy Commission

UNCLASSIFIED



## PREFACE

The Oak Ridge National Laboratory was asked by the Division of Biology and Medicine, U. S. Atomic Energy Commission, to study methods for determining the radiation dose received by persons involved in accidental criticality excursions. A system of dosimetry for this purpose has been devised and partially implemented at various AEC contractor sites in the United States. One objective of Part A of this report is to serve as an information manual for those persons responsible for implementing this system. A review and re-evaluation of the dosimetry of previous accidents is also included in the introduction.

A companion part of this report (ORNL-2748, Part B) deals with a review and analysis of the medical data obtained from previous criticality accidents. It also includes a method of defining human radiation injury and gives recommendations for clinical and laboratory observations for potential future cases. Parts A and B together form a complete analysis of dosimetric and medical information pertinent to acute exposures of humans to mixed radiations, and thus provide a basis for the correlation of biological effects on man with radiation dose.

ACKNOWLEDGMENTS

The following persons contributed to the preparation of this report:

G. S. Hurst }  
R. H. Ritchie } Editors

J. A. Auxier

H. M. Borella<sup>1</sup>

D. M. Davis

E. D. Gupton

J. C. Hart

P. N. Hensley

P. W. Reinhardt

F. W. Sanders

S. C. Sigoloff<sup>1</sup>

*F. J. Davis*

We wish to acknowledge the cooperation of W. T. Ham,<sup>2</sup> P. S. Harris,<sup>3</sup>  
K. Z. Morgan, R. M. Simmons, and especially that of the authors of the  
companion report, Niel Wald<sup>4</sup> and G. E. Thoma, Jr.<sup>5</sup>

---

1 Edgerton, Germeshausen, and Grier, Inc., Las Vegas, Nevada

2 Medical College of Virginia, Richmond

3 Los Alamos Scientific Laboratory, New Mexico

4 University of Pittsburgh

5 St. Louis University Hospital and Southwest Medical Center,  
St. Louis, Mo.

## TABLE OF CONTENTS

	Page
1. Review of Previous Accident Dosimetry Data	
R. H. Ritchie -----	1
1.1. Introduction -----	1
1.2. Los Alamos Accident LASL-I -----	3
1.3. Los Alamos Accident LASL-II -----	6
1.4. Argonne Cases -----	8
1.5. U. S. S. R. Cases -----	9
1.6. Oak Ridge Cases -----	11
1.7. Yugoslavia Cases - -----	12
1.8. Los Alamos Accident LASL-III -----	16
2. Recommended Dosimetry System -----	17
2.1. General Description of the Dosimetry System	
G. S. Hurst -----	17
2.1.1. Neutron Dose -----	19
2.1.2. Determination of the Gamma Dose -----	20
2.1.3. Orientation -----	22
2.1.4. Immediate Indication -----	22
2.2. Threshold Detector Techniques	
F. J. Davis, P. W. Reinhardt, and P. N. Hensley ---	24
2.2.1. Introduction -----	24
2.2.2. Threshold Detector System -----	24
2.2.3. Threshold Detector Counting Equipment -----	26
2.2.4. Operation and Calibration of the Fission Product Counters -----	41

## TABLE OF CONTENTS (continued)

	Page
2.2.5. Operation and Calibration of the Sulfur Counter -----	48
2.2.6. Operation and Calibration of the Gold Counters -	49
2.2.7. Placement of Threshold Detector Stations -----	51
2.2.8. Counting Techniques -----	51
2.2.9. Flux Calculation -----	54
2.2.10. Sensitivity of Various Threshold Detectors -----	62
2.3. Blood Sodium Techniques	
P. W. Reinhardt and F. W. Sanders -----	64
2.3.1. Introduction -----	64
2.3.2. Preparation of Blood Samples -----	64
2.3.3. Blood Na <sup>24</sup> Counting -----	64
2.4. Gamma Dosimetry with Chemical Techniques	
S. C. Sigoloff and H. M. Borella -----	68
2.4.1. Introduction -----	68
2.4.2. Radiation Characteristics -----	68
2.4.3. Spectrophotometric Measurements of pH Changes in Chlor-Phenol Red Indicator -----	73
2.4.4. Evaluation -----	73
2.4.5. Determination of Exposure Dosage -----	75
2.4.6. Shelf Life -----	75

## TABLE OF CONTENTS (continued)

	Page
2.5. Glass Dosimetry	
J. A. Auxier -----	77
2.5.1. General -----	77
2.5.2. Energy Response -----	81
2.5.3. Fast Neutron Response -----	83
2.5.4. Thermal Neutron Response -----	83
2.5.5. Cleaning of Glass and Reader -----	83
2.6. Film Badge for Criticality Accident Applications	
E. D. Gupton, D. M. Davis, and J. C. Hart -----	86
2.6.1. Introduction -----	86
2.6.2. Description of Badge -----	89
2.6.3. Effects of Orientation -----	92
2.6.4. Personnel Screening -----	93
2.7. Assignment of Individual Exposure Doses	
G. S. Hurst -----	95
2.7.1. Neutrons -----	95
2.7.2. Gamma Rays -----	97
3. Outline and Synopsis of ORNL-2748, Part B	
N. Wald and G. E. Thoma, Jr. -----	99
3.1. Outline of ORNL-2748, Part B -----	99
3.2. Synopsis of ORNL-2748, Part B -----	100
3.2.1. Review of Previous Accident Medical Data -----	100
3.2.2. Recommended Clinical Procedures -----	103

## LIST OF TABLES

	Page
I. Fast Neutron Leakage Spectrum from LASL Godiva I -----	5
II. Los Alamos Accident Cases - Serum Na Data -----	7
III. Review of Argonne Accident Cases -----	10
IV. Oak Ridge Y-12 Accident Cases Based on Serum Na Data ----	13
V. Yugoslavian Accident -----	15
VI. Sensitivity and Background of the Various Foils -----	63
VII. Neutron Activation of the ORNL Film Badge -----	94

## LIST OF FIGURES

	Page
1. Dosimetry System Suggested for Nuclear Excursions -----	18
2. Thermal Capture Probability for Unit Incident Flux -----	21
3. Cross Section of Threshold Detectors as a Function of Neutron Energy -----	25
4. Energy Response of Pu <sup>239</sup> Shielded with Various Thicknesses of B <sup>10</sup> -----	27
5. Exploded View of B <sup>10</sup> Container -----	28
6. Schematic Diagram of Fission Foil Counting System -----	30
7. Fission Foil Scintillation Counter -----	31
8. Detailed View of Lead Filter and Crystal -----	33
9. Gold Scintillation Counter -----	34
10. Shield for Sulphur and Gold Scintillation Counter -----	35
11. Sulphur Scintillation Counter -----	36
12. Phototube Coupling for Dual Counters -----	38
13. High Voltage Control for 6364 Photomultiplier -----	39
14. Differential and Integral Count Rate vs Energy Curves for Fission Foil Counters and Cs <sup>137</sup> -----	42
15. C(t) as a Function of Elapsed Time for Pu <sup>239</sup> , U <sup>238</sup> , Np <sup>237</sup> , and U <sup>235</sup> -----	46
16. Photograph of Sulphur in Various Stages of Burning Process --	50
17. Threshold Detector Placement Container -----	52
18. Placement Chart for Threshold Detectors -----	53
19. Sample Data Sheet -----	55
19a. Sample Data Sheet -----	56

## LIST OF FIGURES (continued)

	Page
20. Data Summary Sheet -----	57
21. Flux Correction Factors for Various Exposure Times -----	60
22. Blood Counting Techniques -----	66
23. Counting Geometry for Na <sup>24</sup> in Various Volumes of Blood Serum--	67
24. Chemical Dosimetry Nomenclature - TCE Dosimeter -----	69
25. Chemical Dosimeter with Li, Sn Shield -----	71
26. Energy Dependence of Chemical Dosimeter -----	72
27. Per Cent Transmission at 580 m $\mu$ and 432 m $\mu$ as a Function of pH -----	74
28. Relationship of Ratio $\frac{\%T_{580}}{\%T_{432}}$ vs pH -----	76
29. Size of Glass Rod and Exposure Capsules Relative to Common Objects. (a) and (b) - Tantalum-tin-teflon capsule to correct for energy dependence. (c) - Fluorothene capsule for hard gamma exposures. (d) - Gelatin capsule for low energy unshielded exposure. (e) - A glass rod -----	78
30. The Bausch and Lomb Reader and Low Power Microscope -----	79
31. Microdosimeter Reader - Optical Layout -----	80
32. Luminescent Response of Glass Rods as a Function of Photon Energy for Various Shields -----	82
33. Neutron Response of Glass Rods as a Function of Neutron Energy -----	84
34. Experimental Lithium Shield for Glass Dosimeter -----	85
35. A Typical Low-Dose Calibration Curve for Glass Rods Exposed to Gamma Rays -----	87
36. New Health Physics Multi-Purpose Badge Meter -----	90
37. Preliminary Estimation of Clinical Radiation Injury Following Overexposure -----	105

## 1. REVIEW OF PREVIOUS ACCIDENT DOSIMETRY DATA

### 1.1. Introduction

Since the beginning of research and production activities in the field of nuclear technology dating back to the Manhattan project, there have been seven major nuclear accidents involving significant exposures of personnel to ionizing radiation. In this section these accidents will be reviewed in chronological order. The sequence of events and conditions of exposure which are pertinent to an understanding of the physical dosimetry will be described.

Since the time of the first of these accidents (fourteen years ago) there has been continuous improvement in the techniques and concepts of radiation dosimetry. For example, dose units such as the gram-roentgen are no longer believed to be adequate indices of radiation exposure and time has served to accentuate the complexity of the RBE concept. In this report, an effort has been made to re-evaluate the dose assigned to certain individuals involved in nuclear accidents, using modern techniques of radiation dosimetry.

To put the physical dosimetry of past accidents on a common objective basis, the dose to a given individual is specified in terms of the absorbed dose (in rads) which would have been received by a small mass of soft tissue located at the position of the individual. This dose will be referred to as the first collision dose, consistent with

common usage.<sup>1</sup> It is realized that correlations of biological data with a single dose reading will be far from perfect unless other physical conditions of exposure are specified. Thus, as much information as is available on parameters such as radiation energy and angular distribution will also be considered.

The use of the rem dose unit is avoided entirely in this report. First collision doses will be given in terms of rads to soft tissue for neutrons and gamma rays separately. This procedure is consistent with the desirability of establishing RBE factors for acute irradiation of man from accident data.

The method which has been found<sup>2</sup> most reliable for evaluating the neutron dose to persons exposed in mixed radiation fields is that obtained from measurements of the formation of  $\text{Na}^{24}$  in the body via the reaction  $\text{Na}^{23}(n,\gamma)\text{Na}^{24}$ . The neutron dose to the body may be related in a simple way to the spectrum of incident neutrons as determined from threshold detector measurements. This method of dose measurement might be termed "spectral" dosimetry and is described in detail in Section 2.2 below. The  $\text{Na}^{24}$  activation engendered in the

---

1 This definition of first collision dose is not consistent with the mathematically convenient definition given by Snyder (W. S. Snyder, Health Physics 1, 51 (1958)). His definition refers to the energy per gram imparted to a small volume element of tissue located at a given depth below the surface of the body by neutrons which have made no collisions until they reach the point in question.

2 G. S. Hurst, R. H. Ritchie, and L. C. Emerson, Health Physics 2, No. 2, (1959).

body is very simply related to threshold detector measurements of the neutron spectrum. Hence if one can estimate or measure the neutron spectrum escaping from a critical assembly, the  $\text{Na}^{24}$  activation in a man may be interpreted in terms of the first collision dose at his position. This method has been used below whenever data on spectral distribution of neutrons are available. Estimates of the gamma-to-neutron dose ratio are used to allow one to assign both gamma and neutron doses on the basis of  $\text{Na}^{24}$  activation in the body.

Dose estimates are made only for cases in which the radiation exposure was acute, external, penetrating and generalized. Doses due to alpha and beta radiation, either internal or external to the body, are not considered and are thought to be relatively unimportant in the usual criticality accident.

## 1.2. Los Alamos Accident LASL-1

The first nuclear accident occurred at the Los Alamos Scientific Laboratory, Los Alamos, New Mexico, in August 1945.<sup>3</sup> In a criticality experiment involving a metal system a nuclear excursion occurred and two people were exposed to the mixed radiation field from this assembly. Case LA-1, who died following the accident, was touching the assembly when the chain reaction occurred, and so received a very high dose to his hands and a smaller dose to the bulk of his torso. He was exposed

---

<sup>3</sup> L. H. Hempelman, H. Lisco, and J. G. Hoffman, *Ann. Int. Med.* 36, 279 (1952).

to considerable gamma radiation from fission products while dismantling the experiment and would possibly have survived had he left the room immediately. His actions during this period are not well known and the total dose received is correspondingly uncertain. Neither he nor the other person exposed was wearing a film badge at the time of the accident. Since the number of fissions which occurred in the assembly is not known accurately, the best index of his neutron exposure is the  $\text{Na}^{24}$  activity induced in his blood.

One may relate the  $\text{Na}^{24}$  concentration in the blood to the number of incident neutrons if one knows their distribution in energy.<sup>4</sup> Measurements of the spectrum of neutrons escaping from the Godiva reactor have been made, and are shown in Table I. It is reasonable to assume that this spectrum is very similar to the accident spectrum and that the latter does not vary with distance over the range at which exposure occurred. It is known that the attenuation of the tamper around the critical experiment was not high.<sup>5</sup>

Using the relation between dose per dps of  $\text{Na}^{24}$  per ml of blood serum and the spectral distribution given by the Godiva threshold detector measurements, Table I, one finds for the neutron dose,

$$D_n = 5.0 K \quad (1)$$

---

4 See Section 2.7 below.

5 P. S. Harris, LASL, Private Communication.

Table I

## Fast Neutron Leakage Spectrum from LASL Godiva 1

(Results are shown in terms of the number of neutrons per  $\text{cm}^2$  above the threshold of detectors described in Section 2)

Detector	Relative Flux* ( $\text{n cm}^{-2}$ )
$\text{Pu}^{239}$ (2 cm $\text{B}^{10}$ ) (n,f)	1.00
$\text{Np}^{237}$ (n,f)	0.86**
$\text{U}^{238}$ (n,f)	0.46
$\text{S}^{32}$ (n,p)	0.21

\* Measurements made August 1956. At one meter from Godiva center actual Pu flux was  $3.0 \times 10^{10}$   $\text{n/cm}^2$  for  $2.04 \times 10^{15}$  fissions.

\*\* Includes a correction for the new fission cross section of  $\text{Np}^{237}$ . Value adopted = 1.6 barns based on private communication with R. B. Murray. See also, H. W. Schmitt and R. B. Murray, Bull. Amer. Phys. Soc. 4, No. 5, 321 (June 18, 1959).

where  $K = \text{dps/cm}^3$  of blood serum and  $D_n$  is in rad. It is known that the quantity of  $\text{Na}^{23}$  per  $\text{cm}^3$  of blood serum is remarkably constant in man at the value of  $3.2 \text{ mg/cm}^3$  (see Ref. 1). This fact has been used in converting from activity per unit mass of  $\text{Na}^{23}$  to activity per  $\text{cm}^3$  of blood. One finds a neutron dose of 288 rads for this case, using the blood  $\text{Na}^{24}$  value from Ref. 2 (see Table II).

Case LA-2 was exposed at a greater distance from the reactor than was case LA-1 and did not remain in the vicinity after the excursion. From measurements of the ratio of gamma dose to neutron dose leaking from the Godiva reactor, one may estimate that the gamma-neutron dose ratio was approximately 1/10 in the LASL-I accident, independent of distance from the reactor in the range of distances of LA-1 and LA-2. Table II shows the resulting estimate of dose, again using the  $\text{Na}^{24}$  data of Ref. 3.

### 1.3. Los Alamos Accident LASL-II

The circumstances surrounding the second major radiation exposure at Los Alamos on May 21, 1946, were quite similar to those in the first accident. Personnel film badge data were not available and data from badges located on the walls of the room were not very helpful. Eight persons were exposed to significant doses in this incident. It is felt that none of these victims received uniform total body exposures because of various amounts of partial body shielding.<sup>3</sup>

The neutron doses to the exposed people have been estimated as in the case of the LASL-I accident, i.e. by using neutron spectral

Table II  
Los Alamos Accident Cases - Serum Na Data

Accident	Case	dps/mg Na	K (dps/cc)	D <sub>n</sub> (rad) (5.00 K)	D <sub>γ</sub> (rad)	D <sub>t</sub> (rad)
LASL-I	LA-1	18.0 <sup>(6)</sup>	57.6	288	Uncertain	
	LA-2	1.10 <sup>(6)</sup>	3.5	18	2	20
LASL-II	LA-3	74.8 <sup>(7)</sup>	239	1190	120	1310
	LA-4	13.2 <sup>(7)</sup>	42.2	213	21	234
	LA-6	7.1 <sup>(7)</sup>	22.7	117	12	129
	LA-7	3.0 <sup>(7)</sup>	9.6	48	5	53
	LA-8	2.0 <sup>(7)</sup>	6.4	32	3	35
	LA-9	1.54 <sup>(7)</sup>	4.9	24	2.4	26
	LA-10	1.22 <sup>(7)</sup>	3.9	19	2	21
LASL-III	LA-11		451 <sup>(8)</sup>	2200	6600	8800

6 J. G. Hoffman and L. H. Hempelmann, Am. J. Roentgenol., Rad. Therapy and Nuclear Med. 77, No. 1, 144 (1957).

7 J. G. Hoffman, "Radiation Dose In the Pajarito Accident of May 21, 1946," LA-687, May 26, 1948.

8 P. S. Harris, LASL, Private Communication.

data obtained from the Godiva reactor together with Na<sup>24</sup> activation data for the blood of the patients. Table II shows the doses derived on this basis. It has been assumed that the gamma-to-neutron dose ratio was 1/10 for all those exposed. This is probably a good assumption except for case LA-9 who returned to the scene of the accident twice after his initial exposure.

#### 1.4 Argonne Cases

A reactor criticality accident occurred at the Argonne National Laboratory, Lemont, Illinois, on June 2, 1952.<sup>9</sup> Four persons were exposed to a mixed field of radiation in which the gamma-to-neutron dose ratio was about 10. The critical assembly consisted of a quasi-cylindrical metallic core surrounded by a natural water moderator in a plastic tank. There were no fatalities.

Cases 1, 2, and 3 were wearing film badges which were so blackened that it was necessary to evaluate the doses in terms of the reduced silver left after development of the film. The gamma dose to patient 4 was evaluated from a knowledge of his position and times of exposure to prompt and delayed fission gamma rays. The gamma dose is given by Hasterlik and Marinelli<sup>9</sup> in terms of first collision dose, i.e. the correction for the effect of the body on the dose received by it has been made. The doses were found to be fairly constant over the bodies

---

<sup>9</sup> R. J. Hasterlik and L. O. Marinelli, Proceedings of the International Conference on the Peaceful Uses of Atomic Energy, Vol. 11, p 25 (1956).

of those exposed and can be considered as uniform whole body irradiation.

Threshold detector measurements of the neutron spectrum escaping from this assembly are not available. However, Hasterlik and Marinelli quote accurate neutron dose values determined with proportional counter dosimeters.<sup>10</sup> These were obtained by measuring the ratio of fast neutron dose to gamma dose during an experimental run of the reconstructed reactor and applying this ratio to the film badge readings.

The resulting dose determinations are shown in Table III.

#### 1.5. U.S.S.R. Cases

At some undisclosed time prior to July 1956, a reactor accident occurred in the U.S.S.R. resulting in the "short general external" exposure of two persons to neutrons and gamma rays. The clinical course of the exposures is detailed by A. K. Guskova and G. D. Baisogolov.<sup>11</sup> They assign doses of 300 "r" and 450 "r" to the people but do not give the gamma-neutron ratio in the radiation field. No information is available concerning the structure and composition of the reactor, so that it is not possible to estimate this ratio. In addition, the methods of dosimetry used are not described. The dose assignments must, therefore, be regarded as ambiguous.

---

10 G. S. Hurst, Brit. J. Radiol. 27, 353 (1954).

11 A. K. Guskova and G. D. Baisogolov, Proceedings of the International Conference on the Peaceful Uses of Atomic Energy, Vol. 11, p 35 (1956).

Table III

Review of Argonne Accident Cases<sup>9</sup>

Employee	Gamma Dose* (rad)	Neutron Dose** (rad)	Total Dose (rad)
A-1	145	14.2	159
A-2	116	9.6	126
A-3	55	5.5	60.5
A-4	10	0.8	10.8

\* Gamma Dose - Film badge readings of reduced silver left after development of film, corrected for readings in air for buildup and body shielding.

\*\* Neutron Dose - Based on  $D_Y - D_n$  ratio and film badge doses. Values above are precise to ~ 10% based on dosimetric measurements of reconstructed accident.

### 1.6. Oak Ridge Cases

A criticality accident occurred on June 16, 1958, at the Y 12 Plant at Oak Ridge, Tennessee.<sup>12</sup> Criticality was reached when an aqueous solution of an enriched uranium compound was drained inadvertently into a waste drum having dimensions such that a chain reaction resulted. Eight persons received general whole body doses from the radiations emanating from the critical system, five of these receiving total doses in excess of 200 rads.

Film badges were not worn by any of those exposed to the radiation field. Blood sodium radioactivity was chosen as the most reliable measure of neutron dose in this accident. The neutron dose to a man at a given distance from the assembly was deduced from the  $\text{Na}^{24}$  concentration in his body by employing a "phantom" (in this case, a burro). The phantom was exposed to the neutron field escaping from a "mock-up" reactor of dimensions and composition closely similar to those of the accident assembly. The blood serum  $\text{Na}^{24}$  level of the phantom resulting from irradiation by a measured first collision neutron dose was determined and was used to convert blood  $\text{Na}^{24}$  activity data to first collision neutron dose, assuming that the neutron spectrum did not vary with distance from the reactor. During another run of the same "mock-up" reactor a measurement of the gamma-neutron dose ratio was made and was used to obtain the gamma doses. Corrections

---

<sup>12</sup> Accidental Radiation Excursion at the Y-12 Plant, Y-1234, July 28, 1958; See also Ref. 2.

were made for the different contributions from fission product gamma rays in the two cases. Calculation of the neutron and gamma-ray leakage spectra from the reactor gave dose estimates which agreed well with the measured values.

Table IV shows the doses for the persons exposed. None died as a result of the exposure.

### 1.7. Yugoslavia Cases

In an accidental supercritical excursion of a zero-power reactor on October 15, 1958, at the Boris Kidrich Institute of Nuclear Sciences in Vinca near Belgrade, Yugoslavia, eight persons received above maximum permissible doses of neutrons and gamma rays.<sup>13</sup> One man died as a result of the irradiation.

The facility consisted of a natural uranium, heavy water assembly in a cylindrical tank approximately 2 meters high and 2 meters in diameter. The people were located in the range 5 to 10 meters from the reactor at the time of the excursion.

Although only incomplete information is available concerning the neutron and gamma leakage spectrum from the reactor and the disposition of people and apparatus at the time of the accident, it is possible to make estimates of the doses from Na<sup>24</sup> activation data for the six

---

13 Editors (from an exchange of airmail and radiograms between the Nucleonics office and Pavle Savic, Director of the Boris Kidrich Institute of Nuclear Science), *Nucleonics* 17, No. 4, 106 (1959).

See also references under Table V.

Table IV  
Oak Ridge Y-12 Accident Cases Based on Serum Na Data

Employee	Neutron Dose (rad)	Gamma Dose (rad)	Total Dose (rad)
OR-1	96	269	365
OR-2	89	250	339
OR-3	86	241	327
OR-4	71	199	270
OR-5	62	174	236
OR-6	18	50.5	68.5
OR-7	18	50.5	68.5
OR-8	6	16.8	22.8

patients treated in Paris at the Curie Foundation.<sup>14</sup> One account of the accident<sup>13</sup> states that it is known from both calculation and experiment that the thermal and epithermal leakage from the reactor are equal. It seems reasonable to take the fast neutron leakage spectrum from the reactor to be roughly similar to that measured in the Y-12 accident study.<sup>12</sup> Hence, it has been assumed that the total neutron spectrum in the Yugoslavia case is equal to that in the Y-12 case for epithermal energies ( $> \sim 5$  kev), but that the thermal flux is equal to the total flux above 5 kev.

Using this assumption and Eq. (18) in Section 2.7 below, and taking the amount of Na<sup>23</sup> in each individual to be 105 g,<sup>15</sup> one finds the neutron dose to be

$$D_n = 3.92 A \quad (2)$$

where  $D_n$  is in rad and  $A$  is the total measured Na<sup>24</sup> activity in the body in  $\mu$ c. Table V shows values of  $A$  for the patients together with their estimated doses (Col. 2).

The gamma doses may be deduced from these data, using a reported measurement<sup>13</sup> of a gamma dose of 1 mr/hr at a thermal neutron flux level of  $155 \text{ n/cm}^2 \cdot \text{sec}$  around the reactor when operated in early

---

14 Dr. Raymond Latarjet, Curie Foundation, Paris, Private Communication, February 26, 1959.

15 This is the figure quoted in NBS Handbook 63, p 8, for the standard 70 KG man. Data on body weights of the exposed are not available at this time.

Table V  
Yugoslavian Accident

Case	Na <sup>24</sup> ( $\mu$ c) <sup>(14)</sup>	K(dps/cc blood serum) <sup>(16)</sup>	D <sub>n</sub> (rad) <sup>(17)</sup>	D <sub>γ</sub> (rad) <sup>(18)</sup>	D <sub>t</sub> (rad)
V	82	92.5	320	320	640
M	75	84.6	290	290	580
G	76	85.7	300	300	600
D	63	71.0	250	250	500
H	53	60.0	210	210	420
B	45	50.8	175	175	350

K = 1.13 x  $\mu$ c

$\mu$ c = total  $\mu$ c in exposed individuals

16 Assuming a standard man (70 KG) with 105 grams of Na.

17 Total first collision dose for neutrons, assuming fast spectrum same as at Y-12 and one thermal for each fast D<sub>n</sub> = 3.47 K.

18 Assuming D<sub>γ</sub>/D<sub>n</sub> = 1.0, estimated from Ref. 13, using gamma dose to thermal neutron flux ratio. See also Pavle P. Savić, Bull. Inst. Nuclear Sciences "Boris Kidrich", 9, No. 167, 1 (1959).

experiments. One estimates from this and from measurements of the neutron-gamma dose ratio around similar reactors that the neutron-gamma dose ratio was approximately 1.0. The resulting estimates are given in Table V.

#### 1.8. Los Alamos Accident LASL-III

The most recent radiation accident occurred on December 30, 1958, at the Los Alamos Scientific Laboratory.<sup>19</sup> In the course of a routine plutonium salvage operation, the material attained a critical state. Case LA-11 was standing in close proximity to the critical system and received a lethal dose.

If one assumes that the neutron and gamma-ray fields were comparable with those which were measured in the Y-12 mock-up experiment,<sup>12</sup> then the neutron dose may be approximated as  $D_n = 5.2 K$  where  $K$  is the  $\text{Na}^{24}$  activity in dps per cc of blood serum and  $D_n$  is the neutron dose in rad.  $K$  was found to be 451 dps/mg.<sup>20</sup> This relation between  $D_n$  and  $K$  is nearly the same as that which one derives from the Godiva measurements. One finds a fast neutron dose of 2200 rads and using a neutron-to-gamma dose ratio of 3, one finds a gamma dose of 6600 rads (see Table II).

---

19 H. C. Paxton, R. D. Baker, W. J. Maraman, and Roy Reider, *Nucleonics* 17, No. 4, 107 (1959). See also LAMS-2293, February 1959.

20 P. S. Harris, LASL, Private Communication.

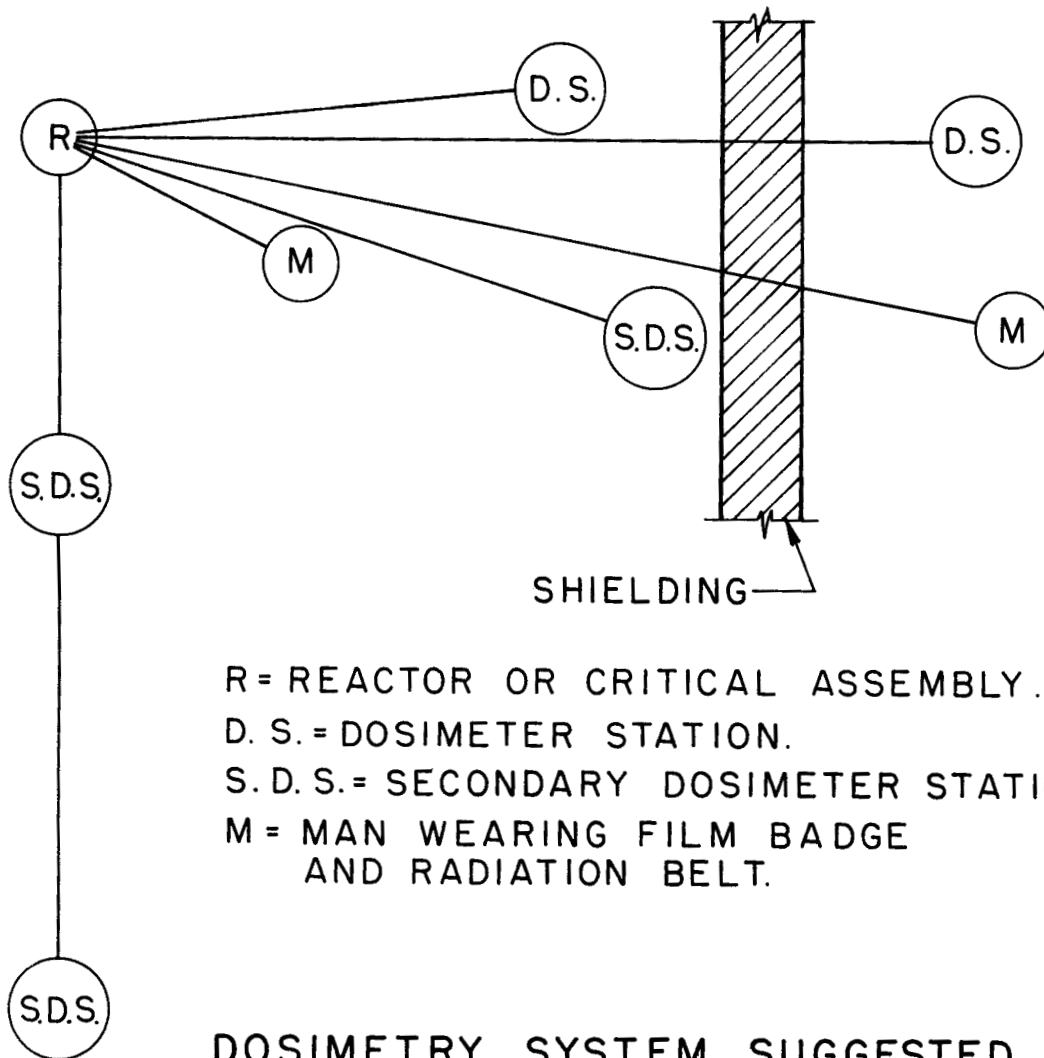
## 2. RECOMMENDED DOSIMETRY SYSTEM

### 2.1. General Description of the Dosimetry System

A system of dosimetry designed to determine the dose received by personnel from criticality incidents must be capable of (1) measuring the dose due to gamma rays in the presence of neutrons with reasonably small uncertainty, say  $\pm 15\%$ ; (2) measuring the neutron dose in the presence of gamma rays with reasonably small uncertainty, say  $\pm 15\%$ ; (3) giving information relative to the orientation of the exposed person so that not only the first collision dose but also the conditions necessary for defining the depth dose distribution can be specified; and (4) giving an immediate indication of the persons who have been exposed so that the exposed and non-exposed personnel can be readily separated.

Because of the fact that the equipment necessary for accomplishing the above objectives is too complicated and large to be worn by the person, much of it must be at fixed locations within the laboratory areas. On the other hand, since the dose varies strongly with distance from the point of excursion and since in general the location of persons cannot be precisely determined, part of this system should be worn on the person. Figure 1 is a diagram of the complete dosimetric system under consideration. The point "R" marks the site of the nuclear excursion. The "dosimeter station" consists of the complete series of threshold detectors which is capable of roughly measuring the spectrum due to fast neutrons and thermal neutrons and also consists of a device

UNCLASSIFIED  
ORNL-LR-DWG. 36558



DOSIMETRY SYSTEM SUGGESTED  
FOR NUCLEAR EXCURSIONS

FIG. 1

suitable for measuring the gamma dose in the presence of neutrons, e.g. glass needles and/or chemical dosimeters. In addition to this fixed station, several other secondary dosimeter stations may be located throughout the area which would contain, for example, only sulfur and gold. It is noted that in the event of intervening shielding between an exposed person and the point R, the dosimeter station should be repeated. The symbol "M" represents locations of a man whose dose we wish to determine. It is noted that the part of the dosimeter system worn by the man is a film badge of the type developed by the Applied Health Physics Group, ORNL,<sup>21</sup> which contains sulfur and gold foils (both bare gold and gold encased in cadmium) for neutron activation measurements. In addition, the man should wear a belt which would contain both gamma and neutron dosimeters at fixed intervals. It is noted that the effective orientation of the individual for neutrons and for gamma rays may be quite different; therefore, the belt should contain not only a gamma measuring device but also neutron monitors. This can take the form of the glass rods spaced at regular intervals for measuring the gamma dose and sulfur and gold samples for measuring the neutron flux. The results which should be obtainable from such a system of dosimetry may be summarized as follows:

#### 2.1.1. Neutron Dose

The neutron dose can be determined by Na<sup>24</sup> activity in

---

21 D. M. Davis, J. C. Hart, and K. Z. Morgan, "Personnel Meters," ORNL CF 58-12-39, January 2, 1959.

the blood plus the threshold detector data on the neutron spectrum. Figure 2 (Ref. 2) shows the probability of  $\text{Na}^{24}$  capture in the blood system as a function of neutron energy. It is noted that the sensitivity for thermal neutrons is roughly one-third the sensitivity for fast neutrons. With this curve and the data obtained by counting blood samples for  $\text{Na}^{24}$ , one can determine the neutron flux; then by multiplying this flux by the spectrum obtained with threshold detector units, one can determine the neutron dose. Corrections for the activation of  $\text{Na}^{23}$  by thermal neutrons can be made by means of the gold in the film badge or in the radiation belt.

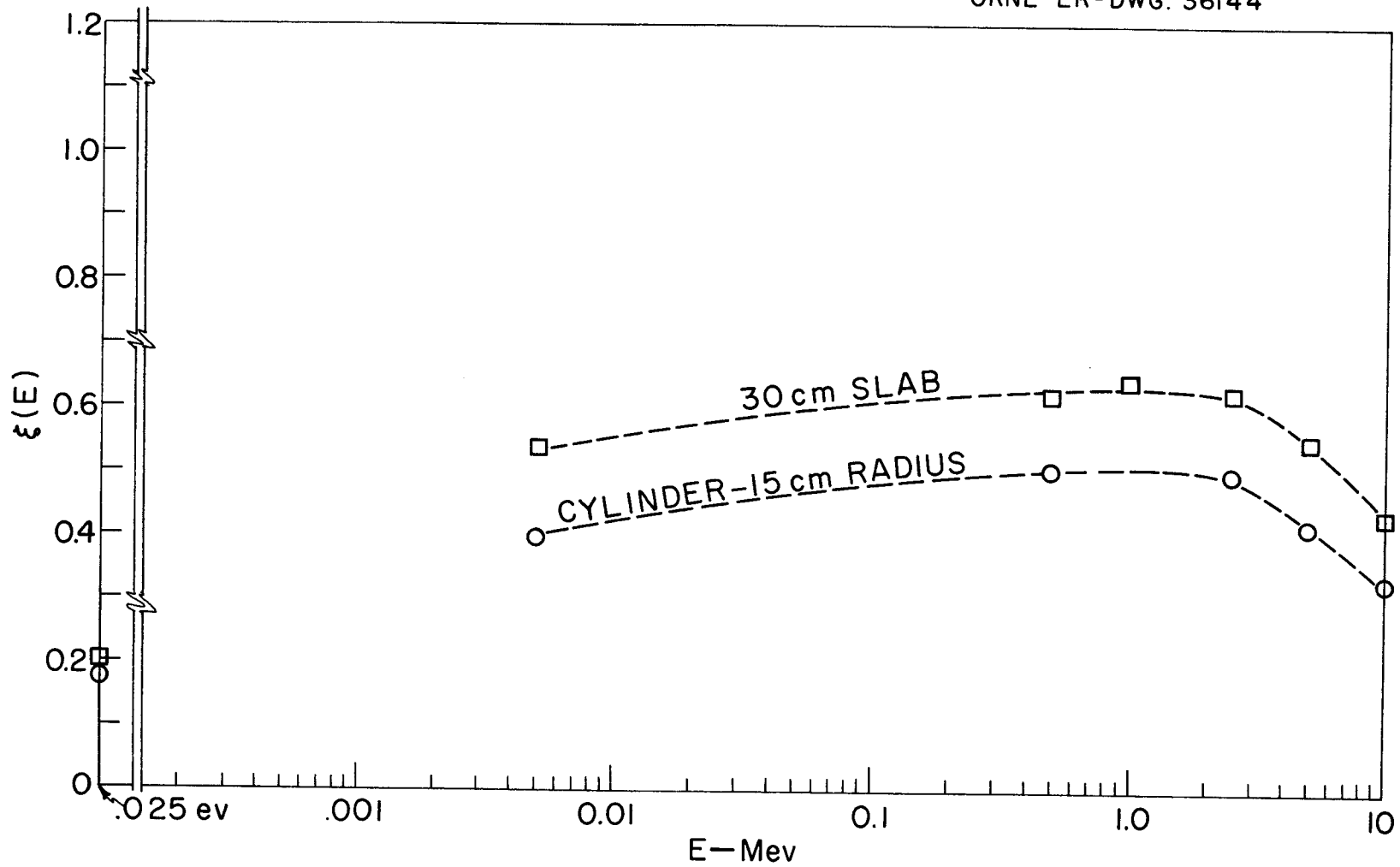
The neutron dose can also be determined by using the neutron dose calculated from the threshold detectors at the dosimeter station and by normalizing the sulfur flux obtained at this station to the sulfur flux obtained for the person either from the radiation belt or from the film badge.

The neutron dose can also be determined from the  $\text{Na}^{24}$  and from direct calculations of the leakage spectrum of fast neutrons.

#### 2.1.2. Determination of the Gamma Dose

The gamma dose can be determined also by three methods:

(1) The  $D_Y - D_n$  ratio can be determined from the dosimeter station since it contains a complete set of threshold detectors for determining the fast neutron dose and contains the chemicals or glass for determining the gamma-ray dose. Use of this experimental ratio in conjunction with the neutron dose determined by the above method leads to a separate



THERMAL CAPTURE PROBABILITY FOR UNIT INCIDENT FLUX

FIG. 2

determination of the gamma-ray dose.

(2) The film in the film badge can also be used to approximate the gamma-ray dose. It is noted that in this case the gamma-ray dose as read by the film will have to be normalized for orientation of the person as determined by the radiation belt.

(3) In some cases the gamma-ray dose can be determined also by calculation of the  $D_{\gamma}/D_n$  ratio, and the application of the neutron dose as determined by the above method.

#### 2.1.3. Orientation

The orientation of an individual can be determined approximately by means of the radiation belt. This then aids in the construction of depth dose curves. For example, an individual may be looking at the reactor at the time of the excursion and obtain the neutron dose through his front section, whereas if he then runs from the point of excursion, he will receive part of the gamma dose through the back. This factor can be taken into account by the information obtained from the radiation belt which measures the effective orientation both for gamma rays and fast neutrons.

#### 2.1.4. Immediate Indication

An immediate indication of the exposed personnel is desirable and this could be obtained through the use of prompt indication of radiation dose by some device worn on the film badge. For example, this can be the self-indicating chemical dosimeter which changes its color immediately on radiation. It is emphasized that the meters

should be sensitive to gamma rays as well as neutrons because in some cases the person could be exposed to large doses of gamma rays and comparatively small doses of neutrons.

Another method of immediate indication is obtainable through the use of an indium foil located in the film badge. This could be read for activation with simple radiation detecting instruments. The gold supplements the indium for the purpose of immediate identification of those exposed to neutrons. Although less sensitive than the indium, it has a longer half-life permitting identification of the highly exposed individuals for several days following exposure. It is noted, however, that the indium and gold are sensitive only to neutrons and not to gamma rays.

The system as outlined in Section 2.1 cannot be completely realized at this time because (1) some of the techniques are not available, and (2) some of the information is not complete. It is recommended that the minimum system consist of the threshold detectors with chemical and/or glass dosimeters and facilities for counting blood  $\text{Na}^{24}$ . With this arrangement the  $D_\gamma$ - $D_n$  ratio would be measured and the neutron dose may be determined from blood  $\text{Na}^{24}$  and the data from the threshold detectors. When available the film badge package and radiation belt could be added which would provide (1) an independent estimate of the gamma dose and (2) a determination of the effective orientation of the person for gamma rays and for neutrons.

## 2.2. Threshold Detector Techniques

### 2.2.1. Introduction

The threshold detector as developed by Hurst et al.<sup>22</sup> and Reinhardt and Davis<sup>23</sup> allows a measurement of the number of neutrons in five energy regions. The thermal flux is determined by exposing Au and Au surrounded with Cd and taking the difference in Au activation. The fast flux is determined by use of Pu<sup>239</sup>, Np<sup>237</sup>, U<sup>238</sup>, and S<sup>32</sup> which provide measurements of the flux above 1 kev, 0.75 Mev, 1.5 Mev, and 2.5 Mev, respectively. From these flux measurements the total neutron dose can be obtained.

### 2.2.2. Threshold Detector System

Figure 3 shows the fission cross sections<sup>24</sup> as a function of energy of Pu<sup>239</sup>, Np<sup>237</sup>, and U<sup>238</sup> and the S<sup>32</sup>(n,p)P<sup>32</sup> cross section for S<sup>32</sup>. Pu<sup>239</sup> has a high thermal neutron fission cross section; thus the thermal neutrons must be removed in order to make it a suitable threshold detector. Np<sup>237</sup> has a competing high thermal neutron capture cross section giving Np<sup>238</sup> which emits a 1.0 Mev gamma ray with a 2.3

---

22 G. S. Hurst, J. A. Harter, P. N. Hensley, W. A. Mills, M. Slater, and P. W. Reinhardt, Rev. Sci. Instr. 27, 153 (1956).

23 P. W. Reinhardt and F. J. Davis, Health Physics 1, 169 (1958).

24 D. J. Hughes and J. A. Harvey, Neutron Cross Sections, BNL-325 (1955); D. J. Hughes and R. B. Schwartz, Neutron Cross Sections-Supplement No. 1, BNL-325 (1957).

See also H. W. Schmitt and R. B. Murray, Bull. Amer. Phys. Soc. 4, No. 5, 321 (June 18, 1959).

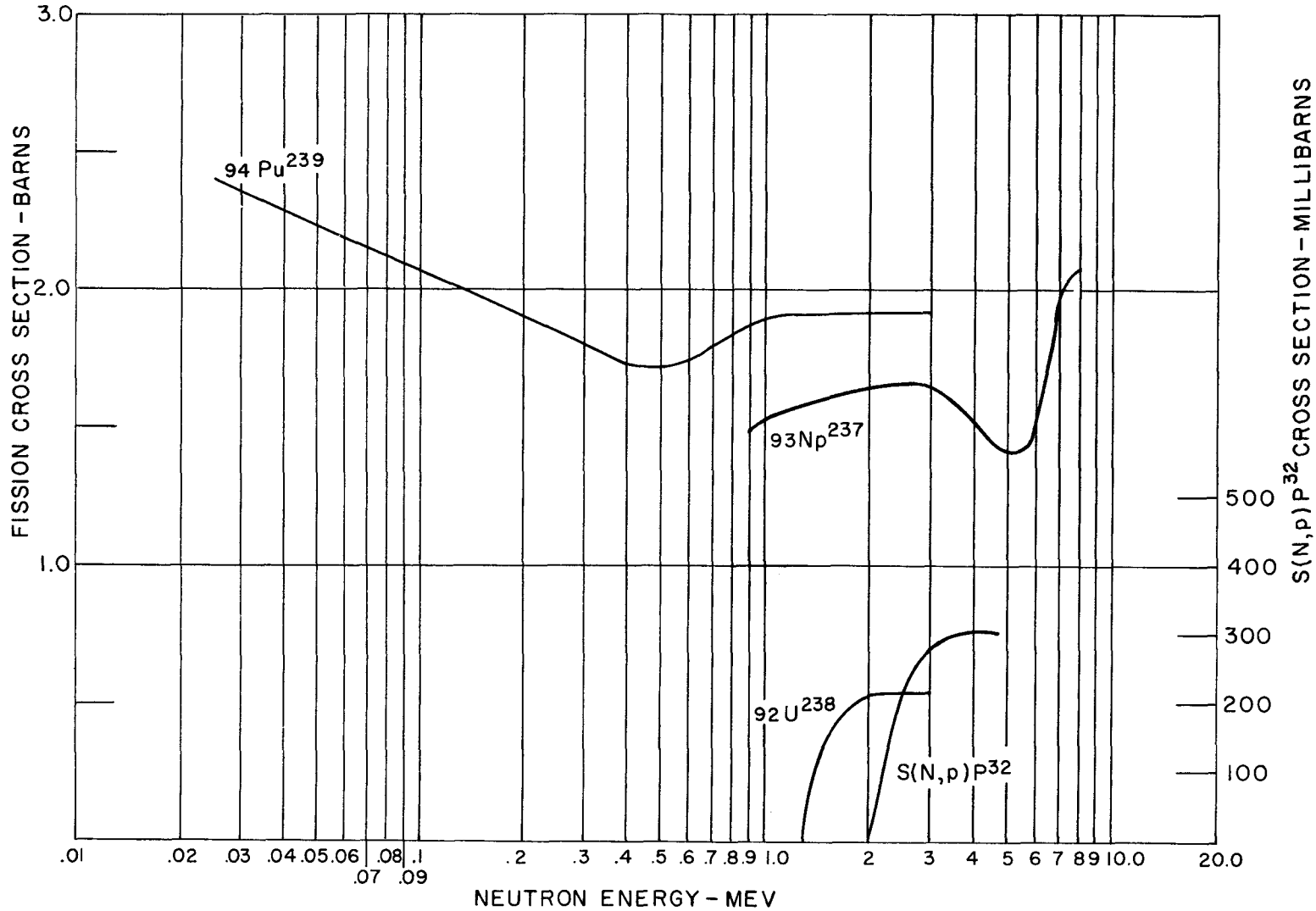


FIG. 3 CROSS SECTION OF THRESHOLD DETECTORS AS A FUNCTION OF NEUTRON ENERGY.

day half life, and  $U^{238}$  usually contains a small amount of  $U^{235}$  which has a high thermal fission cross section. Therefore, it is advantageous to remove the thermal neutrons from all of the fission foils. A  $B^{10}$  shield is used for this purpose.

The response of  $Pu^{239}$  shielded with various thicknesses of  $B^{10}$  is shown in Fig. 4. The effective cross section is defined as

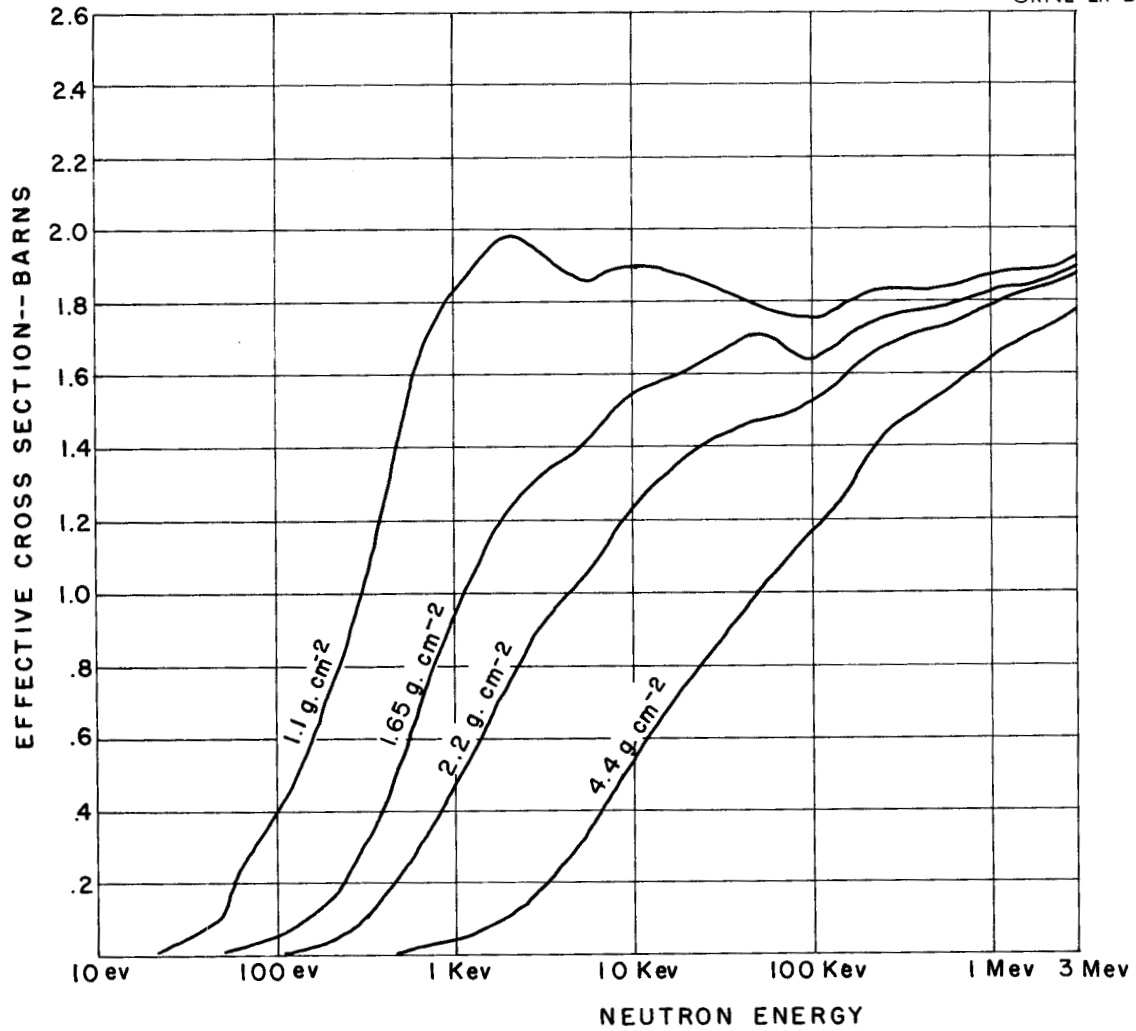
$$\sigma_{\text{eff}} = \sigma_F \exp(-\sigma_B N_B) \quad (3)$$

where  $\sigma_F$  is the fission cross section of  $Pu^{239}$ ,  $\sigma_B$  is the cross section of  $B^{10}(n,\alpha)Li^7$  reaction, and  $N_B$  is the number of  $B^{10}$  atoms per  $\text{cm}^2$  in the boron shield. The cross section  $\sigma_B$  is proportional to  $1/\text{velocity}$  with a value of 3700 barns at the thermal energy, 0.025 ev.

In Fig. 5 is shown an exploded view of a loaded  $B^{10}$  container. The shield is designed so that regardless of the direction of the incoming neutron the desired thickness of  $B^{10}$  is penetrated by neutrons in reaching the cavity in which the fission foils are placed. This insures that the above equation holds for the effective cross section even though the beam is broad. The cavity is lined with 0.025 inch cadmium to capture any neutrons moderated by the shield.

### 2.2.3. Threshold Detector Counting Equipment

All of the various types of foils are counted on scintillation counters making it possible to use the same set of electronics with each type of scintillation detector. Due to the nature of decay the fission foils are counted first, then the fission foil

UNCLASSIFIED  
ORNL-LR-DWG. 9442FIG. 4 ENERGY RESPONSE OF Pu<sup>239</sup> SHIELDED WITH VARIOUS THICKNESSES OF B<sup>10</sup>

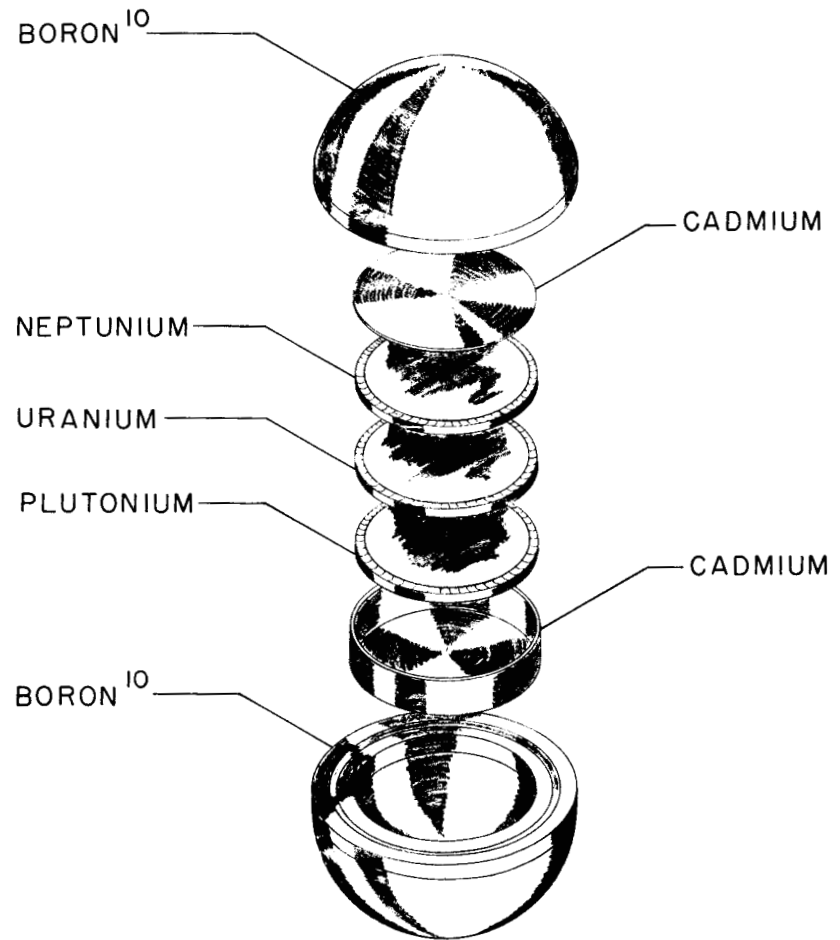
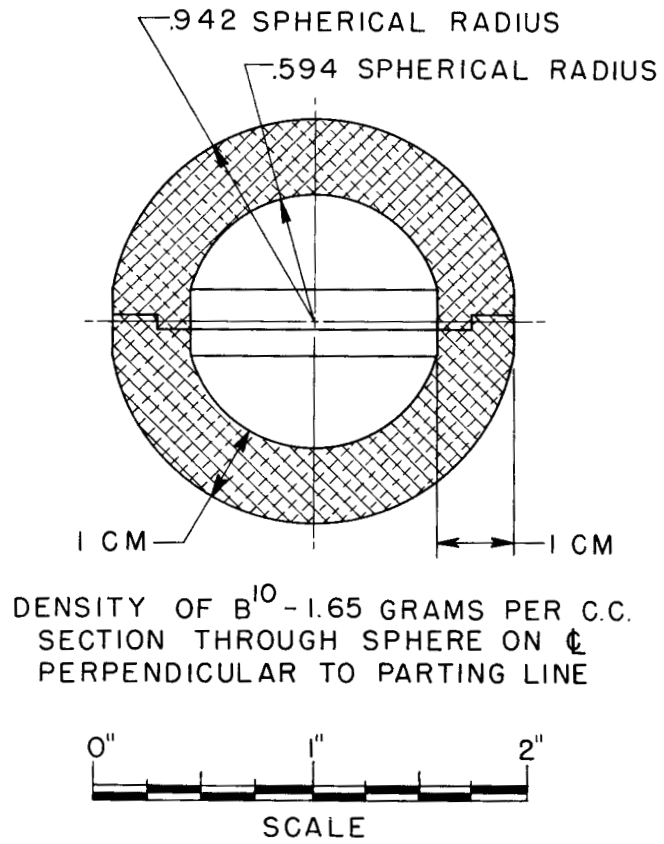


FIG. 5 EXPLODED VIEW OF  $B^{10}$  CONTAINER

scintillation detector is replaced with the gold detector. After the gold has been counted the gold detector is replaced with the sulfur detector. The fission foil scintillation unit is provided with a side access door. By removing one of the two fission foil detectors, the unit is converted into a blood sodium detector.

Figure 6 shows a schematic diagram of the fission foil counter and its associated electronics. The fission foils are counted between two 4 inch x 2 inch sodium iodide crystals. The signals from the photomultipliers are fed through a common pre-amplifier into a linear amplifier. The amplifier discriminator output is fed into a decade scaler whose counting time is controlled by a scaler with preset count of 60 cycle current. The gains of the photomultipliers are individually adjustable by varying the series resistance between the photomultiplier divider network and the high voltage supply.

The fission foil scintillation assembly is shown in Fig. 7. The scintillation detection heads consist of two 4 inch by 2 inch sodium iodide crystals (Harshaw type 16B8) with 6364 DuMont photomultipliers. The detectors are positioned with respect to each other by a spacer assembly. The spacer assembly also provides a sample slide and a lead filter. The sample slide enables one to dispense foils from the outside of the counter shield into the counting position without opening and closing heavily shielded doors. A Cs<sup>137</sup> standard is located in the sample slide at the opposite end from the sample holder. When a fission foil is withdrawn from the counting position, the standard is automatically put into the counting position. A more detailed view of

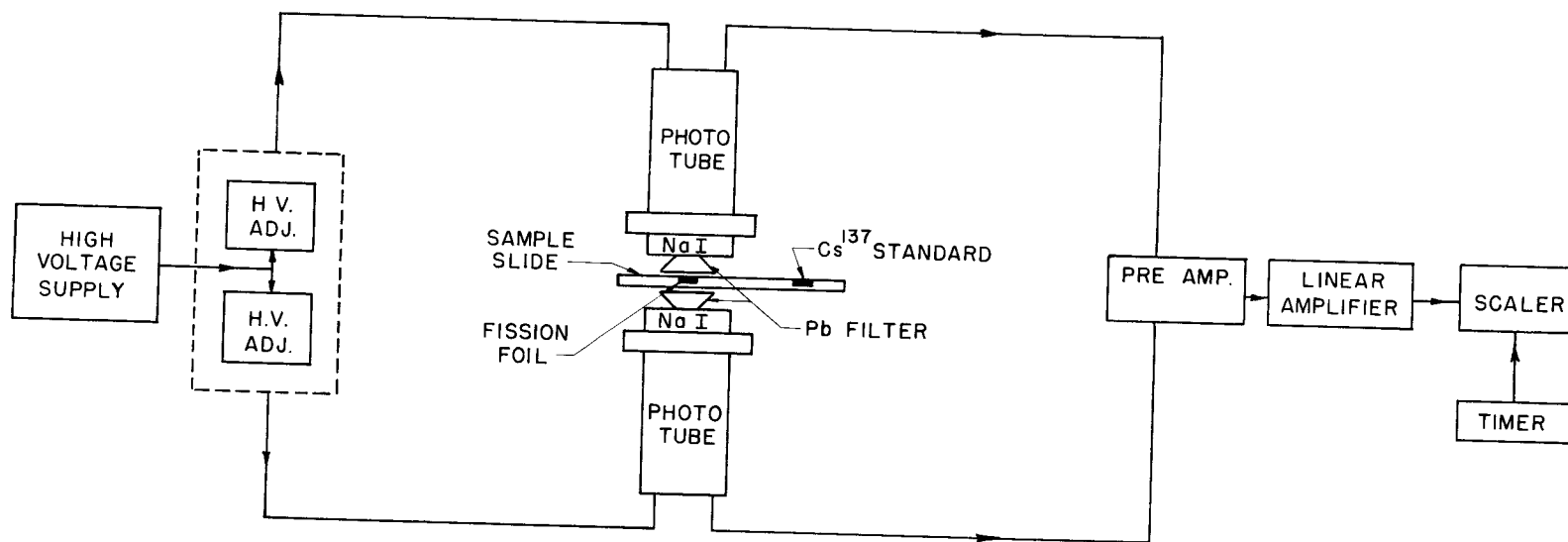


FIG. 6 SCHEMATIC DIAGRAM OF FISSION FOIL COUNTING SYSTEM

UNCLASSIFIED  
ORNL-LR-DWG 36562-A

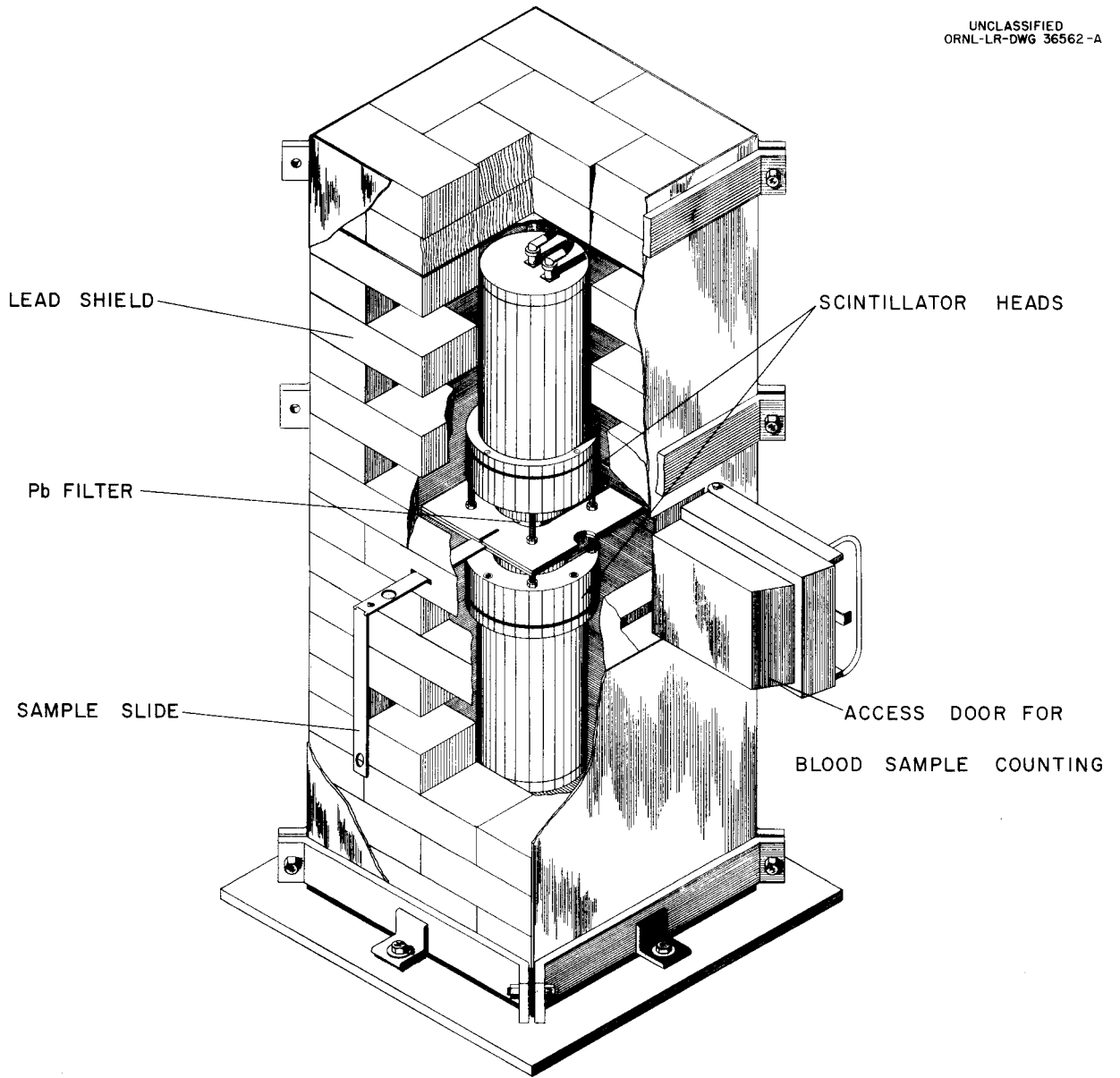


FIG. 7 FISSION FOIL SCINTILLATION COUNTER

the lead filters with respect to the crystals is shown in Fig. 8. The filters were provided primarily for  $\text{Np}^{237}$  counting.  $\text{Np}^{237}$  has a soft gamma background sufficient to overload the amplifier if not filtered out. Close tolerance has been specified for the spacer assembly and lead filters in order to obtain close intercomparison of measurements with a large number of counters.

The gold foil scintillation counter is made up of a 1-1/2 inch sodium iodide crystal (Harshaw type 6D4) and a RCA type 6655 photomultiplier tube shown in Fig. 9. A foil holder for positioning the foil on the crystal is also shown. The foil holder contains a 1/16 inch aluminum filter to eliminate the 0.96 Mev beta. The shield for the gold and sulfur counter is shown in Fig. 10. Access to the counter is obtained by rolling back the top of the shield.

The sulfur counter is shown in Fig. 11. A plastic scintillator 1-7/8 inch x 1/16 inch is used to detect the 1.71 Mev  $\text{P}^{32}$  beta ray. Nel02 plastic scintillator, manufactured by Nuclear Enterprises Ltd., has been found to be most successful. The phototube is a RCA type 6655, the same as used in the gold detector.

The major parts of the electronic equipment are standard components which are commercially available from a number of different manufacturers. The ORNL A-1D linear amplifier model Q-1326-1  $\text{R}_2$  and the Q-1326  $\text{R}_3$  preamplifier have been found quite reliable over long periods of time. For added temperature stability, the resistors in the feed-back loops of both amplifier and preamplifier have been replaced

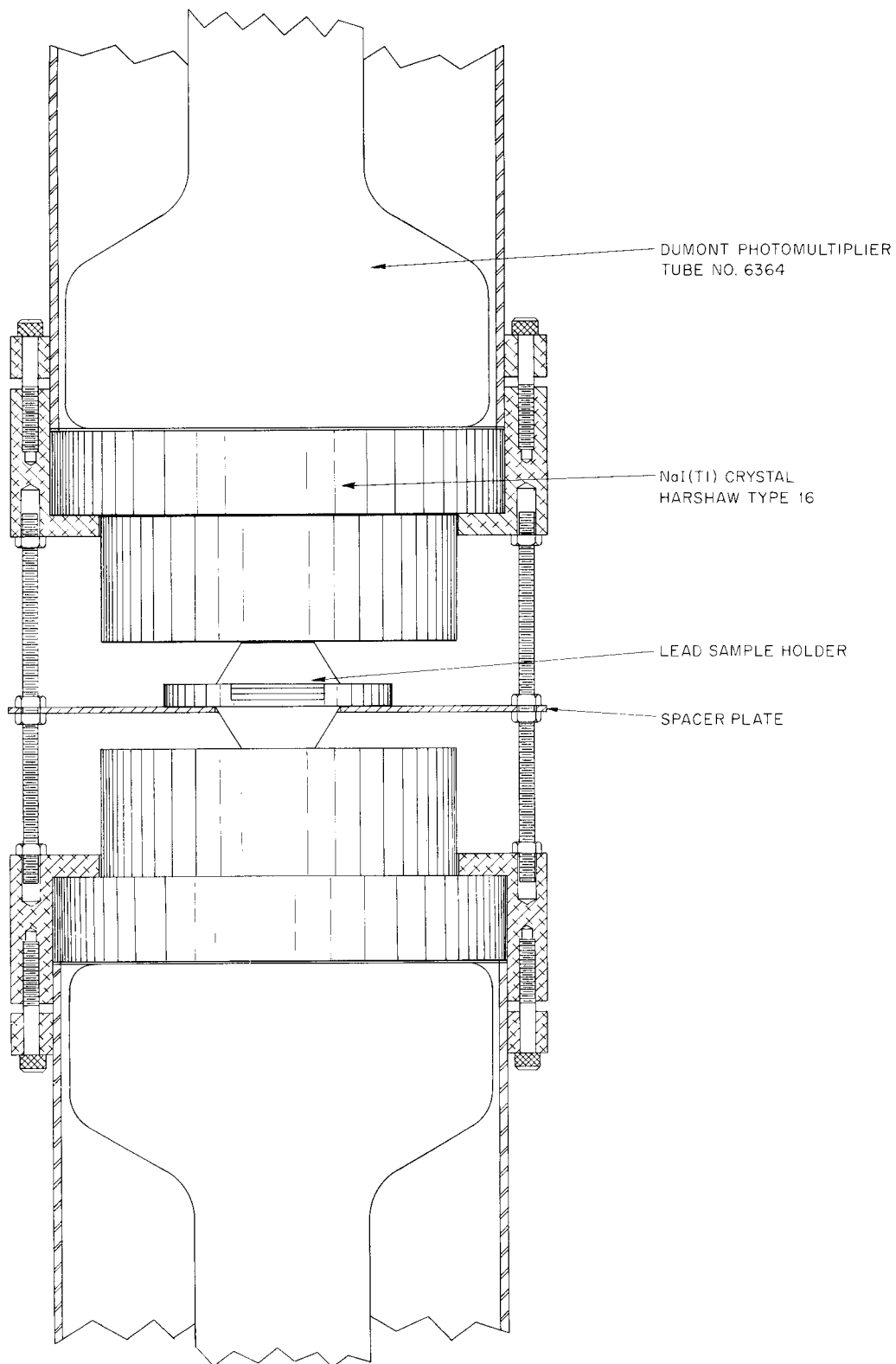
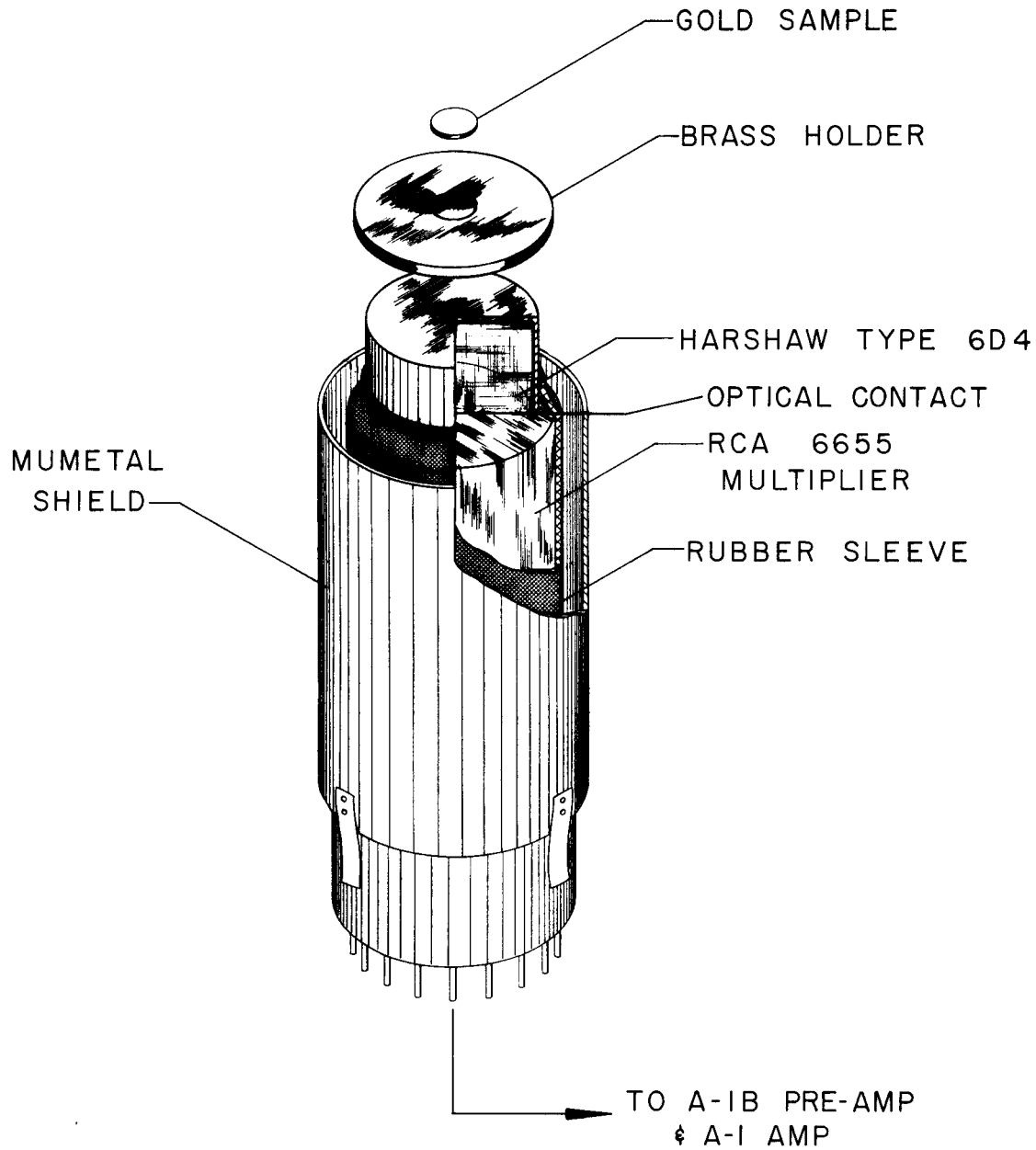


FIG. 8 DETAILED VIEW OF LEAD FILTER AND CRYSTAL



GOLD SCINTILLATION COUNTER  
FIG. 9

UNCLASSIFIED  
ORNL-LR-DWG. 36563-A

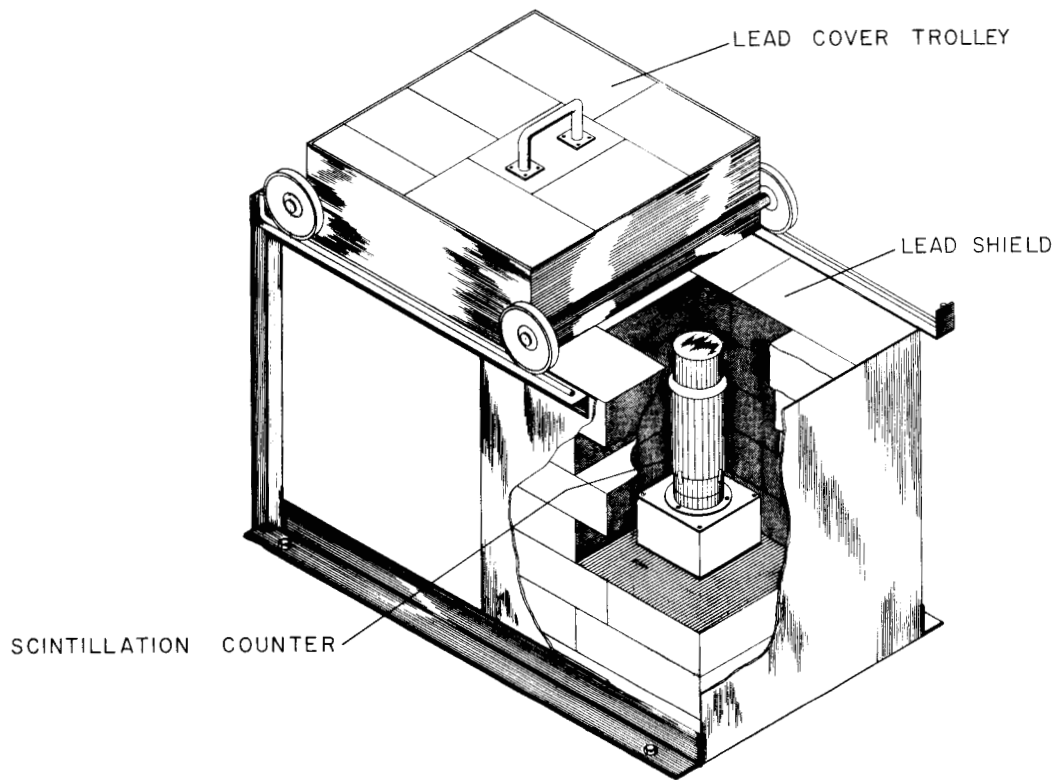
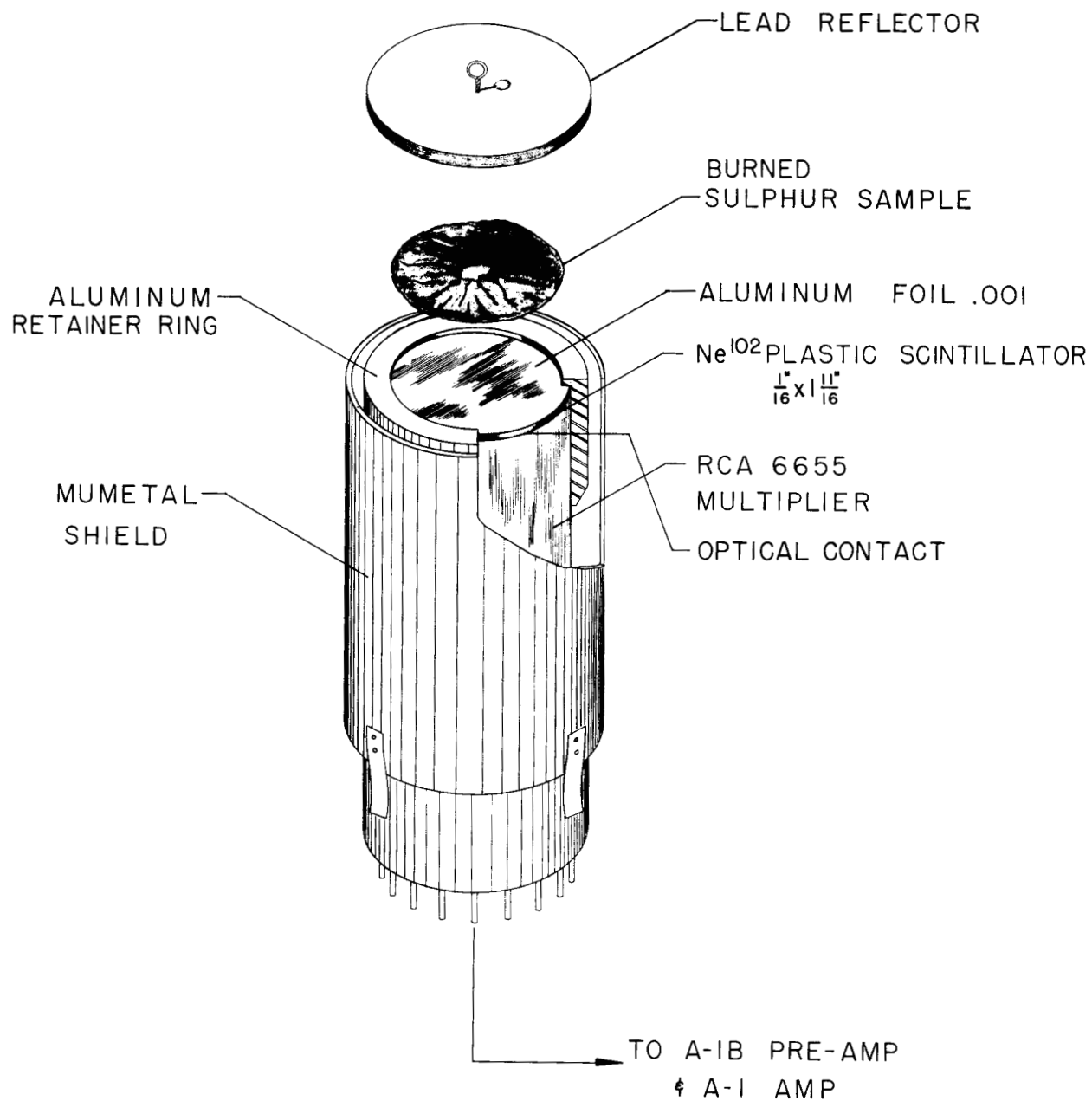


FIG. 10 SHIELD FOR SULPHUR & GOLD SCINTILLATION COUNTER



SULPHUR SCINTILLATION COUNTER  
FIG. II

with IRC type MBC 1% resistors. An additional input connector was added to the preamplifier, as shown in Fig. 12, to accommodate the dual input.

In cases where a large number of foils are to be handled, the ORNL scaler timer model Q-1743 has proven useful. The reset and count operations are controlled from a single switch; the counting time can be quickly manipulated by changing the preset count setting on the timer scaler.

The selector switch shown in the high voltage control schematic diagram, Fig. 13, permits checking the fission foil detectors separately. The resistor network maintains a constant load impedance to the high voltage supply while dropping the voltage on the undesired counter to make it inoperative while adjusting the gain on the other counter.

#### Scintillation Counter Specifications

Amplifier	Atomic 218 or equivalent
Preamplifier	Atomic 219 or equivalent
High Voltage Supply	Positive 500-1500 V, Atomic 312 or equivalent
Scaler	1 $\mu$ -sec resolution
Line Voltage	Regulated 1%
Fission Foil Scintillator	NaI 4 inch by 2 inch Harshaw type 16B8, 10 to 12% resolution
Fission Foil Photo-multiplier	DuMont 6364
Gold Foil Scintillator	NaI 1-1/2 inch by 1 inch Harshaw type 6D4, 10 to 12% resolution
Gold Foil Photomultiplier	RCA 6655
Sulfur Scintillator	1-7/8 inch by 1/16 inch Plastic Ne102, Nuclear Enterprises, Ltd.
Sulfur Photomultiplier	RCA 6655

UNCLASSIFIED  
ORNL-LR-DWG. 36570-A

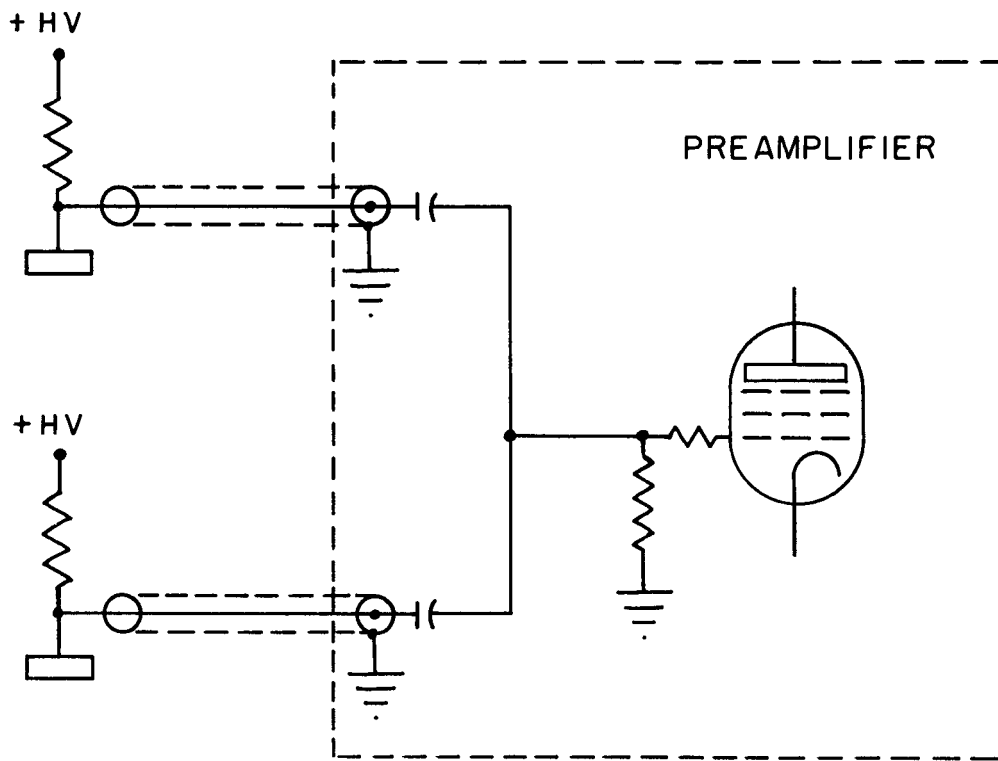


FIG. 12 PHOTOTUBE COUPLING  
FOR DUAL COUNTERS

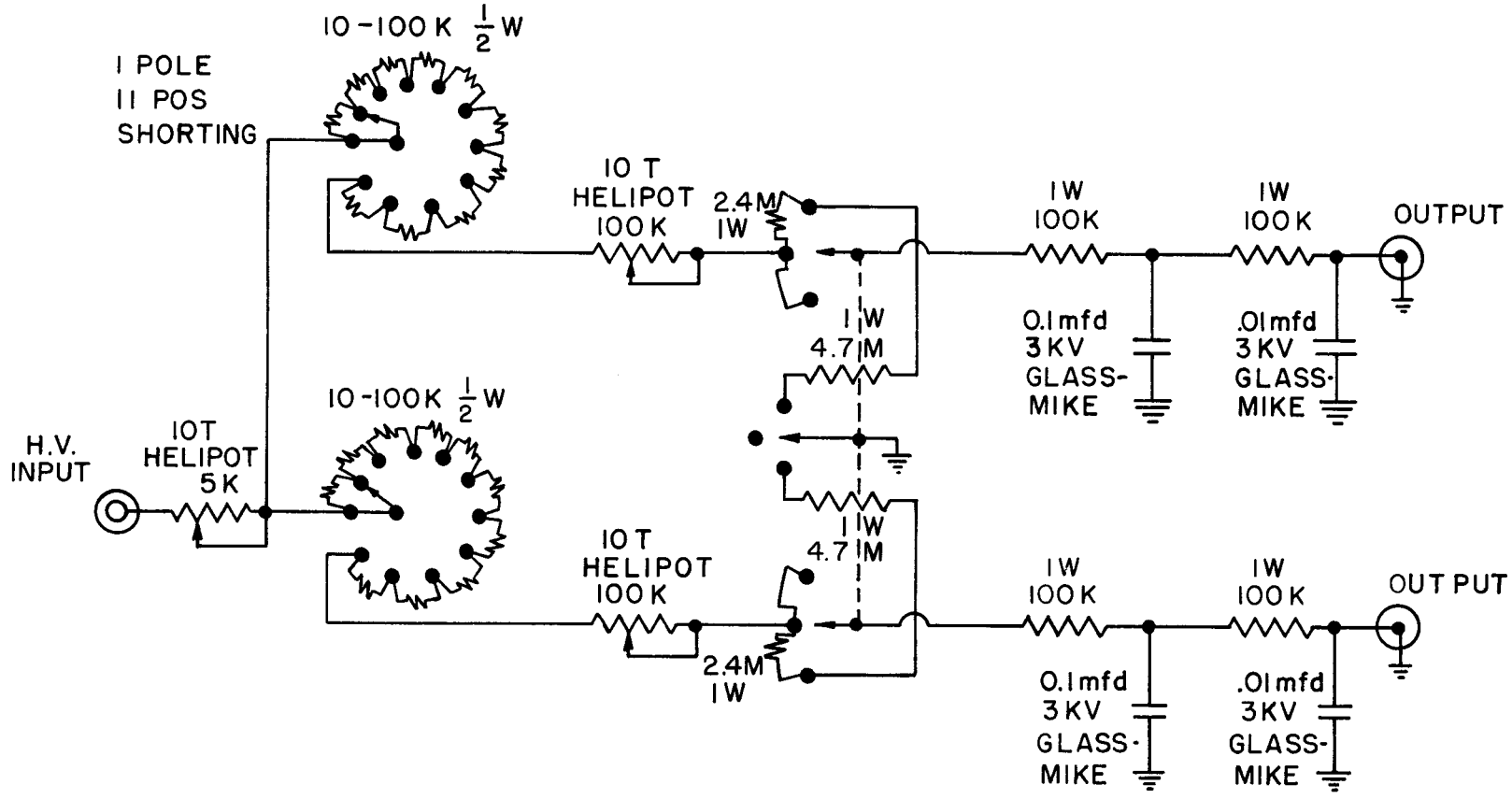


FIG.13 HIGH VOLTAGE CONTROL FOR 6364 PHOTOMULTIPLIER

The following drawings may be obtained from the U. S. Atomic Energy Commission, Technical Information Services Extension, P. O. Box E, Oak Ridge, Tennessee:

ORNL Drawings

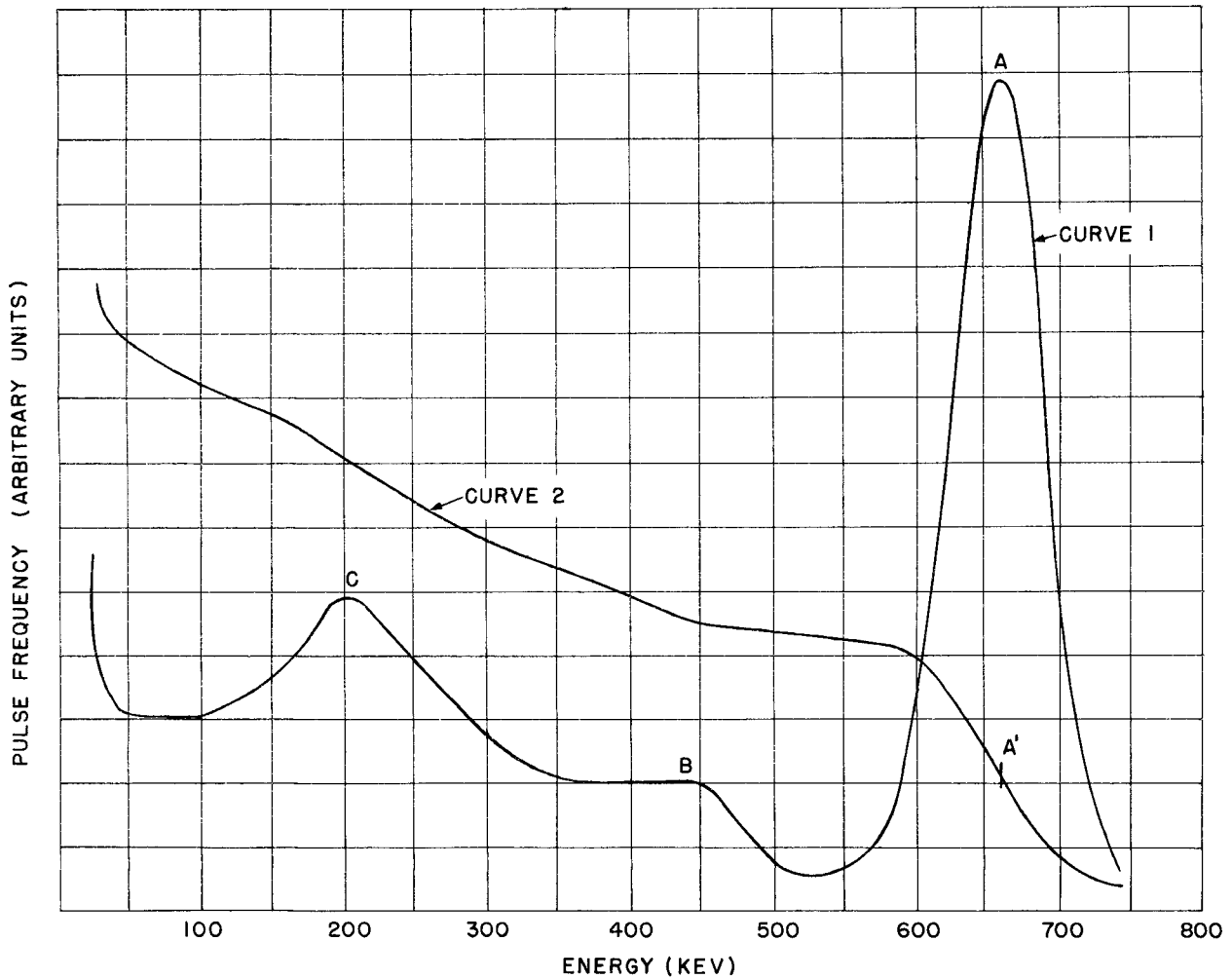
Fission Foil Detector Assembly	HPD D 701-706
Plate, slide and sample holder	HPD D 701
Upper and lower spider ring and sleeve clamp	HPD D 702
Assembly and wiring view of phototube housing	HPD D 703
Stacked and cast lead door frame for lead pig	HPD D 704
Retainer plate, liner, door, and pin details	HPD D 705
Assembly of counter, detail of lead bricks	HPD D 706
Assembly and Materials List for Sulfur and Gold Counter Shield	HPD D 707
Details of Sulfur and Gold Counter Shield	HPD D 708
Gold Counter Cs <sup>137</sup> Holder	HPD D 709
Details of Sulfur Counter	HPD 710
Details of Gold Counter	HPD 711
Sulfur Counter Standard	HPD A 712
B <sup>10</sup> Fission Foil Container	HPD C 713
Details of Sealed Fission Foil Cans	HPD A 714
Details of Np <sup>237</sup> Pressed Sealed Can	HPD A 715
Placement Container Details	HPD D 716
Details 8, 9, 13 for Sulfur and Gold Counter Shield	HPD D 717
Label for Location of Unit	HPD D 718
Photomultiplier Tube and Socket Wiring Diagram (6364 to 6655)	HPD B 719

#### 2.2.4. Operation and Calibration of the Fission Product Counters

In order to make accurate measurements with scintillation counters of the gamma activity induced in the fission foils, it is necessary to maintain a constant bias level. As previously pointed out,  $\text{Np}^{238}$  is produced by neutron capture in  $\text{Np}^{237}$ .  $\text{Np}^{238}$  emits a gamma ray of the order of 1.0 Mev and decays with a 2.1 day half life. If the  $\text{Np}^{237}$  foils are counted at a discriminator setting equivalent to 1.2 Mev the effect due to the 1.0 Mev  $\text{Np}^{238}$  gamma ray is eliminated. Rather than shift the discriminator setting for various types of fission foils, this discrimination level has been adopted for all fission foils.

$\text{Cs}^{137}$  has been found to be a suitable gamma-ray source for standardizing the system. It is a monoenergetic gamma emitter (661 kev) and has a long half life (30 years). It does, however, have the disadvantage that the discriminator setting has to be shifted from the standardization positions to the counting position. For example, with  $\text{Cs}^{137}$  standardization is accomplished by adjusting the gain so that at a discriminator setting of 33.0 volts all pulses of a height greater than those due to the total absorption of the 0.66 Mev gamma rays are accepted. For counting fission foils the discriminator is set at 60.0 volts which then corresponds to an energy of 1.2 Mev.

In order to standardize the proper count rate must be determined for the  $\text{Cs}^{137}$  source to be used with a particular system. Curve 1, Fig. 14, shows the distribution of pulse heights obtained when the crystals are irradiated with 0.66 Mev gamma rays from  $\text{Cs}^{137}$ . The peak

ORNL-LR-Dwg. 12886 -A  
UNCLASSIFIEDFIG. 14 DIFFERENTIAL AND INTEGRAL COUNT RATE vs ENERGY CURVES FOR FISSION  
FOIL COUNTERS AND  $Cs^{137}$ .

at A is due to the total absorption of gamma-ray energy due to the photoelectric effect. Curve 2 in Fig. 14 is the count rate as a function of discriminator setting and, therefore, represents the integral of Curve 1. The point A' at the point of inflection on Curve 2 then corresponds to point A at the peak of Curve 1. Curves 1 and 2 are obtained by plotting the differential and integral output versus pulse height setting from a single-channel pulse height analyzer. When plotting the differential Curve 1 the count rate is plotted against  $E + \Delta E/2$ , where E is the pulse height setting and  $\Delta E$  is the window width. Points A and A' are determined graphically and the count rate at A' is the standard count for that particular Cs<sup>137</sup> source. It is to be noted that the integral count rate in the vicinity of point A', Curve 2, Fig. 14, is quite sensitive to the gain of the counting system. With a sodium iodide crystal having only fair resolution the change in count rate with respect to gain is about 10:1, i.e. a 1% drift in gain will result in a 10% change in the integral count rate.

In the two-crystal counting system the count rate at point A' is determined separately for each crystal and averaged. Following this procedure the average count of the standard should determine the gain within 0.5% of each other.

The gamma activity induced in the foils by neutrons is measured with scintillation counters. From these data one can determine the number of fissions and thereby obtain the neutron flux that produced them. Since the induced activity is measured at some time after fission, it is necessary to correct for fission product decay. The simple power

law does not hold true for all values of  $t$ , making it difficult to calculate decay rates to a high degree of accuracy. Factors which affect the measured decay rate are the exposure time to the neutron flux, the mass of the parent atom, and the pulse height discriminator setting. Decay corrections are therefore made by comparing the count rate of a foil exposed to an unknown flux to a similar foil exposed to a known flux. It has been shown by Hurst et al.<sup>22</sup> that the decay rate for fission products is the same when the fissions are produced by either fast or thermal neutrons. Due to the availability of calibrated thermal neutron sources such as the ORNL standard pile and the Los Alamos water boiler, etc., absolute calibrations are done with thermal neutrons.

Calibration is accomplished by irradiating a thin ( $3/4''$  diameter, 0.100 g)  $\text{Pu}^{239}$  foil with a known thermal neutron flux for a period of five minutes or less and measuring the count rate as a function of time. The thermal neutron flux incident upon the foil is determined by means of small gold foils placed next to the Pu foil.<sup>23</sup> The count rate  $C_T$  due to the thermal activation is corrected to a count rate  $c(t)$  which would have been obtained from a 1 gram foil irradiated with a fast neutron flux equal to  $10^{10}$  n/cm<sup>2</sup>. The normalized count  $c(t)$  would be

$$c(t)_{\text{Pu}^{239}} = \frac{\sigma_F}{\sigma_T} \times \frac{1}{W_{\text{Pu}^{239}}} \times \frac{10^{10}}{F_T} \times C_T \quad (4)$$

where  $\sigma_T$  is the thermal fission cross section for  $\text{Pu}^{239}$ ,  $\sigma_F$  is the fast fission cross section for  $\text{Pu}^{239}$  shielded with  $\text{B}^{10}$ ,  $F_T$  is the thermal flux ( $\text{n/cm}^2$ ) to which the foil has been irradiated,  $W_{\text{Pu}^{239}}$  is the weight in grams of  $\text{Pu}^{239}$  in the calibration foil, and  $C_T$  the count rate obtained from the calibration foil. A curve is then constructed similar to the one shown as Curve A in Fig. 15 by plotting the normalized count rate,  $c(t)$ , against time.

Due to the shift in yield of fission products with the mass of the parent atom the decay curves for the  $\text{U}^{238}$  and  $\text{Np}^{237}$  activation differ from that of  $\text{Pu}^{239}$ . By assuming the perturbations in the decay curve of fission products to be proportional to the atomic mass of the parent atom, one can calculate the decay curves of  $\text{Np}^{237}$  and  $\text{U}^{238}$  from the decay curves of  $\text{Pu}^{239}$  and  $\text{U}^{235}$ . In other words, the  $c(t)$  curve for  $\text{Np}^{237}$  should fall midway between the decay curves of  $\text{Pu}^{239}$  and  $\text{U}^{235}$ .

A more convenient method of correcting for  $\text{Np}^{237}$  and  $\text{U}^{238}$  fission product decay is to calibrate with thermal neutrons the same as for  $\text{Pu}^{239}$  but using  $\text{Np}^{237}$  and  $\text{U}^{238}$  equivalent foils. These are foils made up of a mixture of  $\text{Pu}^{239}$  and  $\text{U}^{235}$  to the proper ratios where they will decay like  $\text{Np}^{237}$  and  $\text{U}^{238}$  but have the effective thermal cross section of  $\text{Pu}^{239}$ .

The amounts of  $\text{U}^{235}$  and  $\text{Pu}^{239}$  which give the same number of fissions in a given thermal flux can be easily calculated by setting the products (fission cross section times the number of atoms) of each nuclide equal to one another.

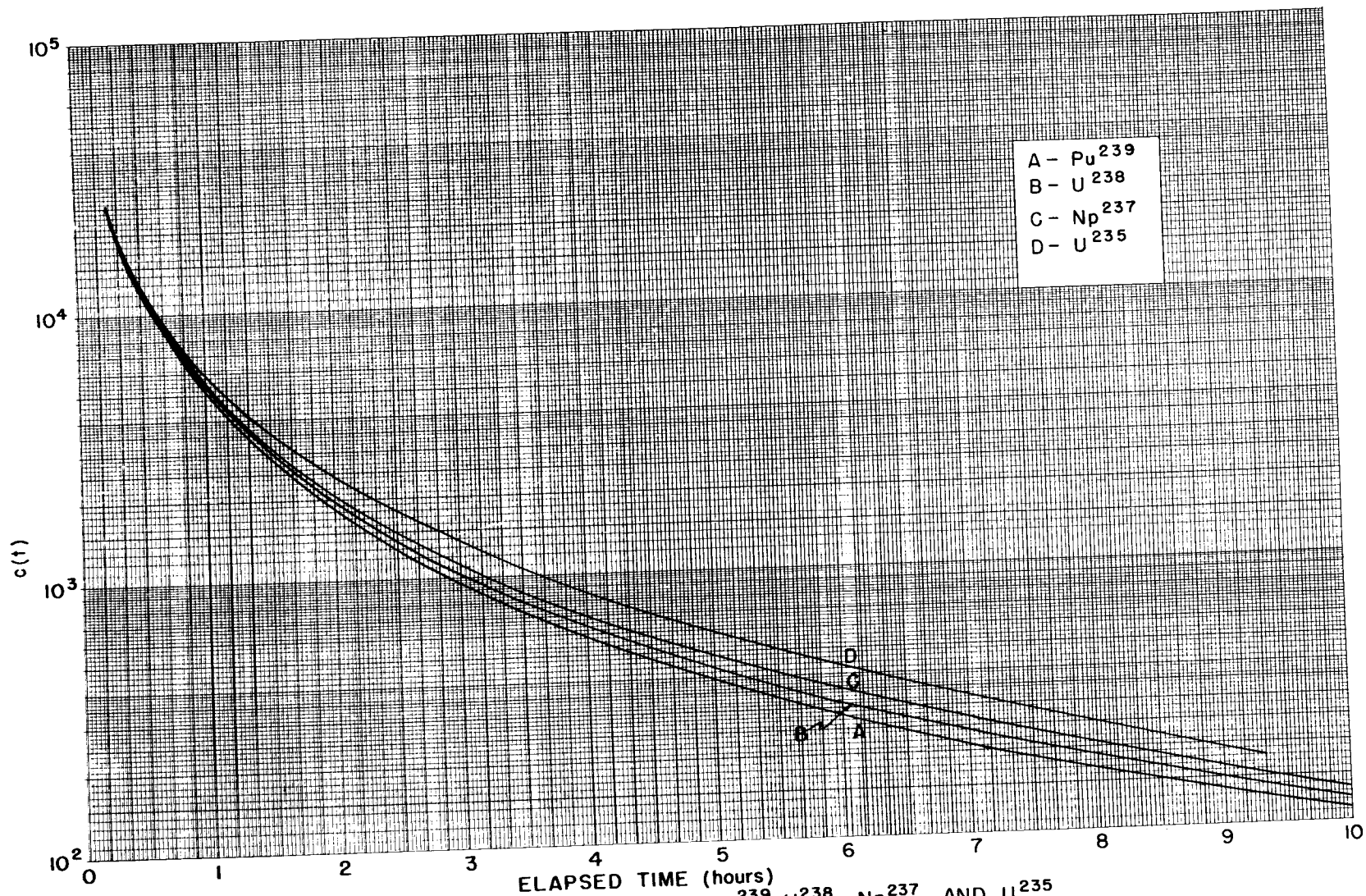


FIG. 15  $c(t)$  AS A FUNCTION OF ELAPSED TIME FOR  $\text{Pu}^{239}$ ,  $\text{U}^{238}$ ,  $\text{Np}^{237}$ , AND  $\text{U}^{235}$ .

$$\frac{\sigma_{\text{Pu}^{239}}}{239} \times W_{\text{Pu}^{239}} = \frac{\sigma_{\text{U}^{235}}}{235} W_{\text{U}^{235}}$$

$$\frac{W_{\text{U}^{235}}}{W_{\text{Pu}^{239}}} = \frac{235 \times \sigma_{\text{Pu}^{239}}}{239 \times \sigma_{\text{U}^{235}}} = \frac{235 \times 793}{239 \times 580} = 1.344$$

where  $W_{\text{U}^{235}}$  and  $W_{\text{Pu}^{239}}$  are the respective weights of  $\text{U}^{235}$  and  $\text{Pu}^{239}$  and  $\sigma_{\text{Pu}^{239}}$  and  $\sigma_{\text{U}^{235}}$  are the thermal cross sections. If one, therefore, takes 1.344 g of  $\text{U}^{235}$  and mixes with 1 g of  $\text{Pu}^{239}$ , one will have a foil which decays like  $\text{Np}^{237}$  but has the effective thermal activation of a 2 g foil of  $\text{Pu}^{239}$ . Actually, our standard  $\text{Np}^{237}$  is made up of 1/20 of these amounts so that it has the effective thermal activation of a 0.1 g  $\text{Pu}^{239}$  foil.

$\text{U}^{238}$  deviates 1/4 as much as  $\text{U}^{235}$ ; therefore, the proper mixture for a 0.100 g equivalent foil would be  $1.344/40 = 0.0336$  g of  $\text{U}^{235}$  and  $0.075$  g of  $\text{Pu}^{239}$ . In computing  $c(t)$  the weight is again considered as 0.100 g.

Curves B and C in Fig. 15 show the  $c(t)$  values for  $\text{U}^{238}$  and  $\text{Np}^{237}$ , respectively, obtained by the previous method. Curve D shown for comparison is the decay of a normalized  $\text{U}^{235}$  foil activated by thermal neutrons.

### 2.2.5. Operation and Calibration of the Sulfur Counter

The  $S^{32}(n,p)P^{32}$  reaction is used to determine the total number of neutrons having energies greater than 2.5 Mev. The reaction produces  $P^{32}$  which is a 1.71 Mev beta emitter with a half life of 14.23 days. The  $P^{32}$  betas from the 1-1/2 inch x 3/8 inch sulfur sample are counted with plastic scintillators as already described. The pulse height discriminator setting was chosen to be just sufficient to exclude photomultiplier noise. At this point the curve (count rate vs pulse height discriminator setting) has a very small slope and thus the count rate is relatively insensitive to small changes in overall gain.

$Cs^{137}$  is used to standardize the sulfur counting system. The standardization count rate is determined at the time of calibration.

The system is calibrated by irradiating a sample of  $P^{31}$  having the same dimensions as the sulfur sample, with a known number of thermal neutrons.  $P^{32}$  atoms are formed by a neutron capture reaction having a cross section of 0.19 barns. Comparison of the  $P^{32}$  cross section with the  $S^{32}(n,p)P^{32}$  cross section of 0.229 barns enables one to make a calibration for fast neutrons on sulfur.

Actual calibration and standardization is performed by irradiating a  $P^{31}$  disc 1-1/2 inches in diameter by 3/8 inch thick to  $10^{10}$  thermal neutrons. The  $P^{31}$  sample is placed in a 0.001 inch thick aluminum dish to prevent contaminating the counter. The discriminator pulse height setting is set to 5 volts and the gain adjusted to give 533 net counts per minute per  $10^{10}$  neutrons. The count rate of the  $Cs^{137}$  standard is

then determined for this discriminator pulse height setting and gain.

Quite often sulfur samples are encountered which do not have sufficient activation to give a significant count rate. It has been shown<sup>23</sup> that by burning out the sulfur in an aluminum dish the P<sup>32</sup> remains in the dish. By burning out the sulfur, the count rate of the standard 1-1/2 inch by 3/8 inch sulfur sample is increased by a factor of approximately 18. The sulfur sample is weighed and then placed in a 0.001 inch thick aluminum dish (Item 2, ORNL Dwg. HPD-C-710). The dish is placed on a hot plate and after the sulfur is melted it is ignited. A Prepo torch has been found useful in igniting the melted sulfur. The time required for a complete burn out of a 21 g sample of sulfur is approximately 45 minutes. Frequently a small amount of unburned sulfur will remain in the dish. This can be removed by applying a very "soft" flame from a torch directly to the sulfur, taking care not to burn through the thin aluminum dish. Figure 16 shows a photograph of the sulfur in various stages of the burning process. After the sulfur has been burned out, the dish is formed into a disc by folding down the sides. When counting the burned sulfur sample, a lead reflector, shown in Fig. 11, is used to increase the counting efficiency.

#### 2.2.6. Operation and Calibration of the Gold Counters

The thermal neutron flux is measured by irradiation of two gold foils, one with and one without a Cd envelope and taking the difference in their activation. Au<sup>198</sup> emits a 0.97 Mev beta followed by a 0.411 Mev gamma and has a 2.69 day half life. The gold foils may

UNCLASSIFIED  
PHOTO 46198

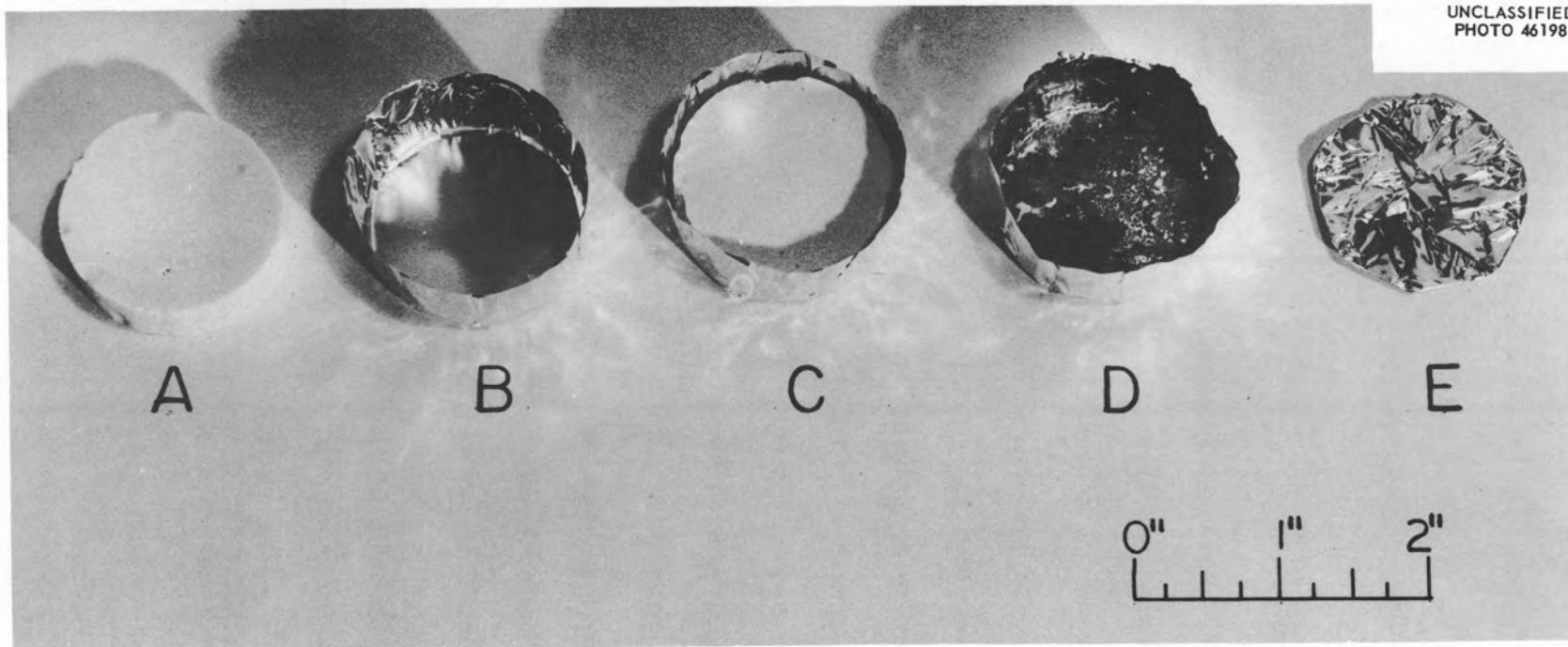


FIG. 16. PHOTOGRAPH OF SULPHUR IN VARIOUS STAGES OF BURNING PROCESS.

be counted on a 1-1/2 inch by 1 inch NaI crystal, as already described.

When counting gold with scintillation detectors, the discriminator pulse height setting is set to accept all pulses greater than those due to 0.33 Mev gammas.  $\text{Cs}^{137}$  is used as a standard and the standardization count rate is determined in the same manner as described for the fission foil system. The standard is mounted in a holder in order to provide reproducible geometry each time the standard is used.

#### 2.2.7. Placement of Threshold Detector Stations

Figure 17 shows a threshold detector container. All fission foils, before loading in the container, should have their background measured on the counting system. Their backgrounds should be recorded in a log book along with their weights and other sample factors. A placement chart which is useful in keeping a record of the threshold detector foils and their locations is shown in Fig. 18.

#### 2.2.8. Counting Techniques

The counting rate of fission products falls off rapidly with the elapsed time since exposure; therefore, it is of utmost importance that the fission foils are recovered and counted as soon as possible after irradiation. The foils should be removed from the exposure container at a pre-arranged location and only the threshold detector foils should be brought to the counting room.

Due to their size (approximately 0.1 g),  $\text{Np}^{237}$  foils are lowest in induced activity and are counted first, followed by  $\text{U}^{238}$  and  $\text{Pu}^{239}$ .

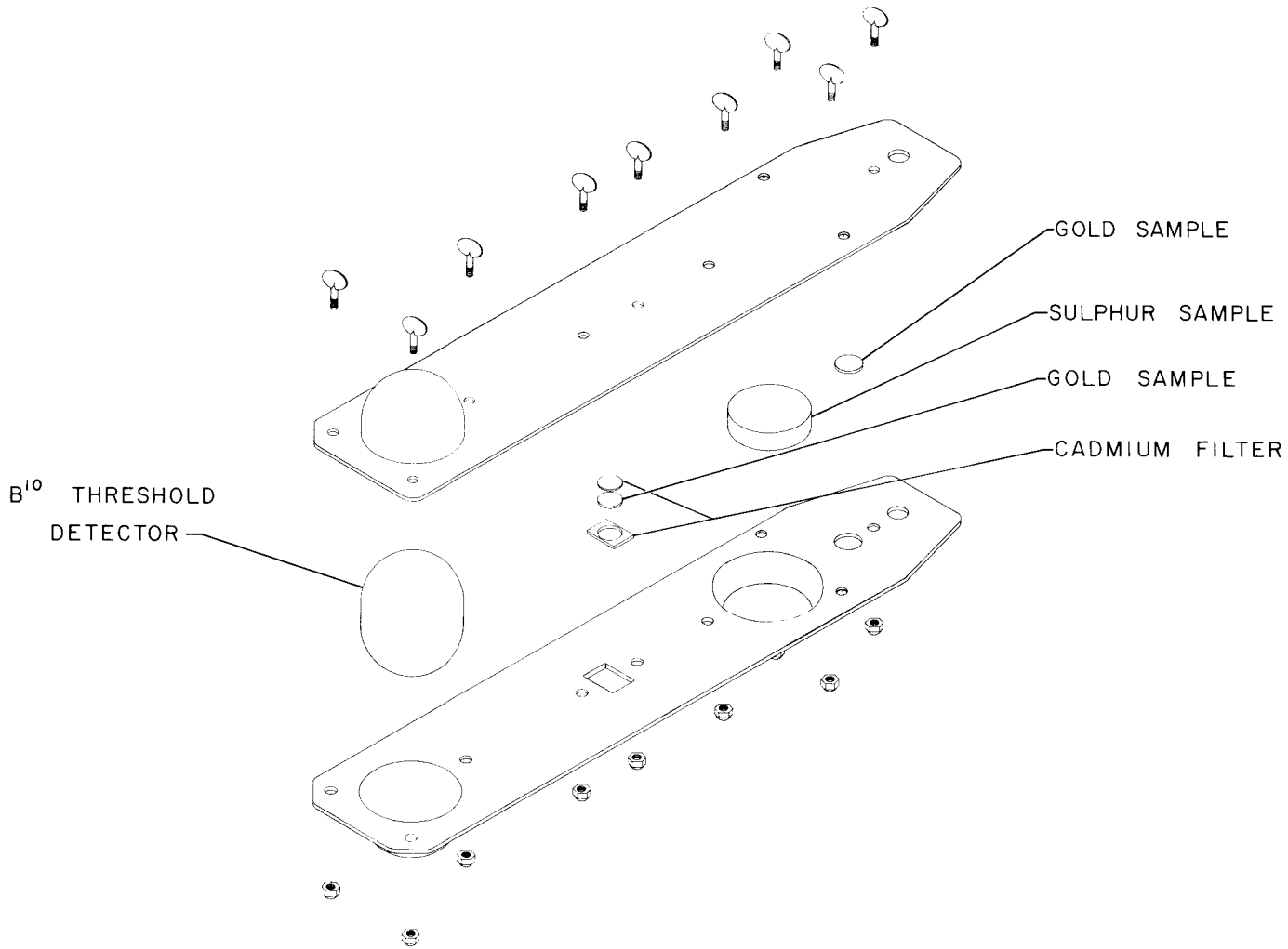


FIG. 17  
THRESHOLD DETECTOR PLACEMENT CONTAINER



Once all of the foils have been counted, several repeat counts should be taken.

Upon completion of fission foil counting, the fission foil detector is disconnected and the gold counter is connected into the system. After the pulse height setting is standardized the gold foils are counted.

Next, the sulfur detector is exchanged with the gold detector and the pulse height setting is again standardized. To avoid contamination of the counter the sulfur discs are placed in the 0.001 inch aluminum burning dishes for counting. If a significant count rate is not obtained, the sulfur discs are then weighed and burned before counting again.

During the first hour or so after irradiation, selenium impurities in the sulfur may contribute selenium activation products causing the count rate to be 10 to 20% too high.

A typical data sheet which is convenient for both recording data and computing flux is shown in Figs. 19 and 19a. A summary sheet which is useful in computing dose is shown in Fig. 20.

#### 2.2.9. Flux Calculation

##### Fission foil flux calculation

As previously pointed out, fission foil fluxes are determined by comparing the foil activations to activation of a foil exposed to a known flux. From Eq. (4) we obtain the normalized count rate  $c(t)$  which is equivalent to the count rate that would be obtained







from a 1 g  $\text{Pu}^{239}$  foil exposed to  $10^{10}$  fast neutrons. The flux (neutrons/cm<sup>2</sup>) for a given count rate of a 1 g foil exposed to an unknown flux would be

$$\text{flux} = \frac{C}{c(t)} \times 10^{10} \quad (5)$$

where  $C$  is the net count rate and the value for  $c(t)$  is taken from Curve A in Fig. 15, corresponding to the elapsed time at which the count rate for the unknown foil was taken.

Since most samples vary in their weight, a sample factor,  $S_f$ , must be applied to Eq. (5).

$$\text{flux}_{\text{Pu}} = \frac{C \times S_f}{c(t)} \times 10^{10} \quad (6)$$

where

$$S_f = \frac{1}{W_{\text{Pu}^{239}}} \quad (7)$$

Fluxes for  $\text{Np}^{237}$  and  $\text{U}^{238}$  are computed using the same general equation as Eq. (6).

$$\text{flux}_{\text{Np}^{237}} = \frac{C \times S_f}{c(t)} \times 10^{10} \quad (8)$$

where  $c(t)_{Np^{237}}$  is the value read from the  $c(t)_{Np}$  curve (Curve C, Fig. 15) corresponding to a time equal to the elapsed time since exposure of the Np foil being measured, but the sample factor now includes the corrections for cross section,

$$S_{f_{Np^{237}}} = \frac{\sigma_{Pu^{239}}}{\sigma_{Np^{237}}} \times \frac{1}{W_{Np^{237}}} = \frac{2}{1.6} \times \frac{1}{W_{Np^{237}}} \quad (9)$$

where  $\sigma_{Pu^{239}}$  and  $\sigma_{Np^{237}}$  are the fast cross sections for  $Pu^{239}$  and  $Np^{237}$ .

The uranium flux is computed similarly:

$$\text{flux}_{U^{238}} = \frac{C \times S_{f_{U^{238}}}}{c(t)_{U^{238}}} \times 10^{10} \quad (10)$$

where

$$S_{f_{U^{238}}} = \frac{\sigma_{Pu^{239}}}{\sigma_{U^{238}}} \times \frac{1}{W_{U^{238}}} = \frac{2}{0.55} \times \frac{1}{W_{U^{238}}} \quad (11)$$

and  $\sigma_{U^{238}}$  is the fast cross section for  $U^{238}$ .

Figure 21 shows flux correction factors to be used when the foils are exposed for times longer than five minutes. The elapsed

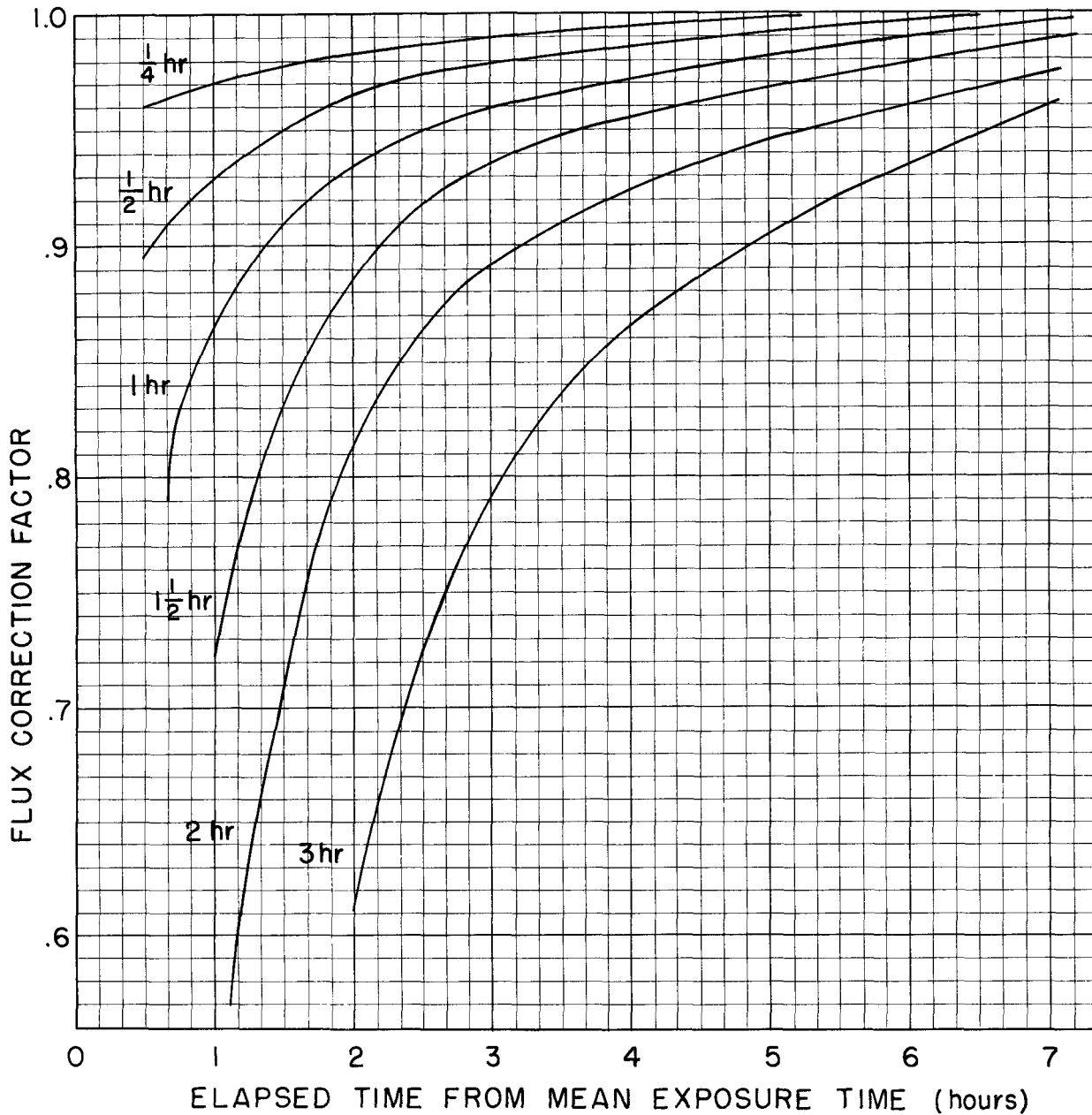
UNCLASSIFIED  
ORNL-LR-DWG. 38936

FIG. 21 FLUX CORRECTION FACTORS FOR VARIOUS EXPOSURE TIMES

time is taken as the time elapsed from the mean of the exposure time.

#### Sulfur flux calculation

The sulfur flux is given by

$$\text{flux}_{S^{32}} = \frac{1.29 \times C}{e^{-\lambda t}} \times 10^7 \quad (12)$$

where  $\lambda$  for  $P^{32}$  is  $2.03 \times 10^{-3}/\text{hr}$ ,  $C$  is in counts per minute obtained for the sulfur sample and counter geometry previously described, and  $t$  is recorded in hours. For a burned-out sample, the flux becomes

$$\text{flux} = 1.33 \times \frac{C}{W_S e^{-\lambda t}} \times 10^7 \quad (13)$$

where  $W_S$  is the weight in grams of the sulfur sample.

#### Thermal flux calculation

The thermal flux is given by

$$F_T = \left( \frac{C_{Au}}{W_{Au}} - \frac{C_{Au Cd}}{W_{Au Cd}} \right) \frac{0.303}{e^{-\lambda t}} \times 10^6 \quad (14)$$

where  $\lambda$  for Au is  $1.07 \times 10^{-2}/\text{hr}$ ,  $C_{Au}$  and  $C_{Au Cd}$  are the counts per minute of the bare and Cd shielded Au,  $W_{Au}$  and  $W_{Au Cd}$  are the weights of the two gold foils and  $t$  is measured in hours.

#### 2.2.10. Sensitivity of Various Threshold Detectors

The sensitivity of the various threshold detectors is shown in Table VI. The counter background and the sample background are shown in columns 2 and 3, respectively. The net number of counts at one hour after exposure to  $10^{10}$  n/cm<sup>2</sup> above the threshold of each particular element is shown in column 4. The last column shows the net count rate produced for a 10 rad Godiva exposure.

Table VI  
Sensitivity and Background of the Various Foils

Type of Foil	Background		Exposure	
	Counter (c/m)	Foil (c/m)	$10^{10}$ n/cm <sup>2</sup> Above Threshold (c/m/g)*	10 rads of Godiva Neutrons (c/m/g)*
Au	50	0	33,700	
Pu	280	970	5,260	<del>1,900</del> 2325
Np	280	0	4,470	<del>1,440</del> 1265
U	280	80	1,440	<del>2,520</del> 215
S "burned"	22	0	750	54

\* 1 hour after exposure

## 2.3. Blood Sodium Techniques

### 2.3.1. Introduction

As mentioned in 2.1 an analysis of  $\text{Na}^{24}$  activity in the blood, together with information on the neutron spectrum obtained with threshold detectors as described in 2.2, leads to a determination of neutron dose received by the individual. In this section the method of  $\text{Na}^{24}$  analysis will be described.

### 2.3.2. Preparation of Blood Samples

Blood samples should be taken from the exposed individuals as soon as possible after exposure, in particular before new sodium is given to the individual through food or medical treatments. The amount of blood required for  $\text{Na}^{24}$  measurements depends on the neutron dose. If it is believed that the dose is more than 100 rads of neutrons, the amount required is only about 10 cc of blood serum; if the dose is less than 10 rads, 100 cc should be taken. It is convenient to count just the blood serum which may be removed from whole blood by first allowing the blood to clot, then centrifugation. After separation the serum is prepared for counting by placing the measured volume into a standard polystyrene box. It is recommended that the total sodium content per cc of serum be determined for each individual. Most clinics are equipped with flame photometers suitable for this purpose.

### 2.3.3. Blood $\text{Na}^{24}$ Counting

The fission foil scintillation counter shown in Figs. 6

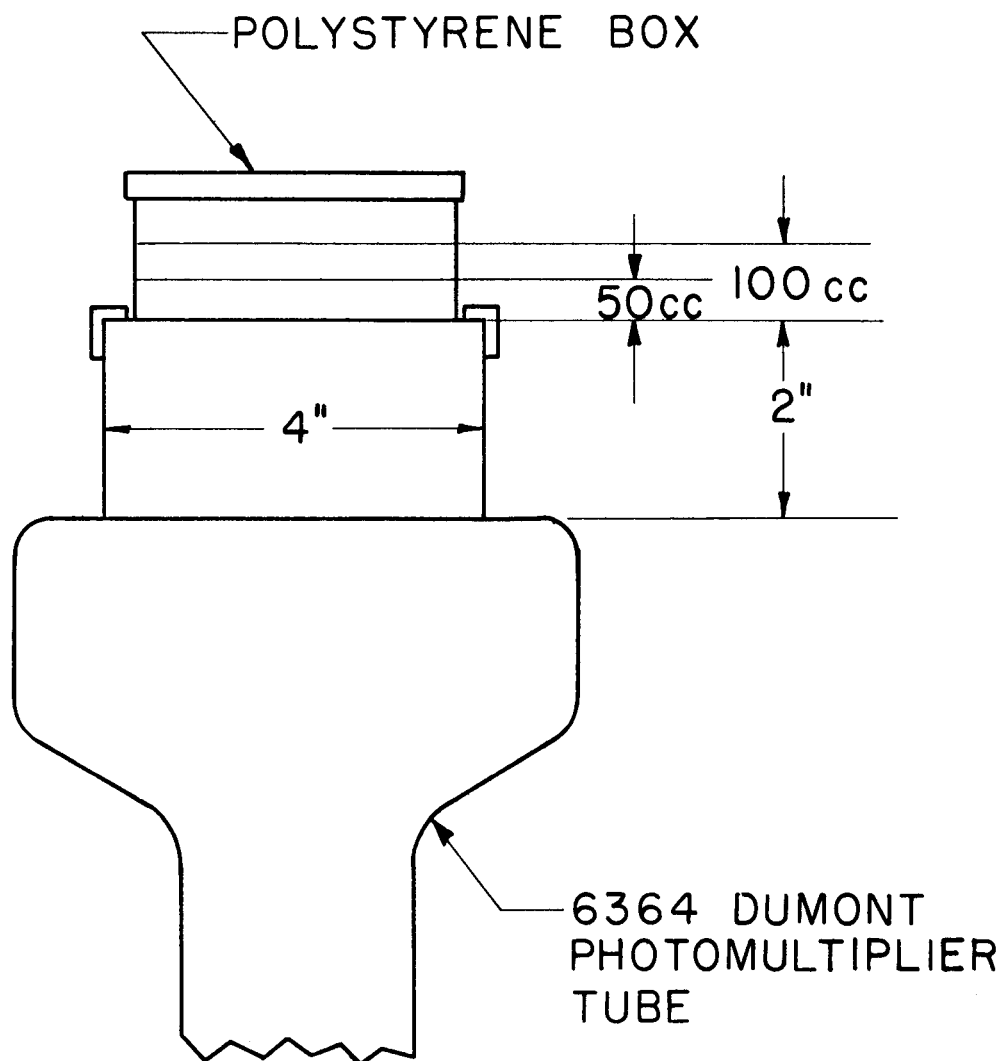
and 7 may be converted easily to a blood  $\text{Na}^{24}$  counter by removing the upper photomultiplier crystal assembly together with the lead filter. Blood samples placed in the polystyrene boxes may now be admitted through the large side door on the lead shield. After doing this the counting arrangement will be as shown in Fig. 22. Under these conditions the counting geometry  $G$  in fractions of  $\text{Na}^{24}$  disintegrations counted is given in Fig. 23, assuming integral pulse height settings of 2.0 Mev and 2.5 Mev. The curves show  $G$  as a function of volume of blood serum in the polystyrene box. If the sample is counted at less than four hours after the exposure, the counter bias should be set at 2.5 Mev so that  $\text{Cl}^{38}$  gamma rays will not be counted.<sup>25</sup>

For planning purposes one may assume that in the case of fission neutrons the number of disintegrations of  $\text{Na}^{24}$  per second and per cc of blood serum is equal to the neutron dose in rads divided by five. Thus a 50 cc sample of blood serum gives a count rate of about 0.7 counts per second per rad compared to a typical background rate of 1.5 counts per second at the 2.0 Mev bias.

---

25 Strictly speaking,  $\text{Cl}^{38}$  (half-life, 37.5 min) may be found at very early counting times. This presents no difficulty since the half-life of  $\text{Na}^{24}$  is 15 hours.

UNCLASSIFIED  
ORNL-LR-DWG. 36216-A



BLOOD COUNTING TECHNIQUES

FIG. 22

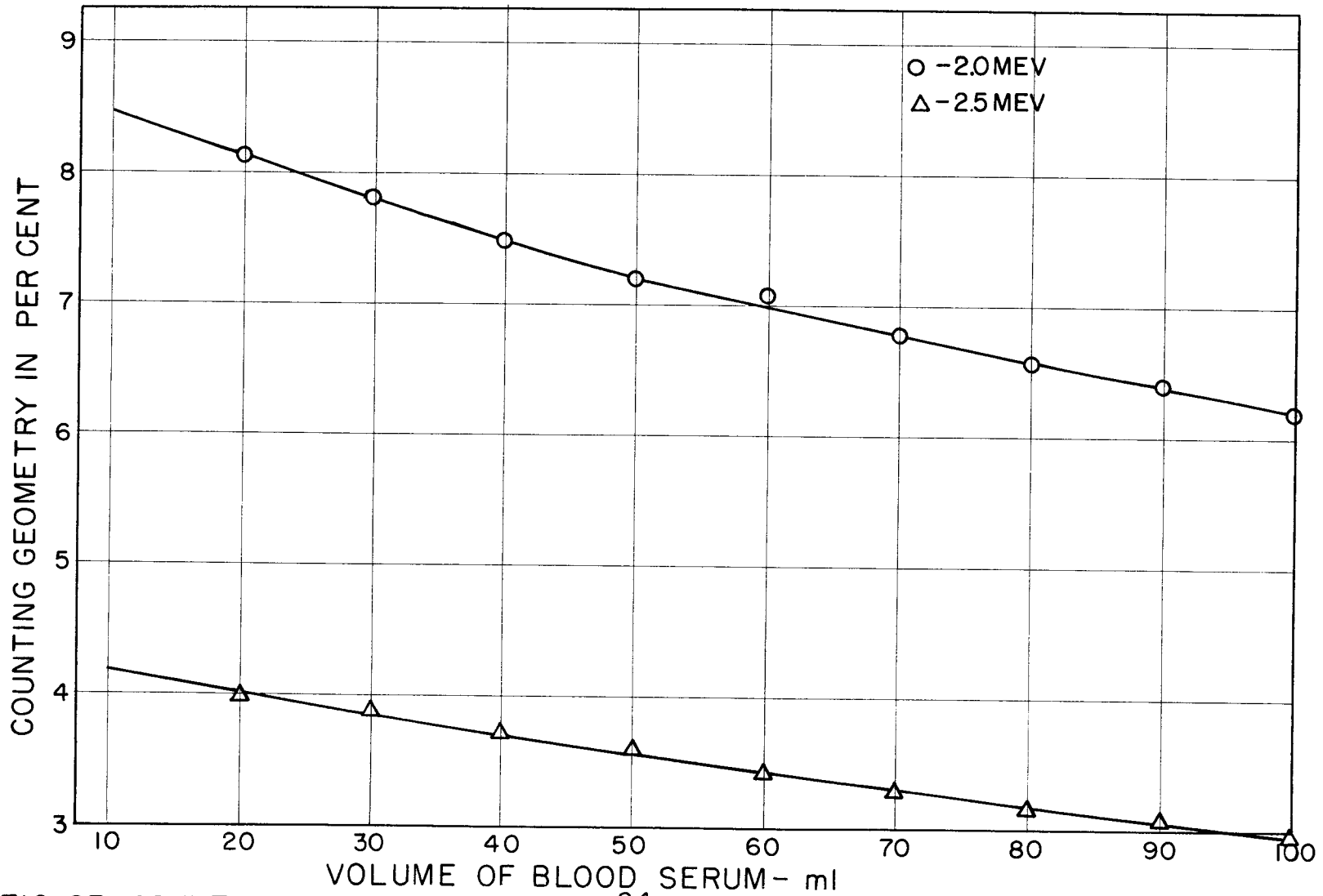


FIG. 23 COUNTING GEOMETRY FOR  $\text{Na}^{24}$  IN VARIOUS VOLUMES OF BLOOD SERUM

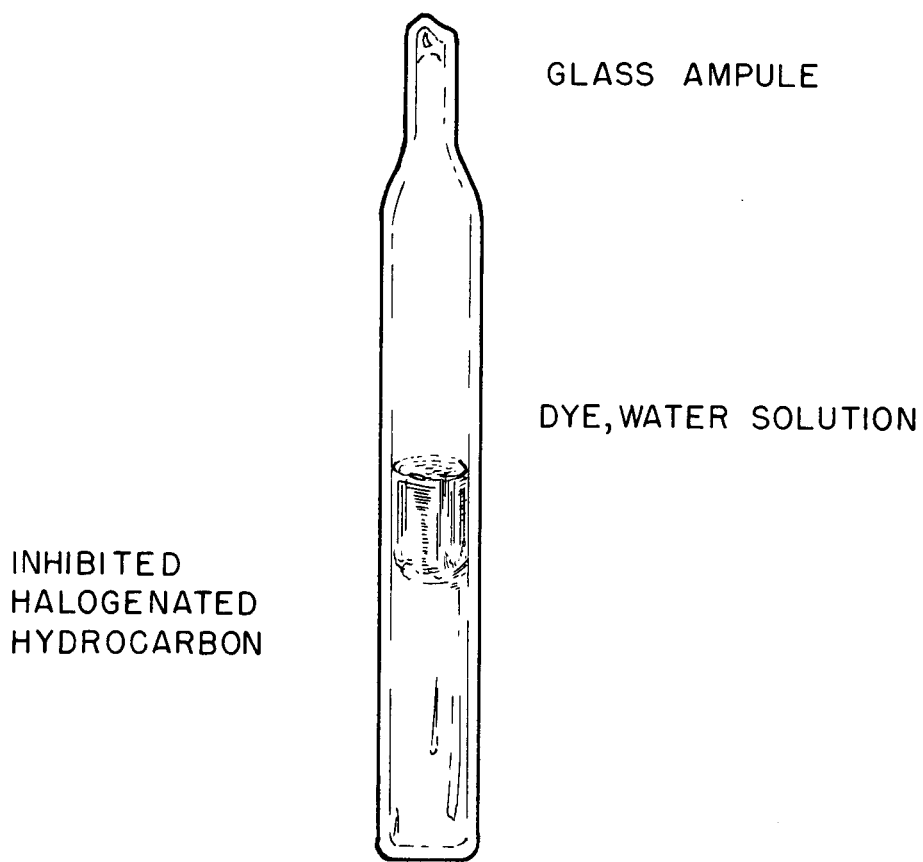
## 2.4. Gamma Dosimetry with Chemical Techniques

### 2.4.1. Introduction

Chemical dosimeter systems generally applicable for the dose range of approximately 5 rads to  $2 \times 10^6$  rads may be used to measure the gamma component in a mixed radiation field. The chemical system as utilized for gamma dosimetry consists of tetrachloroethylene which contains a small amount of free radical chain reaction retarder, overlaid with an aqueous phase containing a pH indicator, Fig. 24. Chemical chain reactions induced by radiation liberate water soluble acids. The amount of acid formed is directly proportional to dose, within a given range. The response may be evaluated by titration of the acid produced by change in conductivity of the solution or by change in pH as measured electrometrically or colorimetrically.

### 2.4.2. Radiation Characteristics

Tetrachloroethylene, when irradiated in a two-phase aqueous system or when irradiated with a soluble pH indicator dye, liberates acidic products. The acid yields are high ( $G_H \pm$  up to 6000), suggesting that a chain mechanism is operative. Chain reactions, although highly sensitive, are often influenced by dose rate, temperature and the presence of impurities. These complicating factors, undesirable in chemical dosimetry, can be made unimportant by the addition of stabilizing agents such as ethyl alcohol, resorcinol and ionol. Although the sensitivity to radiation is thereby greatly reduced ( $G$  value approximately 30), the use of stabilizers has made it



CHEMICAL DOSIMETRY NOMENCLATURE  
TCE DOSIMETER

FIG. 24

possible to produce TCE dosimeters which can register doses in the range 5 rads to  $2 \times 10^6$  rads and which show excellent reproducibility.

The response of this system to fast and thermal neutrons has been adequately investigated. The TCE two-phase system produces approximately 3 to 4% as much acid from a rad of neutrons as is produced by a rad of gamma radiation. The TCE system, because of the lack of hydrogen, absorbs a relatively low amount of energy from the fast neutron portion of a mixed radiation field. When exposed in a lithium shield system, the TCE system will provide relatively accurate values of gamma dose in the presence of fast and thermal neutrons.

The chemical dosimeter designed for the dosimeter stations used in the nuclear accident dosimetry program is housed in a lithium container (Fig. 25). The energy dependence of the chemical dosimeter inside the container is shown in Fig. 26. The dosimeter is electronically evaluated over a range from 15 rads to 30,000 rads, and has the following radiation characteristics:

Rate independence -----	rate independent $\pm 8\%$ to $10^{12}$ rads/hr
Temperature -----	temp. independent $\pm 5\%$ from $5^\circ\text{C}$ to $55^\circ\text{C}$
Energy -----	energy independent $\pm 8\%$ from 90 kev to 10 Mev
Dose linearity -----	linearity of response to $2 \times 10^6$ rads
Shelf life -----	greater than 9 months

UNCLASSIFIED  
ORNL-LR-DWG. 42577

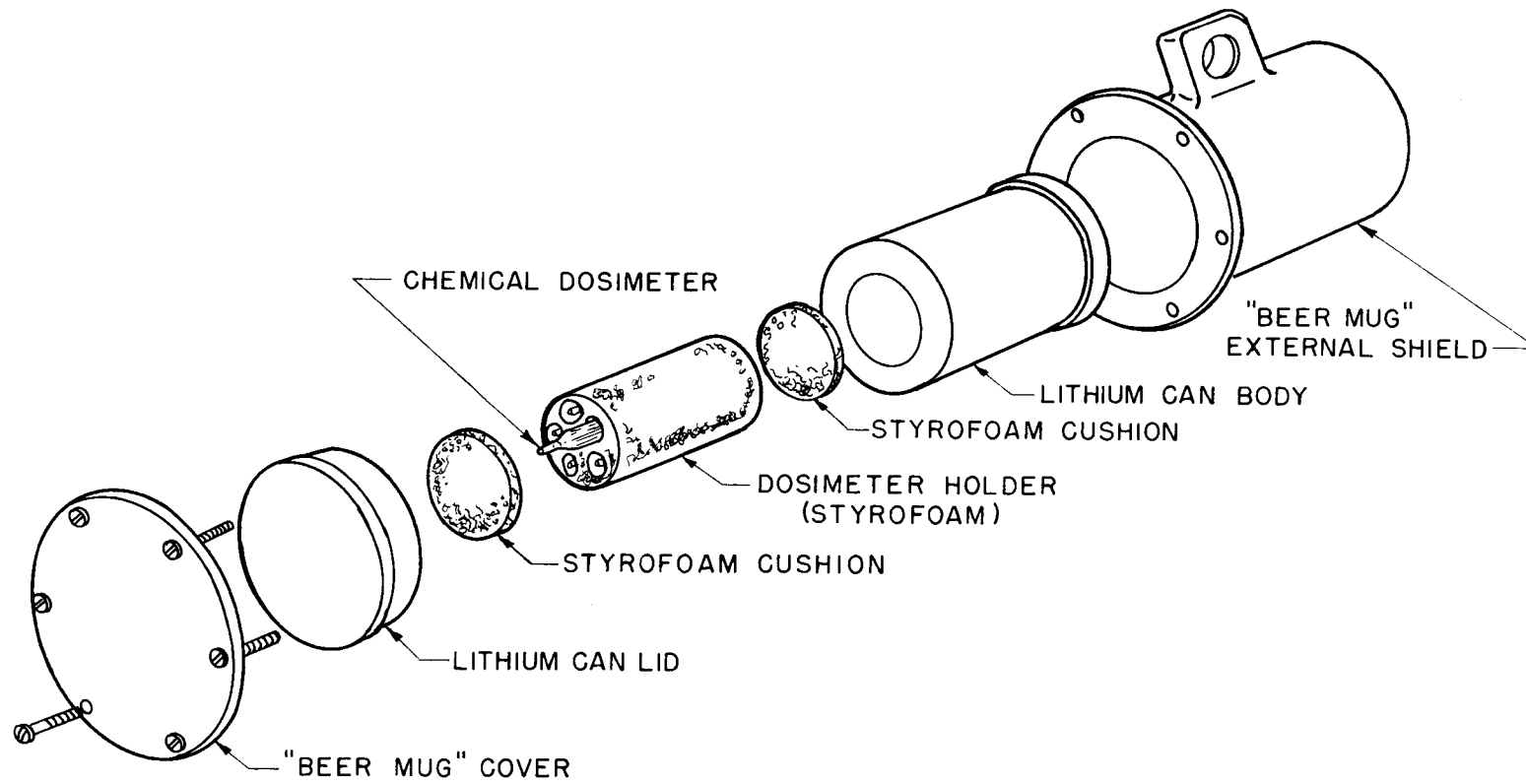


FIG. 25 CHEMICAL DOSIMETER WITH Li, Sn SHIELD

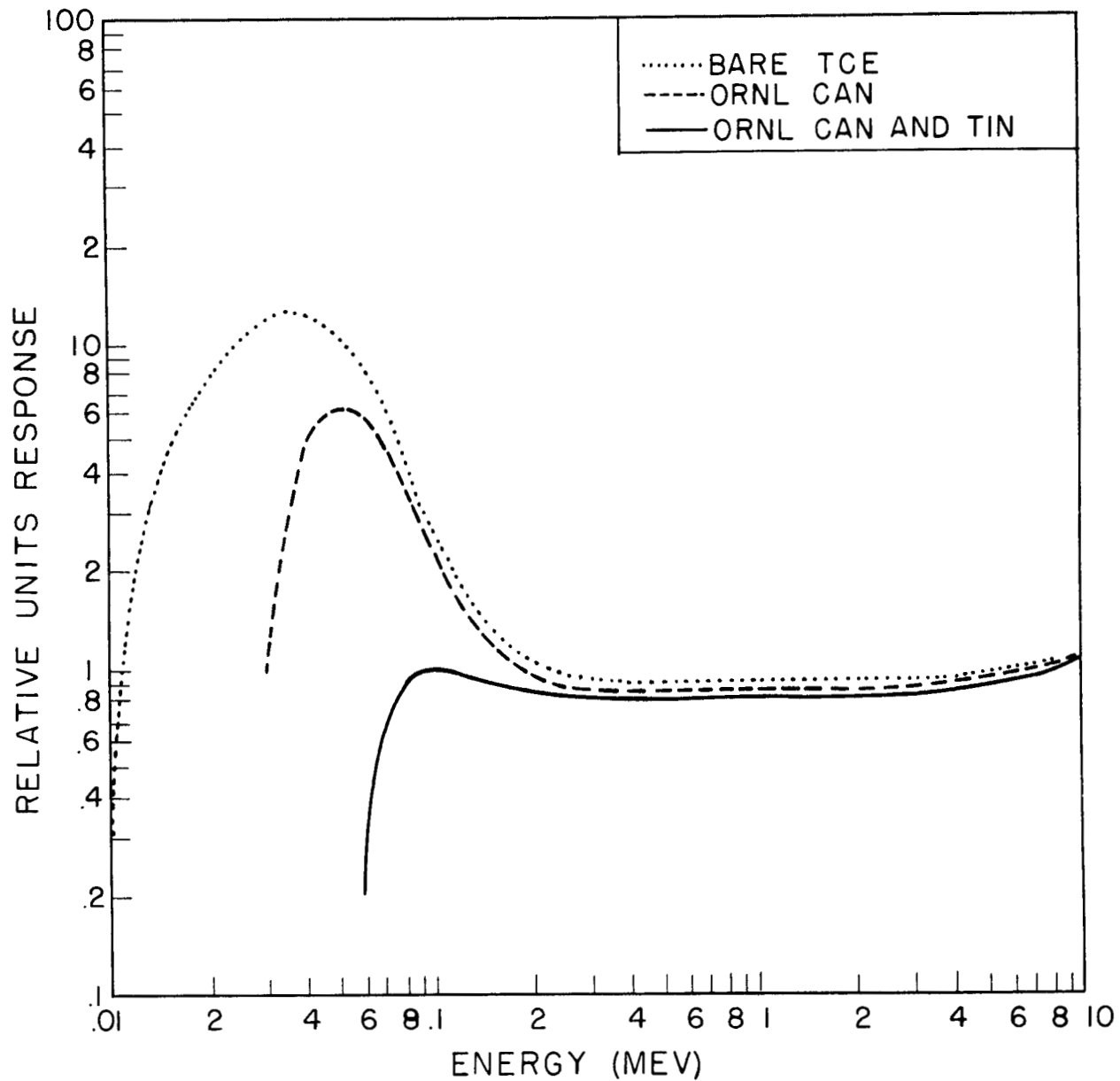
UNCLASSIFIED  
ORNL-LR-DWG. 42578

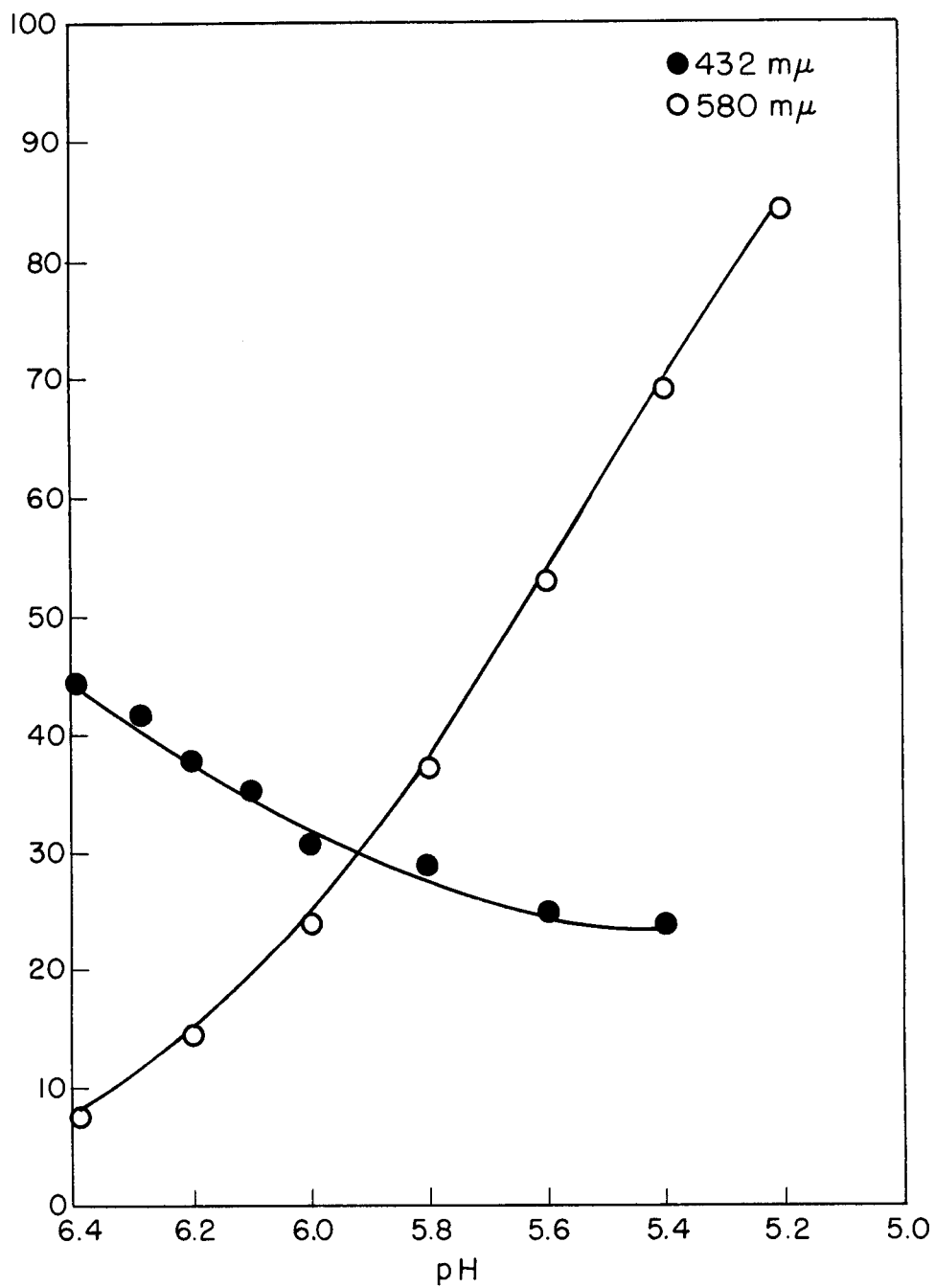
FIG. 26 ENERGY DEPENDENCE OF CHEMICAL DOSIMETER

### 2.4.3. Spectrophotometric Measurements of pH Changes in Chlor Phenol Red Indicator

Chlor Phenol Red, as used in the tetrachloroethylene two-phase dosimeter system, has two peak absorption bands, 580 m $\mu$  and 432 m $\mu$ . As the pH of the dye is reduced from 6.0 to 5.0 (red to yellow), the percentage transmission at 580 m $\mu$  increases while the percentage transmission at 432 m $\mu$  decreases (Fig. 27). The precise evaluation of the pH from the ratio of the percentage transmission at these two peaks is accurate only if the dye concentration, tube size, light source, glass thickness, temperature effects, buffering action, and impurities are controlled and relatively constant.

### 2.4.4. Evaluation

Utilizing a ratio recording, two band, absorption filter colorimeter, it is possible to evaluate easily and accurately the above-mentioned ratio. A special ampoule holder is required to view only the center section of the dye system through a 0.070 inch hole. This hole size was chosen to give minimum glass curvature aberration and an area large enough to reduce the effect of field spots and scratches. The ampoules are height and area positioned by hand. Allowing for changes in glass wall thickness, inside diameter and aberrations of the non-precision ampoules used, reproducibility can be as great as  $\pm 3\%$  with reasonable economy. Ampoules are centrifuged to 5000 rpm prior to readout to remove hydrocarbon droplets from the dye area in the two-phase system.



% TRANSMISSION AT 580 mμ AND  
432 mμ AS A FUNCTION OF pH

FIG. 27

#### 2.4.5. Determination of Exposure Dosage

Dosimeters are produced at a chosen pH value and in the required sensitivities. They are then aged for possible alkali leaching, and color selected for uniformity.

Before exposure, the dosimeters are evaluated for their pre-exposure ratio ( $\%T_{580 \text{ m}\mu} / \%T_{432 \text{ m}\mu}$ ). Dosimeters are then given known dose exposures and spectrophotometrically evaluated for their post-exposure ratio ( $\%T_{580 \text{ m}\mu} / \%T_{432 \text{ m}\mu}$ ). A curve of delta-ratio-units change (post-exposure minus pre-exposure ratio) versus dose is drawn (Fig. 28). Once this curve is drawn, one can convert delta-ratio-units change directly to dose for one specific range of dosimeters. All the dosimeters must start at the bottom of the straight portion of the ratio versus dose curve if linearity is to result. If accidental over-exposure results, the dosimeters are not lost but can be evaluated by titration. If a dosimeter is not exposed to its limit, it can be exposed again provided its total integrated dose range is not exceeded.

#### 2.4.6. Shelf Life

The recommended disposition of chemical dosimeters in the lithium can is:

No. of Chemical Ampoules	Dose Range (rad)
1	25 - 200
2	100 - 800
1	400 - 1600
1	1000 - 30,000

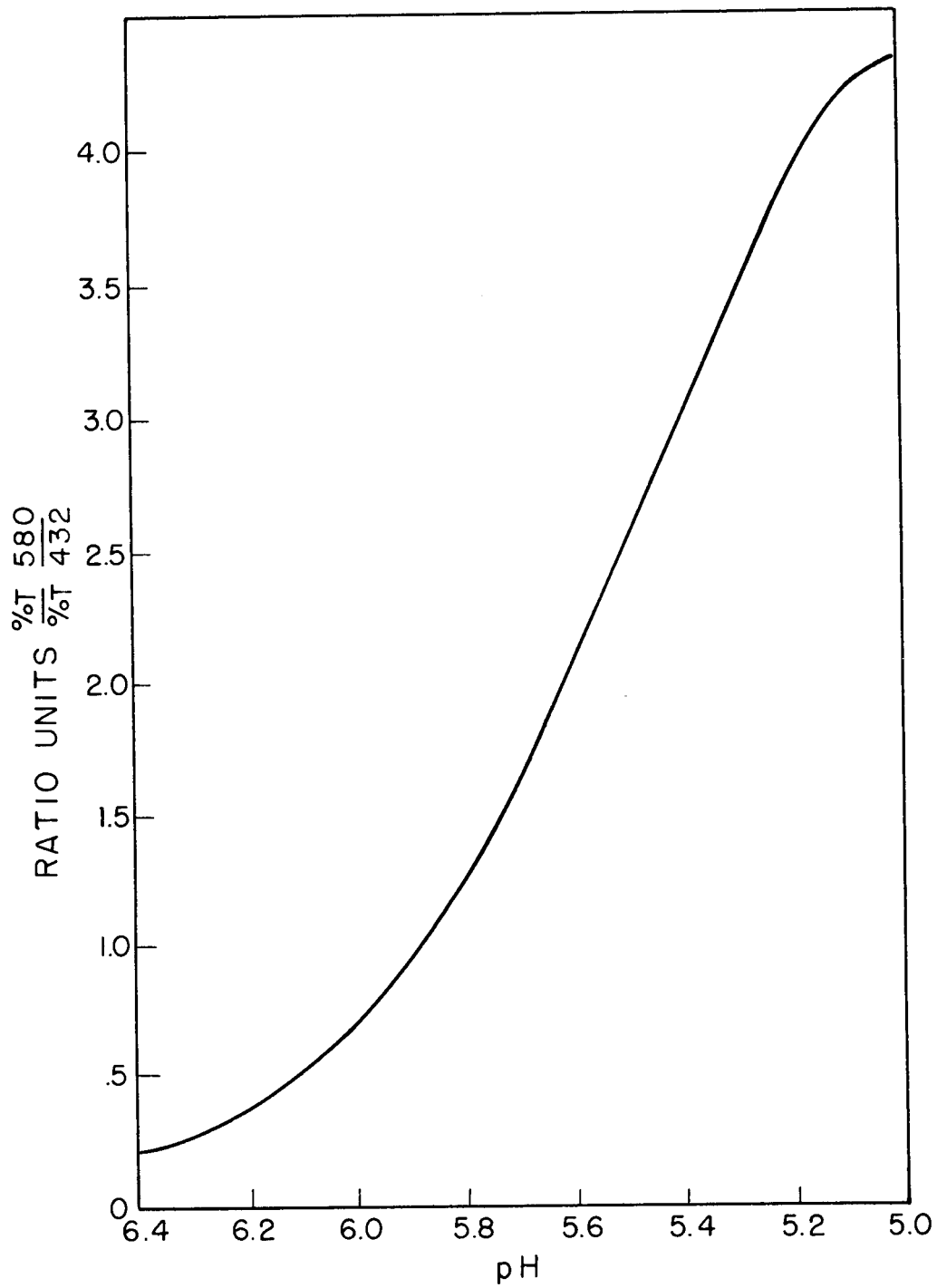


FIG. 28 RELATIONSHIP OF RATIO  $\frac{\%T_{580}}{\%T_{432}}$  vs pH

All these except the lowest range (25 - 200 rad) are stable indefinitely. The lowest range may show appreciable deterioration in nine to twelve months, and for this reason the chemicals should be inspected and possibly replaced every nine months.

## 2.5. Glass Dosimetry

### 2.5.1. General

Metaphosphate glasses containing silver may be used to measure gamma radiation dose in the range of five to several thousand rad. The glass, in the form of small glass rods (1 mm diameter by 6 mm long), Fig. 29, and a convenient reader, Figs. 30 and 31, are commercially available.<sup>26</sup>

Many of the properties of the system have been reported by Schulman<sup>27,28</sup> and others.<sup>29-31</sup> The composition of the glass, by weight, is 46%  $\text{Al}(\text{PO}_3)_3$ , 23%  $\text{Ba}(\text{PO}_3)_2$ , 23%  $\text{KPO}_3$ , and 8%  $\text{AgPO}_3$ . When the glass is exposed to ionizing radiation, loosely bound electrons

---

26 Bausch and Lomb Optical Co., Rochester, N. Y.

27 J. H. Schulman, R. J. Ginther, and C. C. Klick, J. Appl. Phys. 22, 1479 (1951).

28 J. H. Schulman and H. W. Etzel, Science 118, 184 (1953).

29 N. J. Kreidl and G. E. Blair, Nucleonics 14, No. 3, 82 (1956).

30 H. W. Etzel, R. D. Kirk, and J. H. Schulman, Ra-Det 8, No. 2, 49 (1955).

31 A. L. Riegert, H. E. Johns, and J. W. T. Spinks, Nucleonics 14, No. 11, 134 (1956).

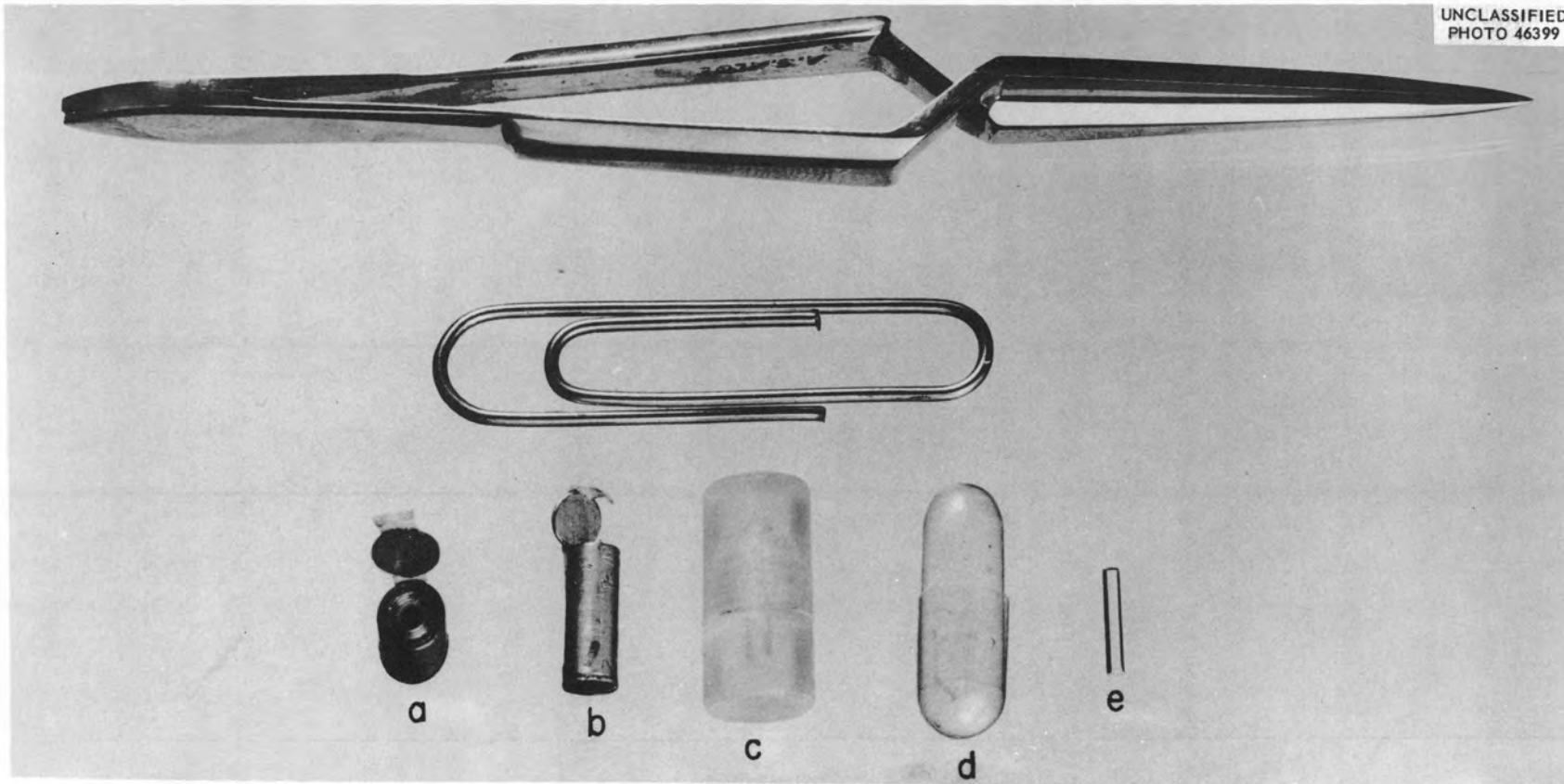
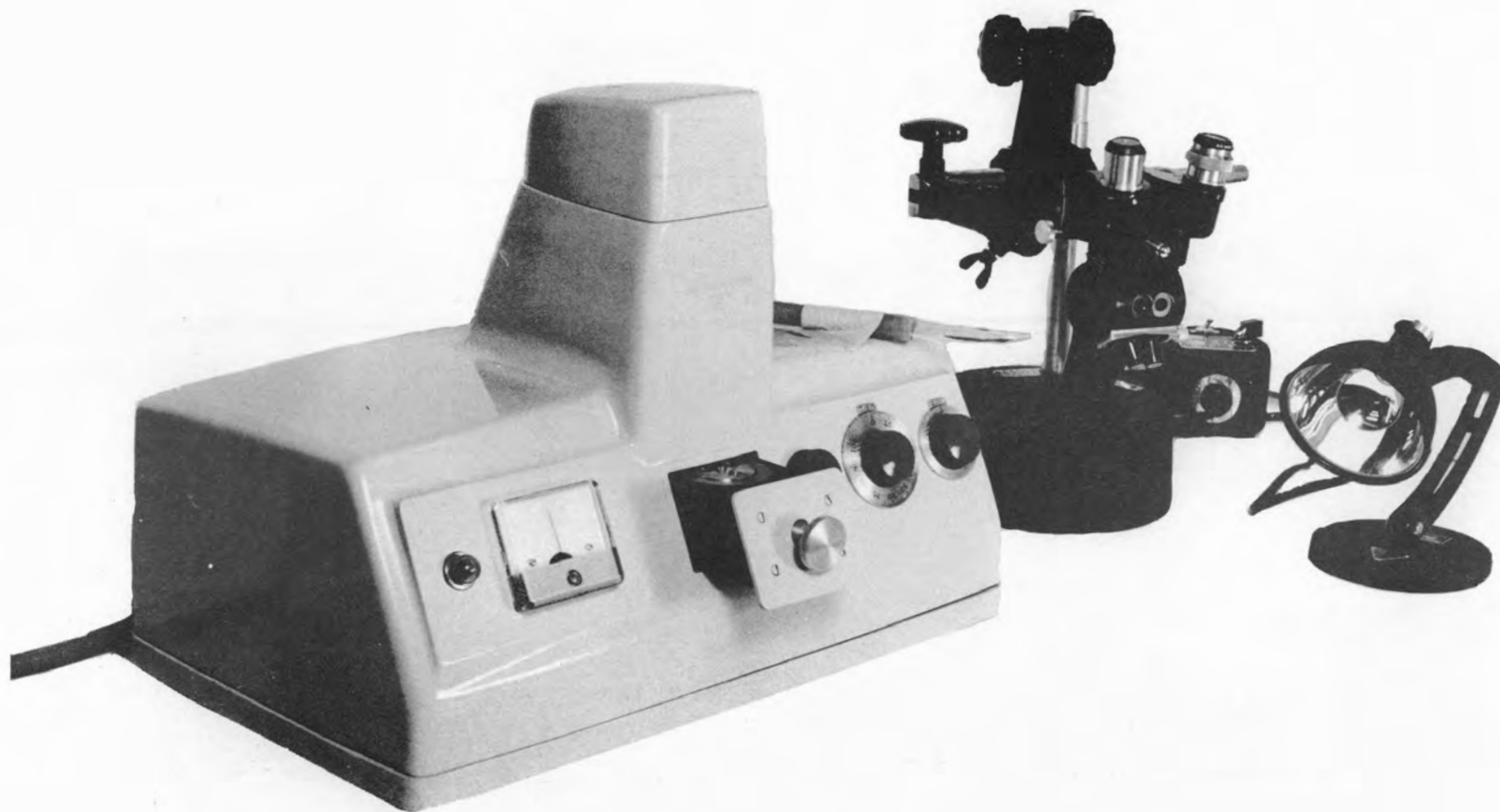


FIG. 29. SIZE OF GLASS ROD AND EXPOSURE CAPSULES RELATIVE TO COMMON OBJECTS. (a) AND (b) - TANTALUM - TIN - TEFLON CAPSULE TO CORRECT FOR ENERGY DEPENDENCE. (c) - FLUOROTHENE CAPSULE FOR HARD GAMMA EXPOSURES. (d) - GELATIN CAPSULE FOR LOW ENERGY UNSHIELDED EXPOSURE. (e) - A GLASS ROD.

UNCLASSIFIED  
PHOTO 46398



79

FIG. 30. THE BAUSCH AND LOMB READER AND LOW POWER MICROSCOPE.

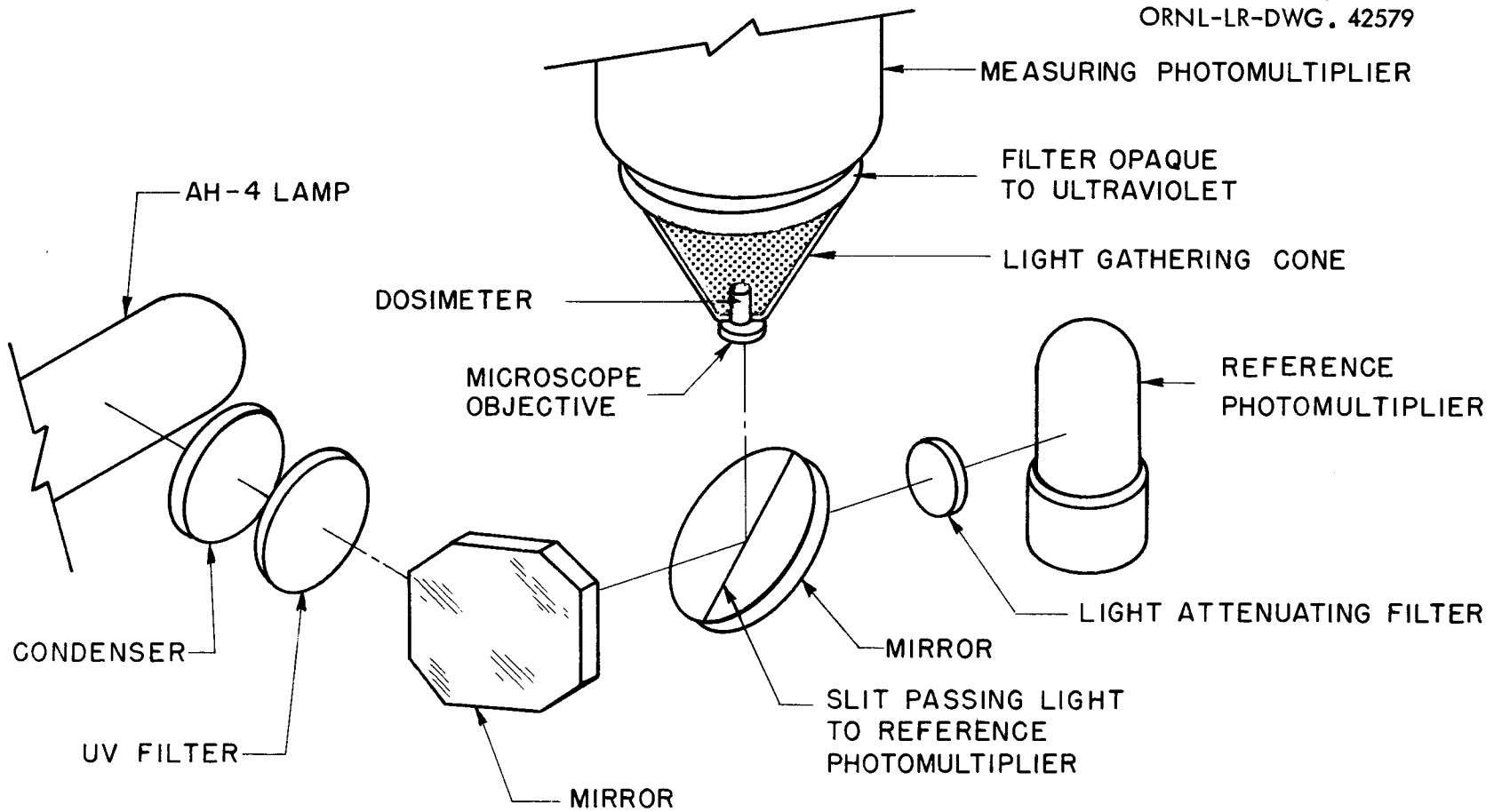


FIG. 31 MICRODOSIMETER READER - OPTICAL LAYOUT

(FROM BAUSCH AND LOMB MICRODOSIMETER CATALOG)

are freed from negative ions and migrate through the glass, some of them are trapped by interstitial silver ions to form a special type of F-center. This F-center, or photoluminescent center, can be excited by ultraviolet light and it then returns to the ground state by emitting a photon in the red region (6400 Å). The stability, temperature dependence, and dose rate effects on the response of the glass to radiation have been described.<sup>27-31</sup> The rods should be read no less than 24 hours after exposure unless they have been specially calibrated for reading at some shorter interval as the response increases for several hours after exposure, after which time the luminescence is stable indefinitely except at elevated temperatures. The system is dose rate independent over a wide range.

#### 2.5.2. Energy Response<sup>32</sup>

From the general description and a knowledge of the response of dosimetric film as a function of photon energy, it might be supposed that the response of the glass per roentgen exposure as a function of photon energy would be similar to that of film. This has been found to be the case and several studies of the energy dependence have been reported.<sup>31,33</sup> The response of the glass, per roentgen, as a function of photon energy is shown in Fig. 32. The response has been normalized to that for Co<sup>60</sup> gamma rays; the lower energy photons are

---

32 Information reported in these sections will appear in more detail in a thesis by W. T. Thornton, Vanderbilt University (to be published as an ORNL report).

33 T. Bowstad and T. Henricksen, Brit. J. Radiol. 31, 163 (1958).

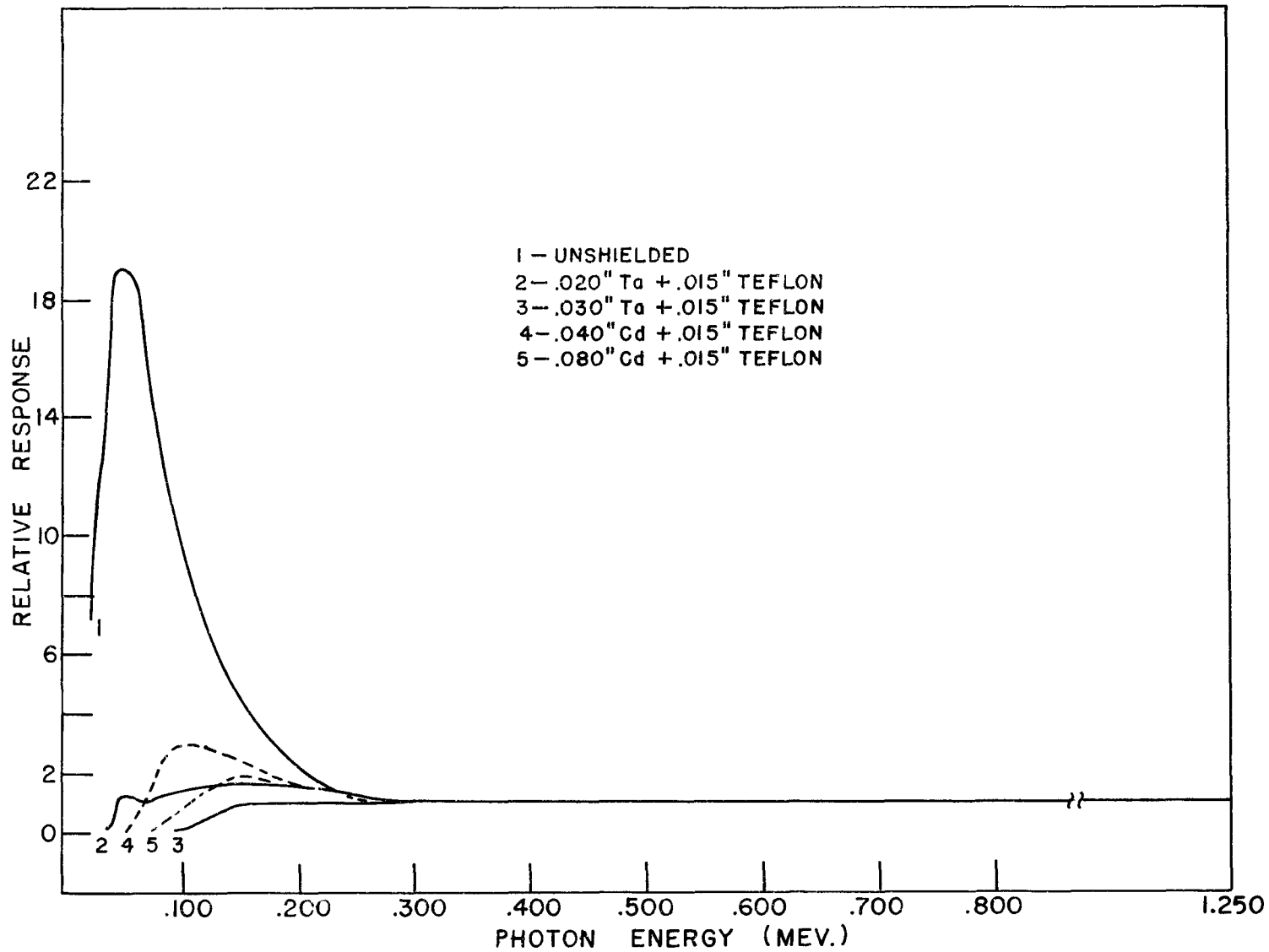


FIG. 32 LUMINESCENT RESPONSE OF GLASS RODS AS A FUNCTION OF PHOTON ENERGY FOR VARIOUS SHIELDS.

from a narrow beam of appropriately filtered X rays. The effectiveness of certain filters or shields placed around the glass and intended to improve the energy response is indicated in Fig. 32. For broad spectra such as the fission gamma spectrum, the 20 mil Ta—15 mil Teflon filter is sufficient for limiting errors due to energy dependence to  $\pm 10\%$ .

### 2.5.3. Fast Neutron Response<sup>32</sup>

The response of the glass rods to fast neutrons is, relative to gamma rays, negligible. Monoenergetic neutron exposures in the region of 0.5 to 1.5 Mev indicate an upper limit of response, relative to Co<sup>60</sup> gamma radiation of less than 1% in this energy region, Fig. 33.

### 2.5.4. Thermal Neutron Response<sup>32</sup>

Exposures of the glass rods in the thermal column of the ORNL graphite reactor yielded a thermal neutron response equivalent to 1 rad of gamma rays for about  $5 \times 10^9$  n<sub>t</sub>/cm<sup>2</sup>. This is sufficiently high to necessitate encapsulation in lithium cans for accurate measurement of gamma radiation coexistent with thermal neutrons. The small dimensions of the glass justify the use of lithium enriched in Li<sup>6</sup>. A research model for possible use in the dosimeter stations is shown in Fig. 34.

### 2.5.5. Cleaning of Glass and Reader

Almost all substances fluoresce when irradiated with

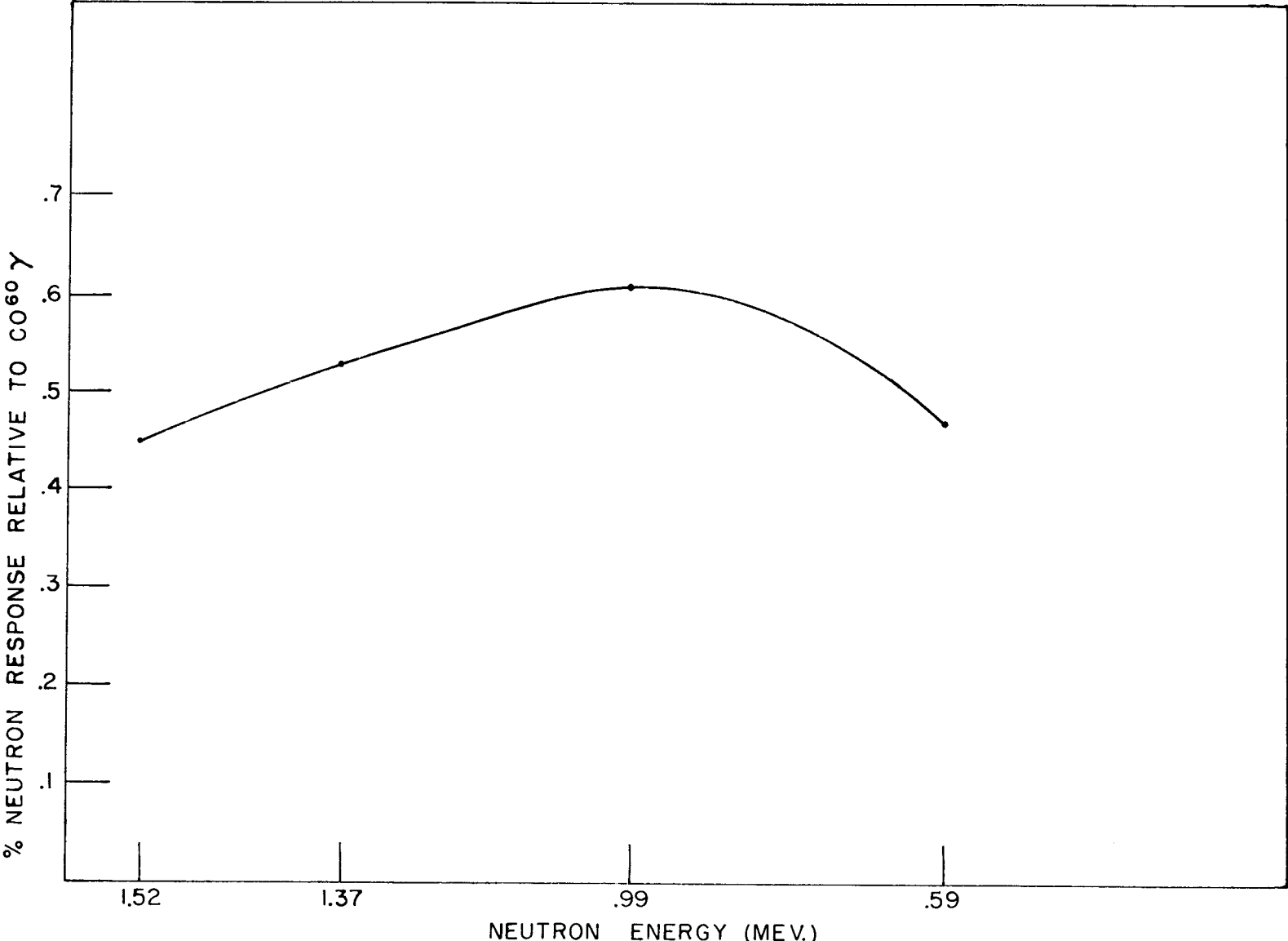


FIG. 33 NEUTRON RESPONSE OF GLASS RODS AS A FUNCTION OF NEUTRON ENERGY

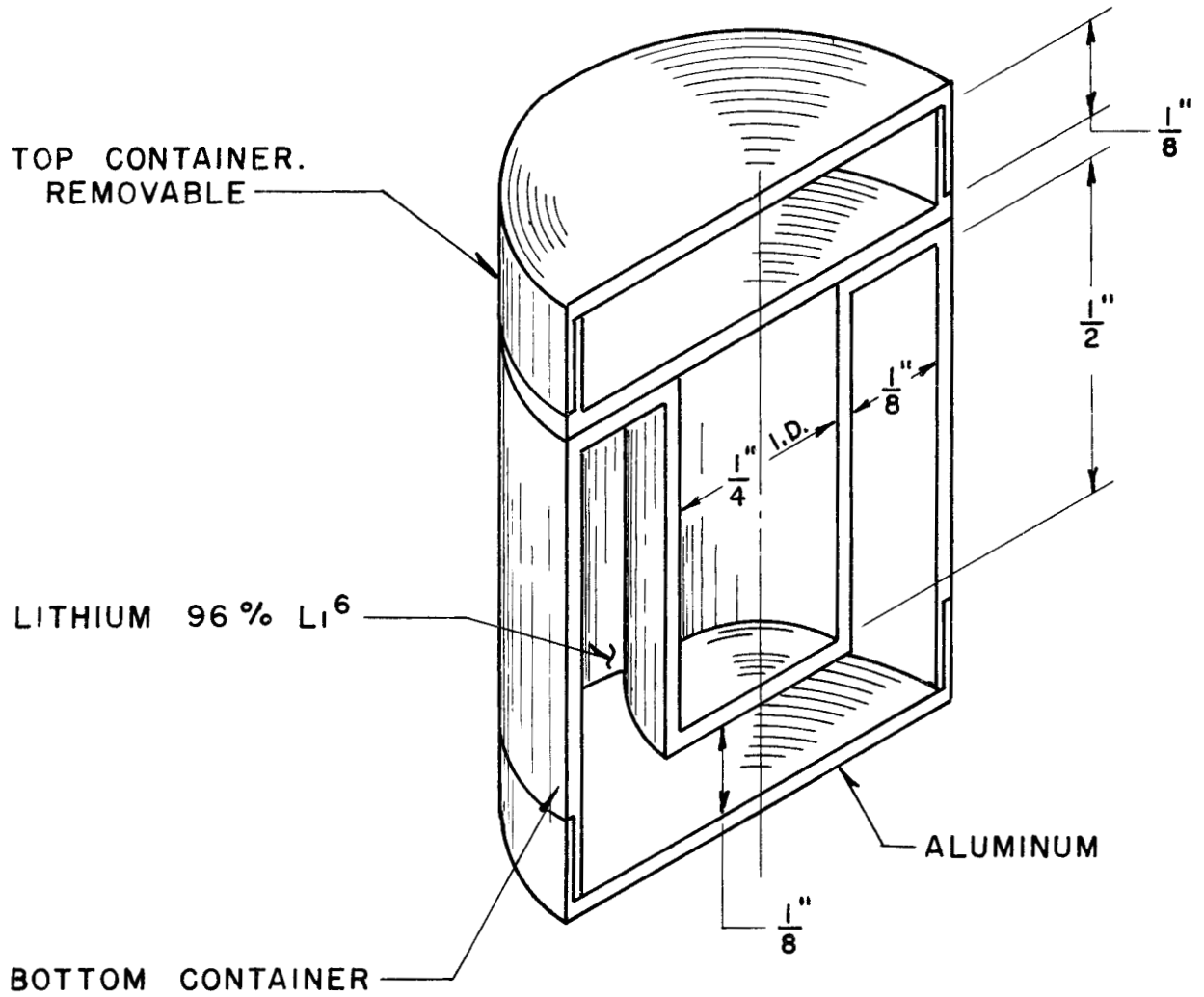


FIG. 34 EXPERIMENTAL LITHIUM SHIELD  
FOR GLASS DOSIMETRY

ultraviolet light. This is particularly true of greases and oils such as found on the hands. The glass rods must be cleaned thoroughly before each reading; clean tweezers, or forceps, and chuck assembly are equally important. It has been found convenient to rinse the rods in acetone, distilled water, and absolute methyl alcohol, in that order, and then to dry them in a stream of filtered and dried air for several seconds. In addition, the rods are held for several more seconds to ascertain that they are back to near room temperature before reading. A low power microscope is used to examine the rods for chips or fractures before reading as the glass is quite friable. The more thorough the cleaning the greater the accuracy, especially at low dose values. A typical low dose calibration curve is shown in Fig. 35 for  $\text{Co}^{60}$  gamma rays.

Operation, care, and maintenance of the reader are adequately described by the manufacturer.

## 2.6. Film Badge for Criticality Accident Applications

### 2.6.1. Introduction

The Oak Ridge National Laboratory badge dosimeter (or badge) has been modified for the addition of materials which permit immediate identification of those persons who may have received medically significant doses due to a combination of neutron and gamma radiation. These modifications supplement the previously incorporated features of the badge, such as provisions for wide range beta-gamma

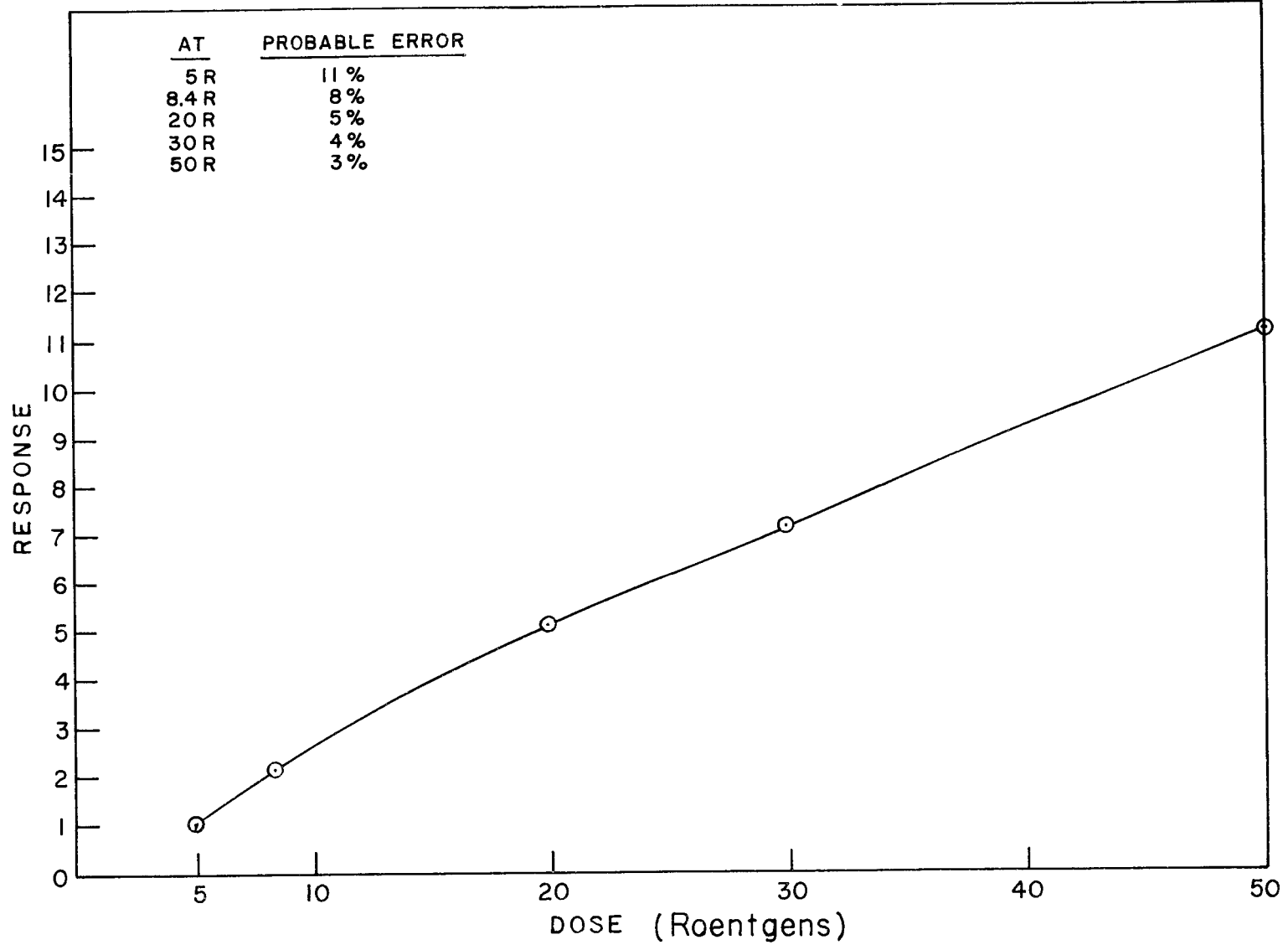


FIG. 35. A TYPICAL LOW-DOSE CALIBRATION CURVE  
FOR GLASS RODS EXPOSED TO GAMMA RAYS.

dosimetry and low level neutron dosimeter.<sup>34</sup>

Film dosimeters of various types have been used since the beginning of the Manhattan Project. The dental size film packets used afford the advantages of small size, negligible weight, low cost, long stability, wide range, and permanent record. Films have some undesirable characteristics, most of which are of minor concern and which may be minimized by available techniques of application, interpretation, and administration. However, the photon energy dependence of the film emulsion has been a problem of prime concern, and many methods for overcoming or circumventing this characteristic have been developed. In all cases, this has been accomplished by a system of filters or absorbers combined into a package or "badge" which contains the film packet.

In many installations the film dosimeter has been combined with the security identification device. This system (1) permits one device to serve for two similar devices, (2) affords excellent administrative control assuring that the dosimeter will be worn, and (3) insures dosimetry coverage for all employees.

The badge dosimeter in which is combined a security device, an adequate system of filters, and a wide range film dosimeter packet, will provide, within the limitations of any small single point dosimeter system, a means of determining personal exposures in facilities where there is no neutron exposure. If only low level

---

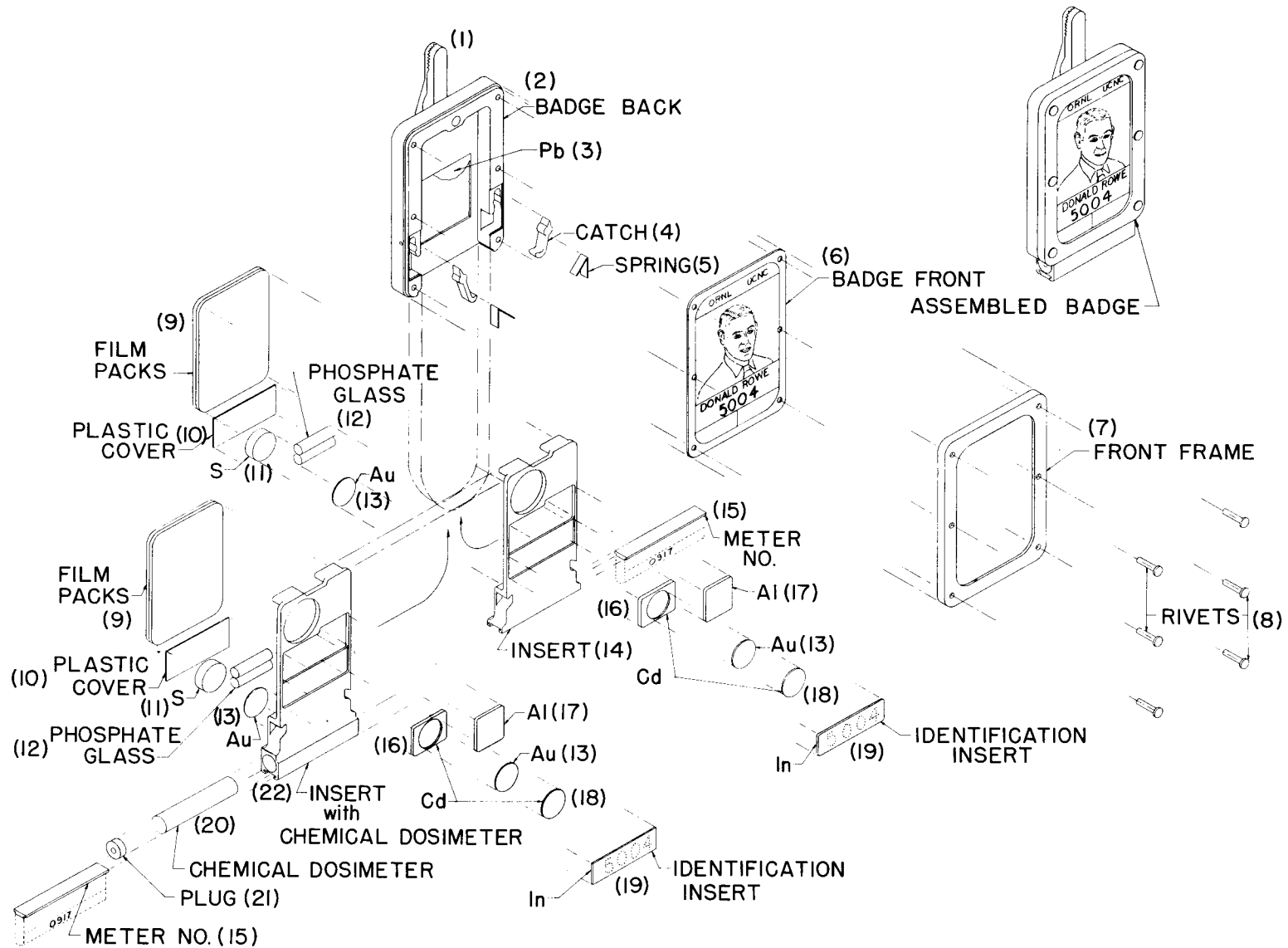
34 E. D. Gupton, Radiol. 66, No. 2, 253 (1956).

neutron doses may be encountered, a nuclear track emulsion may be included to complement the dosimeter film packet. However, the ranges of such emulsions are limited, and this has prompted development of techniques for high level dosage determination.

### 2.6.2. Description of Badge

Figure 36 is an assembly drawing of the recently modified ORNL badge. It provides a compartment for two dosimeter films and a slide arrangement for inserting and removing the films. There are four filters in the front of the badge: (1) a combination filter of 0.020 inch plastic, 0.015 inch cadmium, 0.005 inch gold, 0.015 inch cadmium, and 0.012 inch plastic, in that order from the front surface of the badge; (2) 0.020 inch plastic, 0.040 inch aluminum, and 0.012 inch plastic; (3) 0.082 inch plastic; (4) 0.020 inch plastic. There are two filters in the rear of the badge: (5) 0.062 inch plastic and 0.010 inch lead; and (6) 0.062 inch plastic. A one-half g pellet of elemental sulfur and a 7/16 inch diameter, 0.005 inch thick gold foil are in a cavity in the slide. An indium foil, 1-1/4 inch by 1/4 inch by 0.015 inch thick and perforated with an identification number, is located in the front of the badge. The security device completes the assembly.

Recent improvements include: (1) a tamper-proof insert with magnetically or mechanically operated latch; (2) provisions for inclusion of chemical and/or silver phosphate glass dosimeters when available for personal dosimetry applications; (3) provision for



06

Figure 36 New Health Physics Multi-Purpose Badge Meter.

salvaging components for re-issue; and (4) improvements for increased efficiency in assembly of the badge and administration of the personnel monitoring procedures.

The beta-gamma dosimetry applications of the badge involve a system of four filters in the front of the badge and two filters in the rear of the badge. These filters were selected through experiment to provide an accurate and a simple method for determining various absorbed doses of beta-gamma-X radiation.<sup>35</sup> The du Pont packet 553, with a "hard" gamma dosage range of 50 to 500,000 millirads (first collision, tissue equivalent) under routine conditions of development, is used in conjunction with these filters.<sup>36</sup>

When available for such applications, gamma dosimeters of the chemical or phosphate glass type will be provided and used in the procedure for rapidly determining the highly exposed individuals.

Routine neutron dosimetry is accomplished through use of Eastman NTA film which has a maximum usable usage of approximately 20 to 10,000 millirads from 3 Mev neutrons.

The high level (greater than approximately 10 rads) neutron features depend for accurate dosimetry upon concurrent use with stationary dosimeter stations, as explained in 2.1.

The film badge, Fig. 36, has incorporated in its structure a

---

35 Applied Health Physics Semi-Annual Report, July-December, 1956, Oak Ridge National Laboratory Report CF 57-1-173.

36 The range of this film may be extended by a factor of ten by special developing techniques. (M. Ehrlich and W. Snedegar, Ra-Det 5, Nos. 7-8, 16-18, 1952).

one-half g pellet of sulfur and two 0.005 inch thick by 7/16 inch diameter gold foils, one of which is inserted in the cavity with the sulfur, and the other is a component of the cadmium-gold filter described previously. These items are activated by neutrons such that counting techniques permit determination of the thermal neutron exposure from the two gold foils, and high energy (greater than 2.5 Mev) neutron exposure from the sulfur. The counting procedures are performed with the same counters used in analysis of samples from the dosimeter stations. Exposure to intermediate energy neutrons is determined by referring the data from the badge to that from dosimeter stations in the vicinity of the badge wearer, or by fitting the data from the badge to the spectrum at the point of exposure, if such otherwise is known.

### 2.6.3. Effects of Orientation

The badge alone is not an absolute neutron dosimeter for such exposures, but it permits determination of a "point in space" dose, where the point in space is intimately associated with the person on whom the badge is located. The dose to the badge and the dose to the person will be a function of the relative orientation of the badge with respect to the source of radiation. In any event, the badge would accompany the person throughout the exposure interval and receive a dose proportional to that received by the person. Errors in dosimetry due to lack of knowledge of relative orientation during exposure of person and badge could be reduced appreciably by increasing the number

of dosimeters on the person. However, the problems associated with wearing multiple badges would be rather large. A proposed supplement to the badge and dosimeter stations is a belt which would contain in its structure small detectors which would be located at intervals about the mid-section of the wearer. These would afford information which would permit more nearly accurate determination of tissue dose.

#### 2.6.4. Personnel Screening

Immediately following a nuclear incident, those persons who may have received significant exposure to neutrons may be segregated easily by measurement of the radiation from the activated indium foil in the badge. (Indium 115, which constitutes 96% of that occurring naturally, has a thermal neutron activation cross section of 155 barns with a half life of 54 minutes for the resultant  $\text{In}^{116,37}$ ) Table VII is a listing of resultant dose rate readings obtained subsequent to exposing badges to fast and thermal neutrons in the west animal tunnel of the X-10 graphite reactor and to thermal neutrons in the thermal column of the same reactor. The activated gold foil also serves to identify the persons exposed to neutrons. Although it is less sensitive than the indium, it serves as a valuable compliment since it has a much longer half life than the indium.

In the event of exposure to gamma radiation only, the bare chemical system contained in the badge must be relied on to identify

---

37 "Neutron Cross Sections," AECU-2040, 1952.

Table VII

## Neutron Activation of the ORNL Film Badge

Neutron Exposure	Instrument Reading in Radium Equivalent mr/hr when in "Contact" with Badge (Hours after exposure as indicated)			
	0.5	2	3	6
$10^{11}$ thermal neutrons/cm <sup>2</sup> (thermal column of X-10 graphite reactor)	150 <sup>(38)</sup>	40 <sup>(38)</sup>	20 <sup>(39)</sup>	3 <sup>(39)</sup>
100 rads fast neutron dose + $10^{11}$ thermal neutrons/cm <sup>2</sup> (west animal tunnel of X-10 graphite reactor)	220 <sup>(38)</sup>	70 <sup>(38)</sup>	20 <sup>(39)</sup>	5 <sup>(39)</sup>
$10^9$ thermal neutrons/cm <sup>2</sup> (thermal column of X-10 graphite reactor)	12 <sup>(39)</sup>	3 <sup>(39)</sup>		

38 Readings taken with ORNL Cutie Pie in "contact" with badge.

39 Readings taken with Victoreen model 389C probe in "contact" with badge, shield closed. The shield open to shield closed reading ratio was 2 to 1.

the exposed persons. A gamma dose of 25 rads changes the color from red to yellow. A thermal neutron flux of approximately  $1.5 \times 10^{11}$  n/cm<sup>2</sup> produces the same color change.

## 2.7. Assignment of Individual Exposure Doses

### 2.7.1. Neutrons

It may be shown from Ref. ~~1~~<sup>2</sup> that the first collision neutron dose is related to the sodium activity in a cylindrical phantom having a 15 cm radius, as follows:

$$D_n = 9.5 \times 10^8 \frac{\int_0^\infty D_o(E) \phi(E) dE}{\int_0^\infty \epsilon(E) \phi(E) dE} K \quad (15)$$

where  $D_n$  is the neutron dose in rads,  $\phi(E)dE$  is the number of neutrons between  $E$  and  $E + dE$ ,  $D_o(E)$  is the first collision dose per unit neutron flux at energy  $E$ ,  $\epsilon(E)$  is the probability that neutrons of energy  $E$  will be captured in the phantom as thermal neutrons, and  $K$  is the sodium activity in disintegrations per sec (corrected back to the time of exposure) per cm<sup>3</sup> of blood serum and is equal to corrected counts per sec divided by the geometry correction. The above expression applies to the case where the concentration of sodium in serum is 3.2 mg/cm<sup>3</sup>, a number which is remarkably constant for man and other warm blooded animals.

The integral  $\int_0^{\infty} D_o(E) \phi(E) dE$  may be expressed in terms of the flux measurements made with the threshold detectors as follows:

$$\int_0^{\infty} D_o(E) \phi(E) dE = \left( 0.028 N_T + 1.0 N_{Pu} + 1.4 N_{Np} + 0.6 N_U + 0.7 N_S \right) \times 10^{-9} \quad (16)$$

where the dose is in tissue rads, and the symbol N refers to the number of neutrons per  $\text{cm}^2$  as obtained with each of the detectors.

The integral  $\int_0^{\infty} \epsilon(E) \phi(E) dE$  may be expressed also in terms of the threshold detector data. Using the curve applicable to the 15 cm radius cylinder in Fig. 2, it is seen that

$$\int_0^{\infty} \epsilon(E) \phi(E) dE = 0.18 N_T + 0.50 N_{Pu} \quad (17)$$

Thus,

$$D_n = 0.95K \frac{\left( 0.028 N_T + 1.0 N_{Pu} + 1.4 N_{Np} + 0.6 N_U + 0.7 N_S \right)}{0.18 N_T + 0.5 N_{Pu}} \quad (18)$$

It is important to note that the assignment of the first collision dose given by the above equation holds only if the neutron spectrum at the point where the individual is exposed is essentially the same

as the spectrum at the most favorably located dosimetry station. Experience has shown that the fast spectrum does not drastically change with distance, but the ratio  $N_T/N_{Pu}$  is strongly affected by a number of factors, including distance from the source, slight amounts of intervening shielding, room size, and disposition of materials in the room. For this reason it is suggested that the secondary dosimetry stations, containing Au and S, be used freely. In this case we may adopt the following procedure. The above equation may be modified to account for changes in the  $N_T/N_{Pu}$  ratio by using the Au and S flux, i.e.

$$D_n = 0.95K \frac{(0.028 N_TB + 1.0 N_{Pu} + 1.4 N_{Np} + 0.6 N_U + 0.7 N_S)}{0.18 N_TB + 0.5 N_{Pu}} \quad (19)$$

where  $B = (N_S/N_T)(N_T/N_S)_S$ , and  $(N_T/N_S)_S$  is the ratio of the thermal flux to the sulfur flux evaluated at the secondary station closest to the exposed individual. In many cases the ratio  $N_T/N_{Pu}$  is much less than unity and these extra procedures are not necessary.

### 2.7.2. Gamma Rays

The gamma-ray exposure dose may be determined by

$$D_\gamma = (D_\gamma/D_n) \times D_n \quad (20)$$

where  $(D_\gamma/D_n)$  is the measured gamma to neutron dose ratio, and  $D_n$  is

the neutron dose as determined above. The ratio  $D_Y/D_n$  should not depend strongly on room size, distance or location of material in the room, unless, of course, these materials are located on the ray paths drawn from the source to the individual. The ratio  $D_Y/D_n$  for the most suitably located dosimetry station should be used.

### 3. OUTLINE AND SYNOPSIS OF ORNL-2748, PART B

#### 3.1. Outline of ORNL-2748, Part B

Radiation Accidents: Medical Aspects of Neutron and Gamma-Ray Exposures, N. Wald, M.D., and G. E. Thoma, Jr., M.D.

#### 1. REVIEW OF PREVIOUS ACCIDENT MEDICAL DATA

##### 1.1. Radiation Syndrome

- 1.1.1. Dose response relationship
- 1.1.2. Radiation injury groups
- 1.1.3. Hypothetical clinical case illustrations

##### 1.2. Analysis of Accident Cases

##### 1.2.1. Clinical signs and symptoms

- 1.2.1.1. initial stage
- 1.2.1.2. manifest illness stage

##### 1.2.2. Laboratory findings

- 1.2.2.1. methods of presentation and analysis
- 1.2.2.2. hematology
- 1.2.2.3. biochemistry
- 1.2.2.4. miscellaneous

##### 1.2.3. Clinical management

#### 2. RECOMMENDED CLINICAL PROCEDURES

##### 2.1. Diagnostic Procedures

- 2.1.1. Recommendations for injury groups
- 2.1.2. Utilization of data

##### 2.2. Clinical Management

- 2.2.1. Recommendations for injury groups

### 3.2. Synopsis of ORNL-2748, Part B

#### 3.2.1. Review of Previous Accident Medical Data

##### Radiation syndrome

When man is exposed to a single whole-body dose of ionizing radiation, he exhibits certain clinical signs, symptoms and laboratory findings which are collectively termed the radiation syndrome. The frequency and severity of these manifestations are roughly related to the dose received and the sensitivity of the individual patient. Exposures to less than 100 rads rarely result in clinical symptomatology, so that for our present purposes the radiation syndrome may be thought of as those clinical findings associated with a total-body dose of radiation of over 100 rads.

The typical chronologic sequence of events following a large whole-body radiation exposure can be divided into four clinical stages: the initial or prodromal stage, the latent period, the manifest illness stage, and the recovery stage. The prodromal clinical findings include anorexia, nausea, vomiting, extreme sweating, fatigue, and prostration. These symptoms remit in about two days and the patient enters the latent period. After two to three weeks of well being a number of developments begin within a short time of each other. These include fever, overt or occult infections, scalp hyperesthesia and epilation, purpura and hemorrhage, diarrhea, ileus, cardiovascular collapse, severe lethargy and changes in sensorium. By approximately the end of the sixth week after exposure the situation is usually resolved. Clinical improvement of the surviving patients is rapid, but fatigue often persists for many

months.

About 15% of patients exposed to a dose of 100 rads may be expected to show some of the signs and symptoms of the syndrome. The frequency increases sharply up to approximately 200 rads at which level most of those exposed may be expected to exhibit some clinical symptomatology. A fatal outcome is probably inevitable above about the 800 rad dose level. In the accidents reviewed in this report, death did not occur in any treated patients with known exposure to less than 500 rads.

In spite of the fact that there is a generally useful relationship between magnitude of radiation dose and severity of clinical sequelae, it is considered essential to approach the problem of individual patient management from a somewhat different standpoint. Even if ideal conditions existed and all of the dosimetric procedures discussed in Part A of this report were performed, the response of one person to a known exposure would still differ from that of another. It has, therefore, been deemed useful in the management of radiation accidents to arbitrarily divide patients showing various symptoms and signs of the acute radiation syndrome into five different "radiation injury" groups. The pertinent characteristics of each group may be summarized as follows:

Group I: Most of these patients are completely asymptomatic; a few may have minimal prodromal symptoms.

Group II: These patients develop the acute radiation syndrome in a mild form. After transient prodromal nausea and vomiting, laboratory

and mild clinical evidence of hematopoietic derangement dominates the picture.

Group III: A serious course occurs in these patients: Complications of hematologic malfunction are severe and, in the upper part of the group, some evidence of gastrointestinal damage may also be present.

Group IV: An accelerated version of the acute radiation syndrome occurs. Complications of gastrointestinal injury dominate the clinical picture. The severity of hematopoietic disturbances are related to the length of survival time following exposure.

Group V: These patients have a fulminating fatal course with marked central nervous system impairment.

A case report of a hypothetical patient typical of each group is presented in detail.

#### Analysis of accident cases

Clinical data of all pertinent accident cases were reviewed and the patients were assigned thereby to the appropriate radiation injury groups.

Anorexia, nausea and vomiting were present in all patients in Group III and above within an hour after exposure. These generally continued for about two days. In Group II the triad was somewhat slower in appearing, beginning within six hours, but continued intermittently for about the same duration. Two of the eight patients did not vomit at all. Only four of the fourteen Group I patients had

anorexia or nausea, and only two of them vomited.

Diarrhea only occurred in the Group IV and V cases. All three of these patients died. It appeared on day 4 in both Group IV patients, and in 45 minutes in the Group V patient.

Other symptoms which were frequent almost exclusively in Group III and above included conjunctivitis, erythema, sweating, and paresthesias. Immediate central nervous system symptomatology including ataxia and disorientation was seen only in Group V.

Patients in Group I showed no clinical evidence of illness after the initial stage subsided. Those in higher groups developed further signs of the acute radiation syndrome, as described above, in varying degrees of severity.

A method, called "profile scoring", was developed for grading the severity of radiation injury as indicated by laboratory tests. Where the same tests, performed in many individual cases, fell into reasonably uniform time periods, results were tabulated and reported as mean scores for the various radiation injury groups. This was possible only in the category of hematologic tests.

### 3.2.2. Recommended Clinical Procedures

#### Diagnostic procedures

In a given accident the exposure dose and the patient's response to it are the two means by which logical clinical management can be planned. Therefore, the highest priority diagnostic recommendations in the early post-exposure period are planned for the

accumulation of sufficient information to establish the response "profile" of the individual under study in comparison with those of others who reacted in a similar manner to whatever dose of radiation. Detailed methods for performance of this comparison are given. When this information is available, reasonable estimation of prognosis and management planning can proceed even in the absence of dosimetry information. It is highly desirable, of course, to obtain dosimetry information as soon as possible to supplement the clinical estimate of injury.

#### Clinical management

It is desirable for all cases with a possibility of acute injurious radiation over-exposure to be hospitalized for close observation and bed rest. Using the initial signs and symptoms and the blood count profile scores (made up of scores for counts of erythrocytes or hematocrit, leucocytes, neutrophils, lymphocytes and platelets), it is possible to determine tentatively the severity of the radiation injury which an accident patient will develop. The procedure is graphically illustrated in Fig. 37.

Patients assigned by this method to radiation injury Group II or above should be continued as hospitalized patients under adequate medical care. Recommendations of helpful procedures in medical management of these cases are made in detail. The other patients can be assured of their favorable prognosis and released from in-patient care when asymptomatic. Suggested follow-up procedures are tabulated for all injury groups.

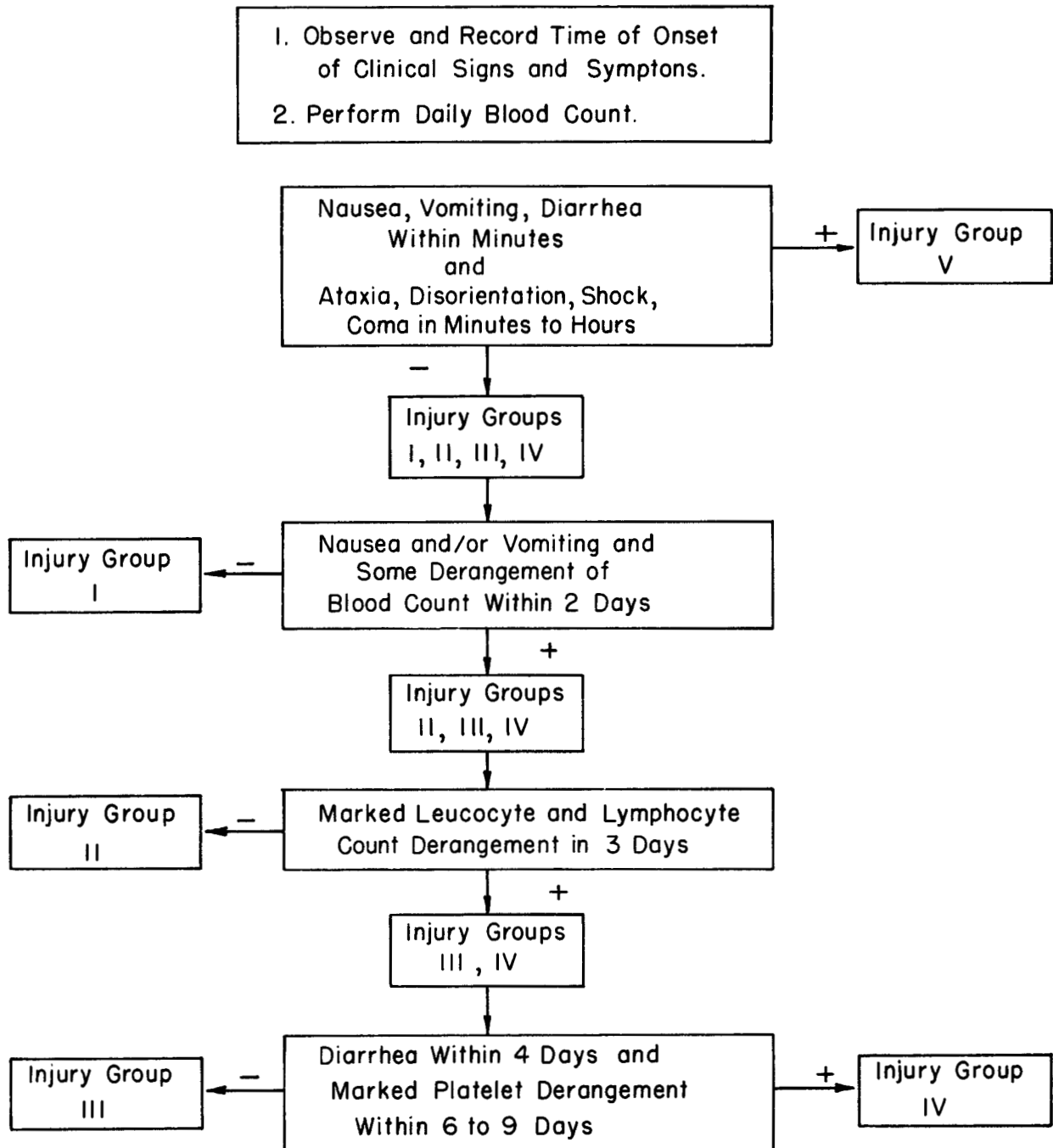
UNCLASSIFIED  
ORNL-LR-DWG. 41433

FIG. 37 PRELIMINARY ESTIMATION OF CLINICAL RADIATION INJURY FOLLOWING OVEREXPOSURE



ORNL-2748  
Health and Safety  
TID-4500 (15th ed.)

Distribution  
Second Issue

1-100. G. S. Hurst